FABRICATION OF 3D-PRINTED DEVICES AND THEIR APPLICATIONS IN FLOW-BASED TECHNIQUES FOR QUALITY CONTROL OF GABA-SUPPLEMENTED PRODUCTS AND CLINICAL DIAGNOSIS OF KIDNEY DISEASE

BHOONNARASA KASETSOONTORN

A THESIS SUBMITTED IN PARTIAL FULFILLMENT OF THE REQUIREMENT FOR THE DEGREE OF DOCTOR OF PHILOSOPHY IN APPLIED CHEMISTRY

DEPARTMENT OF CHEMISTRY
FACULTY OF SCIENCE
KING MONGKUT'S INSTITUTE OF TECHNOLOGY LADKRABANG

2020
KMITL-2020-SC-D-010-049

FABRICATION OF 3D-PRINTED DEVICES AND THEIR APPLICATIONS IN FLOW-BASED TECHNIQUES FOR QUALITY CONTROL OF GABA-SUPPLEMENTED PRODUCTS AND CLINICAL DIAGNOSIS OF KIDNEY DISEASE

BHOONNARASA KASETSOONTORN

A THESIS SUBMITTED IN PARTIAL FULFILLMENT OF THE REQUIREMENT FOR THE DEGREE OF DOCTOR OF PHILOSOPHY IN APPLIED CHEMISTRY

DEPARTMENT OF CHEMISTRY
FACULTY OF SCIENCE
KING MONGKUT'S INSTITUTE OF TECHNOLOGY LADKRABANG

2020
KMITL-2020-SC-D-010-049

Thesis Title	Fabrication of 3D-printed devices and their applications in flow-based techniques for quality control of GABA-supplemented products and clinical diagnosis of kidney disease
Student Name	Miss Bhoonnarasa Kasetsoontorn
Student ID	57605008
Degree	Doctor of Philosophy (Applied Chemistry)
Department	Chemistry
Year	2020
Thesis Advisor	Asst. Prof. Dr. Nathawut Choengchan

Abstract

In this work, two 3D-printed devices for quality control of GABA-supplemented products and clinical diagnosis of kidney disease were presented. The first device is a dialysis unit which was designed for direct analysis of solid and liquid samples. The homemade unit was constructed using a 3D printer due to its simple and fast fabrication ability. The dialysis unit is composed of cylindrical-shaped donor and acceptor chambers. A stainless steel sieve is installed inside the donor chamber. SEM images clearly showed that the sieve prevented membrane blockage by suspension particles in the sample. Multiple dialysis units were connected to a sequential injection (SI) system for serial determination of gamma-aminobutyric acid (GABA) in solid and liquid samples. The dialysate from each dialysis unit was consecutively aspirated into the SI flow line for on-line derivatization of GABA with 2- hydroxy- 1- naphthaldehyde (3.0% w/v). The derivative was detected spectrophotometrically at 425 nm. The linear calibration range extended to 1000 mg L^{-1} GABA ($r^2 > 0.99$) with high precision (1.2 %RSD). The developed system was applied to analysis of dietary supplements, grains of germinated brown rice and milk. The samples were directly introduced into the donor chamber either as powder or liquids. The measured GABA content using the developed method was compared using high performance liquid chromatography, with good agreement using Pearson's

correlation (r^2 = 0.9999). The method has high accuracy based on recovery studies (99.8 ± 1.5%) and high sample throughput (64 samples h^{-1}).

The second devise is 3D printed detection flow cell which was applied to a flow-based system for the determination of albumin based on chemiluminescence (CL) detection. Gold nanoparticles (AuNPs)-catalyzed luminol CL were employed as the detection reaction. In the presence of albumin, aggregation of the AuNPs was induced and this inhibited the CL light caused by the luminol-H_2O_2 system. The AuNPs were synthesized using the Turkevich's method. Surface plasmon peak of the as-prepared colloidal gold was located at 520 nm. TEM image showed that monodispersed nanoparticles were observed (average size: 18.4 ± 0.04 nm). The AuNPs were off-line mixed with the standard/sample for 10 min. Aliquots of 500 μL of the mixed solution and 400 μL of 0.01 mol L^{-1} luminol in 0.1 mol L^{-1} NaOH were injected into the FI manifold. A detection flow cell was designed as spiral configuration and was attached in front of the photomultiplier tube. This flow cell was fabricated quickly and easily using three-dimensional printing technology. Increasing in the concentration of albumin resulted in decreasing in the CL intensity. Calibration plot was observed from the concentration range of 0.1 to 70 mg albumin L^{-1} with good linearity (r^2 > 0.99). The detection limit was 0.05 mg L^{-1} (3SD/slope) with a relative standard deviation of 0.57 %. High sample throughput (66 samples h^{-1}) was also achieved.

Keywords: 3D printed device, dialysis, direct analysis, flow cell, chemiluminescence, GABA, gold nanoparticle, albumin, urine.

Acknowledgments

I would like to acknowledge financial and instrumental supports from Department of Chemistry, Faculty of Science, King Mongkut's Institute of Technology Ladkrabang (KMITL) and FIRST Lab @ KMITL as well as Applied Analytical Chemistry Research Unit.

I would like to acknowledge committees, Asst. Prof. Dr. Nuanlaor Ratanawimarnwong, Asst. Prof. Dr. Wiboon Praditweangkum, Assoc. Prof. Dr. Ekarat Detsri and Assoc. Prof. Dr. Saowapak Teerasong for their useful comments and suggessions which help improvement of thesis.

Finally, I would like to sincere acknowledge Asst. Prof. Dr. Nathawut Choengchan, my advisor, for all his supports of my work. I also appreciate all contributions from my colleagues.

Miss Bhoonnarasa Kasetsoontorn

Contents

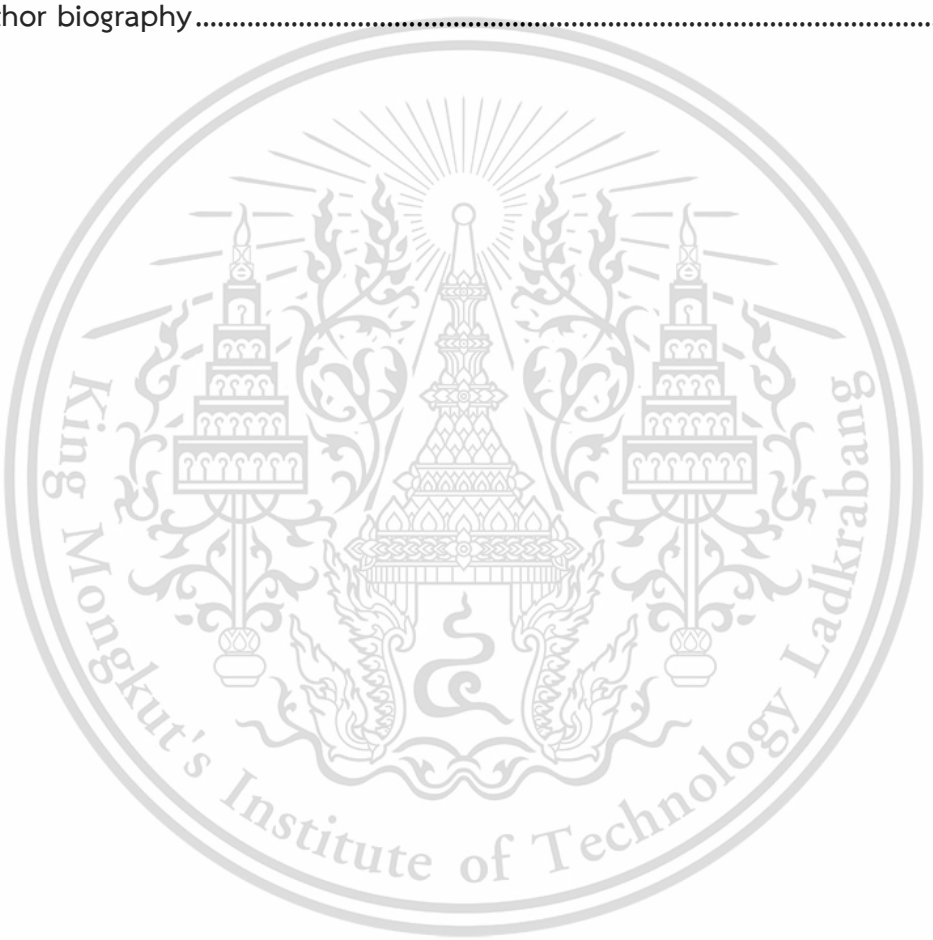

List of Tables

List of Figures

Abbreviations / Symbols

GABA	Gamma-aminobutyric acid
GAD	Glutamate decarboxylase
Da	Dalton
GFR	Glomerular filtration rate
AM	Additive manufacturing
2D	Two dimensions
3D	Three dimensions
CAD	Computer aided design
SLA	Stereolithography
DLP	Digital light projector
FIA	Flow injection analysis
MSD	Membrane sampling device
SIA	Sequential Injection Analysis
MPV	Multi-position valve
SP	Syringe pump
HC	Holding coil
MC	Mixing coil
UV	Ultra violet
VIS	Visible
T	Transmittance
A	Absorbance
I	Intensity
NIR	Near infrared
CL	Chemiluminescence
HN	2-hydroxy-1-naphthaldehyde
CSF	Cerebral spinal fluid
HPLC	High performance liquid chromatography
DAD	Diode array detector
BAs	Biogenic amines
PUT	Putrescine
SPM	Spermine

SPD	Spermidine
HIST	Histamine
TYRA	Tyramine
DOP	Dopamine
SOS	Second order scattering
PIM	Polymer inclusion membrane
BSA	Bovine serum albumin
RLS	Rayleigh light scattering
Alizarin Red S	1,2-dihydroxyanthraquinone-3-sulfonate
SAM	Self-assembled monolayer
PPA	Solyphosphoric acid
QCM	Crystal microbalance
PMMA	Poly (methyl methacrylate)
PMT	Photomultiplier tube
AuNPs	Gold nanoparticles
HSA	Human serum albumin
nm	Nanometer
mg	Milligram
μg	Microgram
ng	Nanogram
pg	Picogram
dL	Deciliter
SD	Standard deviation
RSD	Relative standard deviation
r^2	Coefficient of determination
LOD	Limit of detection
LOQ	Limit of quantitation

Chapter 1
Introduction

1.1 Research Motivation

Nowadays, 3D printing is a well-known technique that offers many advantages such as the ability to fabricate complicated structures that are difficult to construct by traditional machining. It is low cost, fast, and reduces wastage of material to a minimum. 3D printing is now a preferred method for designing and making prototypes of new devices in various fields. 3D printed devices for analytical applications are now receiving increasing attention. The combination of simple-to-fabricate 3D printed devices with flow-based techniques opens up a new approach for integration of automated analytical methods.

In this work, we aimed to develop methods for quantitative analysis of gamma-aminobutyric acid (GABA) in food supplement products and for urinary albumin that relied on "in-house" 3D printed devices and a flow-based system. Our developed methods were used in the following two research topics: 1) a direct analysis of gamma-aminobutyric acid in food supplement products and beverages employing a 3D printed dialysis unit and sequential injection for automated derivatization and determination and 2) an automated analysis of albumin in urine with a flow injection system and a 3D printed flow cell.

1.1.1 Determination of gamma-aminobutyric acid in foodstuff and beverages exploiting a 3D printed dialysis unit and sequential injection.

More efficient and rapid direct analysis of samples has always been a challenge for analytical chemists. Usually, a pre-treatment/preparation step is required to achieve a desired selectivity. Dialysis with a membrane is one of sample clean-up methods for separating low-molecular weight analytes from interfering macromolecules, colloids, and suspended particles in a sample matrix. Various designs of dialysis units have been applied to flow injection system. Most dialysis units have a sandwich design with rectangular geometry. They hold a flat sheet of hydrophilic membrane between their upper and the lower plates. The use of this sandwich-type dialysis unit as part of an automated flow system has been shown to be very effective

for removal of particulate matter in liquid samples such as serum [1], milk [2], pharmaceutical products [3], and fruit juices [4]. Some studies employed concentric-type dialysis unit or microdialyzer for analysis of solids [5]. However, those devices were not suitable for direct analysis. Prior sample preparation was necessary before the devices could be applied [6]. Therefore, in this work, we designed a new dialysis unit suitable for direct analysis of both liquid and solid samples. The unit comprised cylindrical donor and acceptor chambers. In contrast to other dialysis units, this unit incorporated a stainless-steel sieve inside the donor chamber. Because of this sieve, membrane clogging from macromolecules in a sample matrix was prevented. The dialysis unit was constructed by 3D printing based on stereolithography. The advantage of 3D printing is its capability to construct components that cannot be easily manufactured using conventional means. It is a one-step production process suitable for producing prototypes at low running cost.

Gamma-aminobutyric acid (GABA) has been considered a health promoting substance that can reduce anxiety, promote relaxation, reduce insomnia and reduce blood pressure. Nowadays, since there are a large number of commercial dietary GABA supplemented products on the market, it is necessary that GABA concentrations in these products are as labeled as detected in the quality control process. Automated determination of GABA is, therefore, necessary. Various analytical methods have been employed for quantitative analysis of GABA, including high performance liquid chromatography (HPLC) [7], flow injection (FI) [8], and sequential injection (SI) [9]. Chromatographic techniques provide high selectivity, but flow-based methods offer rapid determination. Nevertheless, all these methods are not applicable for automated direct analysis of samples. Complex sample preparation protocols requiring extensive time and labor are the norm.

In this work, multiple dialysis units were connected to a sequential injection (SI) system for conservative determination of gamma-aminobutyric acid (GABA) of solid and liquid samples. The dialysate from each dialysis unit was consecutively aspirated into the SI flow line for on-line derivatization of GABA with 2-hydroxy-1-naphthaldehyde. The developed system was applied to analysis of dietary supplements, grains of germinated brown rice, tea, and milk. The samples were directly introduced into the donor chamber either as powder or liquid.

1.1.2 Flow-based systems with 3D printed flow cells for quantitative measurement of Albumin in urine based on using the AuNPs-catalyzed chemiluminescence detection.

Kidney disease is a global health problem. Urinary albumin excretion is one of the important key parameters for diagnosis of kidney dysfunction. Urinary albumin concentration of lower than 30 mg L^{-1} is regarded as normal. The concentration in the range of 30 – 300 mg L^{-1} is denoted as 'microalbuminuria' which is relevance to the preliminary stage of kidney failure. A concentration of greater than 300 mg L^{-1} is considered 'albuminuria' or 'proteinuria' that represents a severe stage. Therefore, accurate measurement of urinary albumin gives more accurate clinical diagnosis of kidney disease—an accurate measurement method is utmost essential. Turbidimetric immunoassay is commonly used to measure urinary albumin in hospital laboratory. The advantages of this method are high selectivity, precision, and high accuracy. However, it is complicated and consumes long analysis time.

Currently, gold nanoparticles (AuNPs) are probably the most outstanding kind of metal nanoparticles because of their chemical inertness, easy modification, simple control of particle size, and high extinction coefficient. Some works have reported that AuNPs can easily form conjugate with BSA through electrostatic interaction [10]. AuNPs can be also exploited as a catalyst for a chemiluminescence (CL) reaction between luminol-H_2O_2 [11]. In this work, the reported properties of AuNPs were applied as a detection principle for monitoring the concentration of albumin in urine by using a flow injection technique for automated albumin monitoring. This system can produce accurate findings of a large number of samples rapidly, making it practical for clinical diagnosis. Simple and fast three-dimensional (3D) printing technology was employed in construction of spiral flow-through cells. 3D printed flow cells truly made it practical for chemists to assemble an analytical system without the need to rely on parts that a manufacturer may not readily provide.

1.2 Objectives of the study

1) To develop a direct analysis method using a newly designed 3D printed dialysis unit for determination of GABA in both liquid and solid samples of food supplement products.

2) To develop an automated flow-based injection system employing 3D printed flow cell for on-line quantitative measurement of albumin in urine.

1.3 Scopes of the developments

1) Development of a fully automated direct analysis method with a newly designed and constructed 3D printed dialysis unit for determination of gamma-aminobutyric acid in food supplement products and beverages.

Firstly, GABA detection reaction is investigated by spectrophotometry. The chemical and physical parameters affecting the sensitivity of determination is studied in order to determine the optimal conditions for the determination. Analytical performances of 3D printed dialysis units connected to the SI system are evaluated. The method is validated against a conventional high-performance liquid chromatography method.

2) Development of an automated flow-based system employing 3D printed flow cell for on-line quantitative measurement of albumin in urine

3D flow cells are fabricated with a KINGS 600 3D printer (China) with Nd: YVO_4 solid state laser (355 nm) as the light source and a fixed scanning speed of 10.0 ms^{-1}. Detection of albumin by CL level is based on aggregation of AuNPs due to the presence of albumin. CL is generated by a luminol-H_2O_2 system. Optimal conditions for detection is also investigated. The analytical performance of the system is evaluated.

1.4 Benefits of the study

1) Achievement of a simple and accurate direct analysis method of GABA in both liquid and solid samples using a newly designed 3D printed dialysis unit for the determination of GABA in food supplement products and beverages.

2) An automated flow-based system with 3D printed flow cells for on-line quantitative measurement of albumin in urine was successfully developed.

Chapter 2
Theory and Literature Reviews

2.1 General information of GABA and albumin

2.1.1 Gamma aminobutyric acid (GABA) [12]

The GABA (Gamma-aminobutyric acid) molecule is the nucleotide known in biochemistry as the "molecular currency" of intracellular energy transfer; that is, ATP is able to store and transport chemical energy within cells. ATP also plays an important role in the synthesis of nucleic acids. GABA with Chemical Formula $C_4H_9NO_2$, and Molar mass 103.12 g mol^{-1} is synthesized from glutamate using the reaction of decarboxylation which shown in Figure 2.1.

Figure 2.1. Decarboxylation of L-glutamate to GABA by glutamate decarboxylase (GAD). PLP: pyridoxal-5'-phosphate.

GABA is the inhibitory neurotransmitter in the mammalian central nervous system. It plays a role in regulating neuronal excitability throughout the nervous system that makes human brain relaxing and anti-anxiety [13]. GABA is also directly responsible for anterior pituitary encouraged which increases the amount of human growth hormone and the regulation of muscle tone. In medicine, GABA is used for some neurological disorder treatment such as sleep disorder [13] and anxiety. There is also more scientifically and medicinally relevant evidence that GABA has a blood-pressure-lowering effect, low density lipoprotein-lowering effect and preventive effect on Alzheimer's disease [13]. As a result of these properties, GABA has also become a popular supplement in recent years.

2.1.2 Albumin [15]

Albumin is one of the most important proteins, which is made in the liver. It consists of a single polypeptide chain of 585 amino acids with a molecular weight of 66500 Da [14]. Serum albumin is a heart-shaped globular protein with three homologous domains: domain I (residue 1–195), II (residue 196–383) and III (residue 384–585). Each domain possesses two subdomains A and B formed by six and four **α**-helices, respectively. The hydrophobic pocket of subdomain IIA and IIIA, popularly known as Sudlow's site I and II, respectively accommodate the aromatic and heterocyclic compounds (Figure 2.2.)

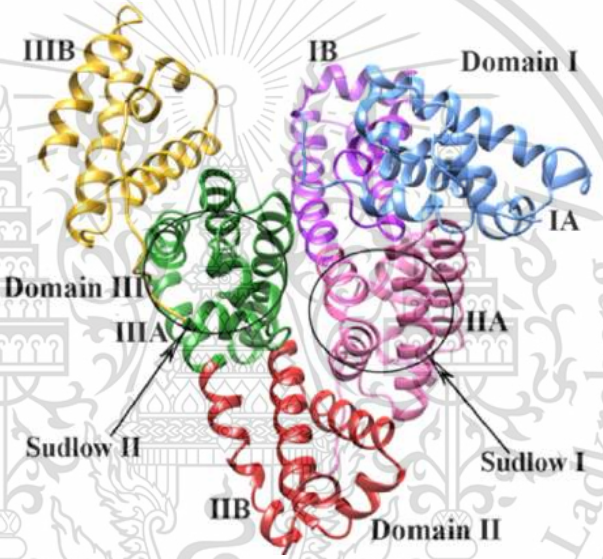

Figure 2.2. The structure of serum albumin representing domains, subdomains, and Sudlow's binding sites I and II [15].

Serum albumin provides the colloid osmotic pressure that regulates passage of water and diffusible solutes through the capillaries. Albumin serves in the transport of fatty acids, hormones, steroids, metals, vitamins, and drugs. Albumin has a negative charge at normal blood pH (7.35 - 7.45), attracts and retains cations, especially Na^+ in the vascular compartment. Because of its negative charge, albumin is also able to furnish some of the anions needed to balance the cations of the plasma [16]. Usually, albumin is not found in urine except in cases of renal dysfunction such as diabetic nephropathy. Diabetic nephropathy refers to kidney disease that is specific

to diabetes. Although kidney biopsy is required to diagnose diabetic glomerulopathy definitively, in most cases, careful screening of diabetic patients can identify people with diabetic nephropathy without the need for kidney biopsy. Diabetic nephropathy is based in part on the finding of elevated urinary albumin excretion, which is divided into: (1) microalbuminuria (the urinary albumin excretion between 30 and 300 mg L^{-1}), a modest elevation of albumin thought to be associated with stable kidney function, and (2) macroalbuminuria (values above 300 mg L^{-1} of albuminuria), a higher elevation of albumin associated with progressive decline in glomerular filtration rate (GFR), an increase in systemic blood pressure, and a high risk of kidney failure [17].

2.2 3D printing technique to fabricate the devices using as part of developed techniques for determination of GABA and albumin [18]

3D printing is technique, also known as additive manufacturing (AM), is a manufacturing process where a 3D printer creates three-dimensional objects by depositing materials layer by layer in accordance to the object's 3D digital model. The AM process begins with a 3D model of the object, usually created by computer aided design (CAD) software or a scan of an existing artifact. Specialized software slices this model into cross-sectional layers, creating a computer file that is sent to the AM machine. The AM machine then creates the object by forming each layer via the selective placement (or forming) of material.

2.2.1 Stereolithography (SLA)

A method and apparatus for making solid objects by successively "printing" thin layers of a curable material, e.g., a UV curable material, one on top of the other. There are two important configurations: free surface approach (bath configuration) and constrained surface approach (bat configuration). In both configurations objects are built in a layer-by-layer manner by spatially controlled photopolymerization of a liquid resin which is performed with either a scanning laser or a digital light projector (DLP). The bath configuration is the classical setup for SLA in which a UV beam traces a 2D cross section onto a substrate submerged in a tank of photoactive resin that polymerizes upon illumination as shown in Figure 2.3. After completion of the 2D cross section, the substrate is lowered further into the resin by

a predefined distance, and the UV beam begins the addition of the next layer, which is polymerized on top of the previous layer. In between layers, a blade loaded with resin levels the surface of the resin to ensure a uniform layer of liquid prior to another round of UV light exposure. In this configuration the height of the printed object is restricted to the tank size. Chemical reactions with ambient air, resin waste and extensive cleaning procedures are serious concern of bottom-up approach.

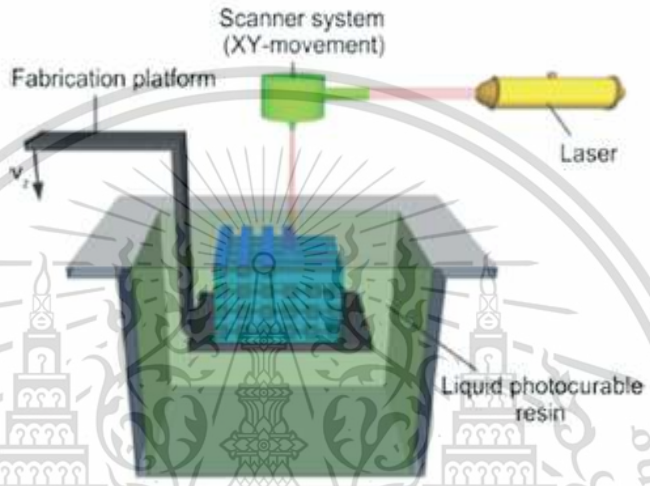

Figure 2.3. SLA printing configurations [19].

2.3 Flow injection system

2.3.1 Flow injection analysis [20]

Flow injection analysis (FIA) is based in sample injection into a flowing carrier stream to which reagents are added at confluence points. In this way, the concentration gradient is formed by dispersion of the sample zone, and the transient signal reflects the gradient of the sample zone, as it passes through the detector. Figure 2.4. shows some of the common components those are used for the various unit operations in the flow-based analytical process, i.e. propulsion, injection, reaction/mixing/modification, detection and data analysis. The assemblage of pumps valves, flow tubes and detector are often referred to collectively as the manifold.

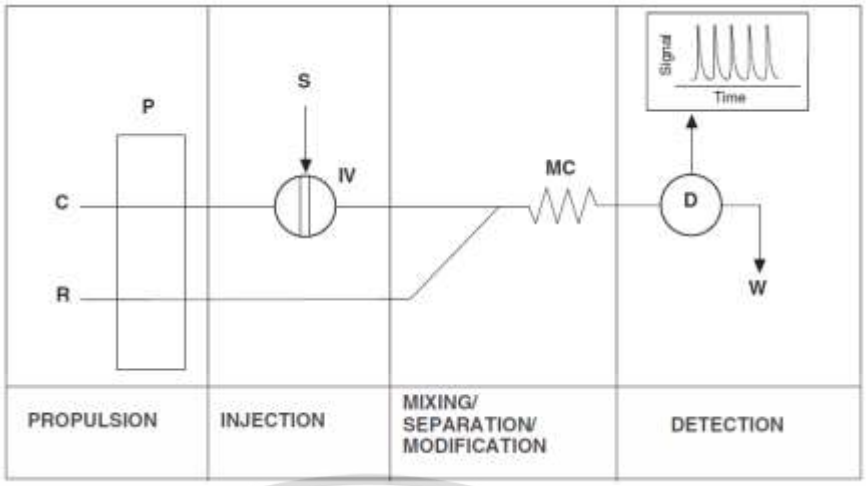

Figure 2.4. Schematic diagram of a simple flow injection analysis (FIA) system [20].

The FIA technique combines several analytical functions into a method performed in a flowing stream, usually under computer control, in a short period of time, with simple and robust hardware, with high precision, with relatively little waste, and covering a broad concentration range. An FIA method can be generally divided into three stages, those were described below.

I. Injection stage: In which the sample is measured and injected into the flowing carrier stream. The device most commonly used to measure and inject the sample into the FIA carrier stream is a two-position six-port commutating sample injection valve, the two positions being commonly termed load and inject.

II. Sample processing stage: In which the analyte is transformed into a species that can be measured by the detector and have its concentration manipulated into a range that is compatible with the detector. Dilution is a very common operation for process FIA and SIA monitors. There are several different ways to perform dilution such as dispersion, electronic dilution, gradient chamber, and membrane sampling, which was employed in many works [1-4, 33] and described in next paragraph.

The use of a membrane sampling device (MSD) for dilution is relatively simple. A donor stream flows on one side of the membrane and an acceptor stream on the other side. The sample is injected into the donor stream and, as the sample segment passes over the membrane, a fraction of it is transported to the acceptor stream. The dilution factor depends on the sample volume injected, the thickness of

the membrane, the surface area of the membrane, the channel dimensions in the MSD, and the flow rates of the two streams.

In addition to dilution, MSDs can be used for other sample processing operations, such as matrix modification, sampling of gas streams, solvent extraction, and analyte enrichment. Two membrane sampling designs that have been used widely differ in the membrane geometry: the parallel plate (or sandwich) design and the tubular design. In the sandwich design (Figure 2.5.), a planar membrane is securely placed between two inert plates. Two carrier lines, i.e. a donor stream and an acceptor stream, pass through the MSD in separate conduits separated by the planar membrane. The donor stream can be either gaseous or liquid, whereas the acceptor stream is liquid. The plates have engraved channels on their surfaces facing the membrane that define the volume for both the donor and acceptor streams. Separate tubing connections at the ends of each channel provide flow in and out for each stream. For gas–liquid separations, the gaseous analyte is introduced by the donor carrier stream into the planar membrane device where it diffuses through the membrane and dissolves into the liquid carrier stream. Only gases that can permeate the membrane and dissolve in the acceptor stream or react chemically with a reagent in the acceptor stream will be transported across the membrane. Hence, the selectivity advantage is dependent primarily on the membrane material. The acceptor stream is pumped through the planar membrane device and then out toward the detector.

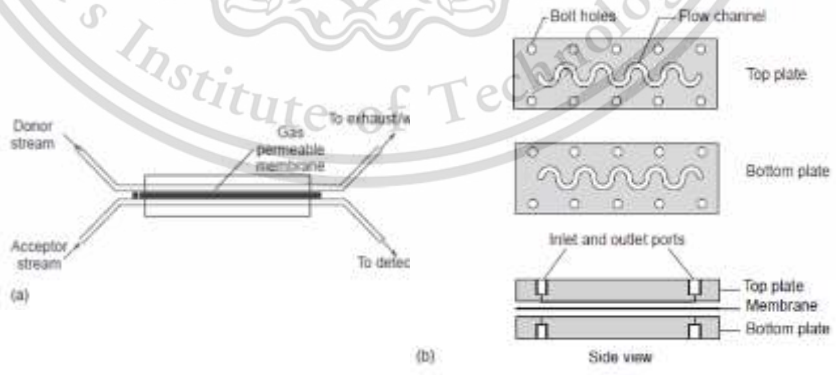

Figure 2.5. (a) Diagram of a parallel-plate membrane sampler for gas–liquid separation (side view). (b) Detailed views of diffusion plates used in the parallel-plate membrane design [20].

III. Detection stage: Where the analyte, or a derivative of it, generates a response that is used for quantitation. A large variety of flow-through detectors are used in FIA, primarily based on ultraviolet–visible optical or electrochemical transducers.

2.3.2 Sequential Injection Analysis [20]

Sequential Injection Analysis (SIA), which is a second generation of FIA, has the primary advantages of simpler and more compact hardware, greater method flexibility, and less waste generation. The SIA technique offers an automated approach to sample handling that enables manual wet chemistry procedures to be executed in a rapid, precise, and efficient manner. Small solution zones are manipulated under controlled dispersion conditions in narrow-bore tubing. It is readily seen that this definition is quite similar to that given above for FIA. SIA does not require an injection valve. Rather, a multi-position valve (MPV) replaces the injection valve, as depicted in Figure 2.6.

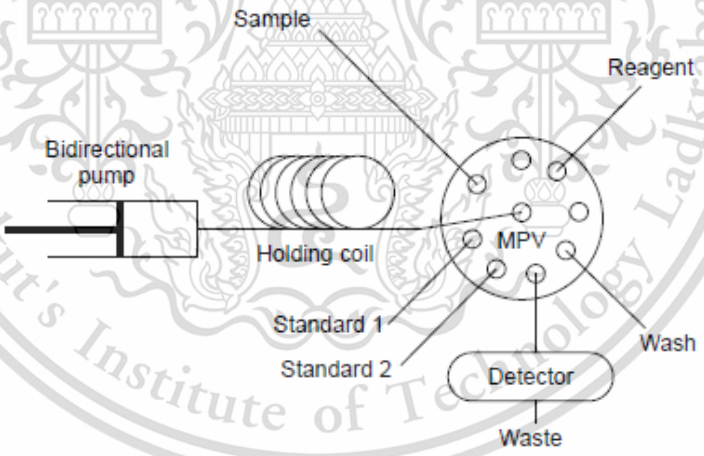

Figure 2.6. Diagram of an SIA manifold [20].

Usually, in SIA system, the peristaltic pump is replaced with a syringe pump and a coil, called the holding coil, is added between the pump and selection valve. To achieve the same measurement as described above for FIA, the syringe is first filled with a carrier solution that contains the reagent. Then the selection valve is advanced to a port that is connected to the sample line. the volume of sample is

precisely drawn into the holding coil. The sample volume is determined by the computerized flow program. The selection valve is then advanced to a port that is connected to the detector, the direction of flow is reversed, and the carrier transports the sample through the reactor to the flow cell of the detector. Again, a detectable species is formed and is registered as a peak by the detector. The concentration of the analyte in the sample is determined in a similar as for FIA.

2.4 Spectrophotometric techniques for determination of GABA and Albumin

2.4.1 UV UV-visible spectrophotometry [21]

UV UV-visible spectrophotometry is a technique that uses the absorbance of light by an analyte (the substance to be analyzed) at a certain wavelength to determine the analyte concentration. UV/VIS (ultra violet/visible) spectrophotometry uses light in UV and visible part of the electromagnetic spectrum. Light of this wavelength is able to affect the excitation of electrons in the atomic or molecular ground state to higher energy levels, giving rise to an absorbance at wavelengths specific to each molecule. Figure 2.7. illustrates the basic structure of spectrophotometers. It consists of a light source, a collimator, a monochromator, a wavelength selector, a cuvette for sample solution, a photoelectric detector, and a digital display or a meter. Detailed mechanism is described below.

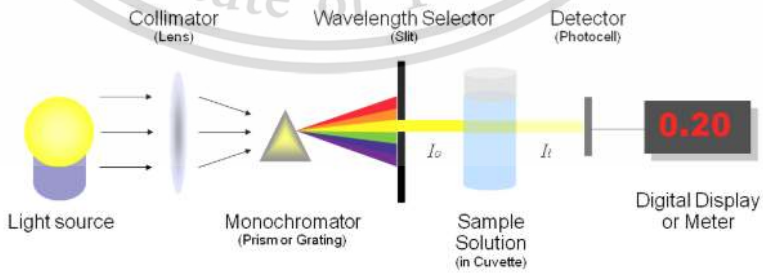

Figure 2.7. Basic structure of spectrophotometers, I_0 is the intensity of the incident light and I_t is the intensity of the transmitted light [22].

When a beam of radiation (light) passes through a substance or a solution, some of the light may be absorbed and the remainder transmitted through the sample. the ratio of the intensity of the light entering the sample (I_o) to that exiting the sample (I) at a particular wavelength is defined as the transmittance (T). The absorbance (A) of a sample is the negative logarithm of the transmittance.

2.4.1.1 Lambert's Law

The proportion of incident light absorbed by a transparent medium is independent of the intensity of the light (provided that there is no other physical or chemical change to the medium). Therefore, successive layers of equal thickness will transmit an equal proportion of the incident energy. Lambert's law is expressed by equation 1.

$$T = \frac{I}{I_0} \quad (1)$$

Where I is the intensity of the transmitted light, I_0 is the intensity of the incident light, and T is the Transmittance.

It is customary to express transmittance as a percentage:

$$\%T = \frac{I}{I_0} \times 100 \quad (2)$$

2.4.1.2 Beer's Law

The absorption of light is directly proportional to both the concentration of the absorbing medium and the thickness of the medium in the light path. A combination of the two laws (known jointly as the Beer-Lambert Law) defines the relationship between absorbance (A) and transmittance (T).

$$A = -\log \frac{I}{I_0} = \log \frac{1}{T} = \varepsilon bc \quad (3)$$

Where A is absorbance (no unit of measurement), ε is molar absorptivity (L^{-1} mol^{-1} cm^{-1}), b is path length (cm) and c is molar concentration (mol L^{-1}).

2.4.2 Fluorescence and chemiluminescence spectroscopies [23]

Fluorescence is photon emission processes that occur during molecular relaxation from electronic excited states. These photonic processes involve transitions between electronic and vibrational states of polyatomic fluorescent molecules (fluorophores). Fluorophores play the central role in fluorescence spectroscopy. Fluorophores are the components in molecules that cause them to fluorescence. Majorly fluorophores are the molecule which contain aromatic rings such as Tyrosine, Tryptophan, Fluorescein etc.

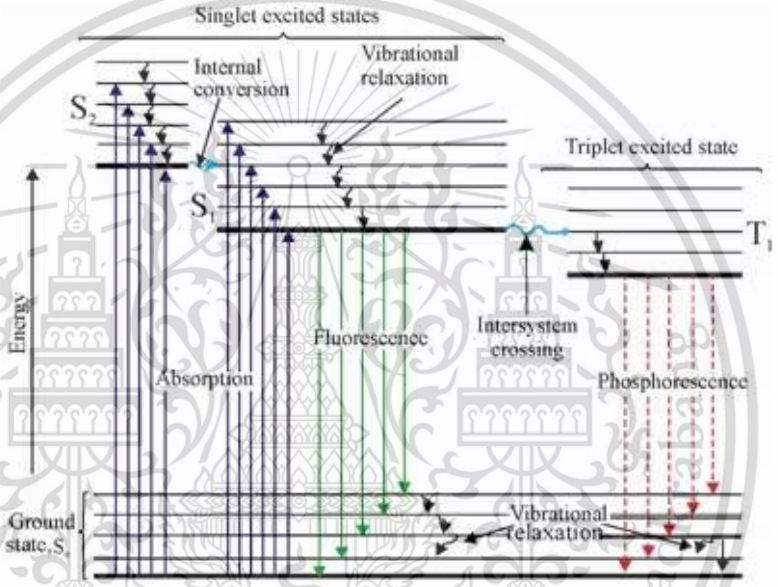

Figure 2.8. Jablonski Diagram [24]

The Jablonski diagram (Figure 2.8.) offers a convenient representation of the excited state structure and the relevant transitions. Molecules that have become electronically excited subsequent to the absorption of visible (400~700 nm), UV (200~400 nm), or NIR (700~1100 nm) radiation. Excitation process to the excited state from the ground state is very fast. After excitation, the molecule is quickly relaxed to the lowest vibrational level of the excited electronic state. This rapid vibrational relaxation process occurs on the time scale of femto seconds to picoseconds. Fluorescence emission occurs as the fluorophore decay from the singlet electronic excited states to an allowable vibrational level in the electronic ground state.

2.4.2.1 Instrumentation of spectrofluorometer [25]

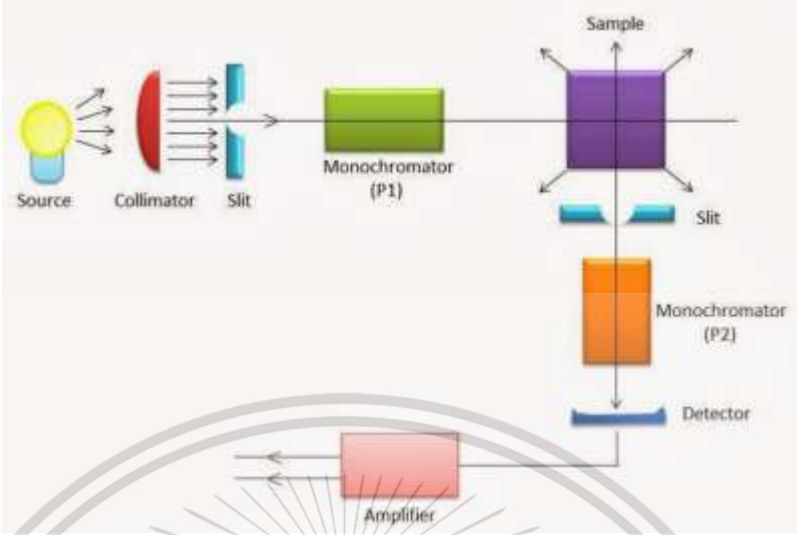

Figure 2.9. Schematic diagram of a spectrofluorometer [26].

A diagram of a typical fluorimeter is shown in Figure 2.9. It consists of a light source, two monochromators, a sample holder and a detector. There are two monochromators, one for selection of the excitation wavelength, another for analysis of the emitted light. The detector is at 90 degrees to the excitation beam. Upon excitation of the sample molecules, the fluorescence is emitted in all directions and is detected by photocell at right angles to the excitation light beam. The lamp source used is a xenon arc lamp that emits radiation in the UV, visible and near-infrared regions. The light is directed by an optical system to the excitation monochromator, which allows either preselection of wavelength or scanning of certain wavelength range. The exciting light then passes into the sample chamber which contains fluorescence cuvette. A special fluorescent cuvette with four translucent quartz or glass sides is used. When the excited light impinges on the sample cell, molecules in the solution are excited and some will emit light. Light emitted at right angles to the beam is analyzed by the emission monochromator. The wavelength analysis of emitted light is carried out by measuring the intensity of fluorescence at preselected wavelength. The analyzer monochromator directs emitted light of the preselected wavelength to the detector. A photomultiplier tube serves as the detector to measure the intensity of the light. The output current from the photomultiplier is fed to some measuring device that indicates the extent of fluorescence.

2.4.2.2 Chemiluminescence (CL) [27]

Chemiluminescence (CL) is defined as the emission of electromagnetic radiation (usually in the visible or near-infrared region) produced by a chemical reaction. In CL, reactions generally yield one of the reaction products in an electronic excited state producing light on falling to the ground state. As can be seen in Figure 2.8., the process of light emission in CL is the same as in photoluminescence, except for the excitation process. In fluorescence and phosphorescence, the electronically excited state is produced by absorption of ultraviolet or visible light, returning to the ground state (S_0) from the lowest singlet excited state (S_1) or from the triplet excited state (T_1) (Figure 2.8.).

1. Luminol-hydrogen peroxide chemiluminescence

In this reaction, a small amount of luminol (3-aminophthalhydrazide or 5-amino-2,3-dihydro- 1,4-phthalazinedione) is dissolved in a basic aqueous solution. To this solution is added a solution of a mild oxidizing agent, which is 0.3% hydrogen peroxide in the demonstration in Figure 2.10. (Bleach is also used in some recipes as the oxidizing agent.) The reaction occurred by the following mechanism.

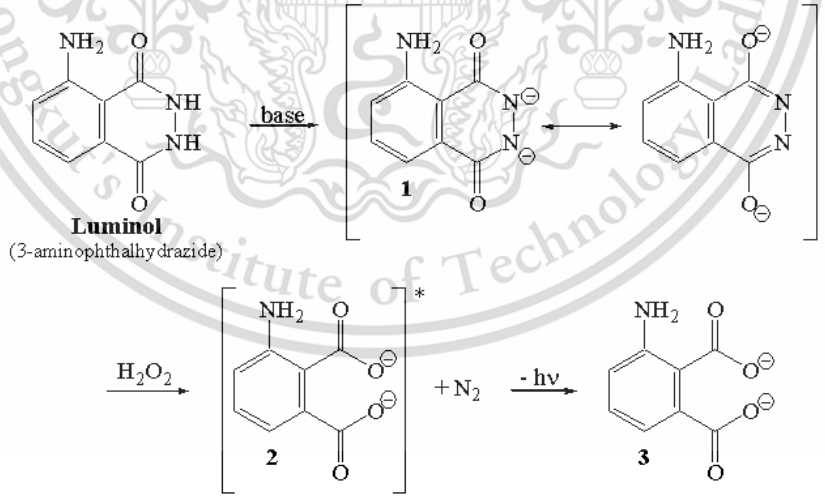

Figure 2.10. The mechanism of the CL reaction between luminol and hydrogen peroxide.

2. The gold nanoparticle- catalyzed luminol-hydrogen peroxide chemiluminescence [10]

The reaction of luminol with hydrogen peroxide in alkaline solution in the absence of a catalyst underwent weak CL, it is assumed that the catalyst gold nanoparticles may interact with the reactants or the intermediates of the reaction of luminol with hydrogen peroxide. When gold nanoparticles were used as the catalysts, epoxidation reactions were also reported to take place on the surface of gold nanoparticles via the reversible generation of O-O bond. In addition, The O-O bond of H_2O_2 might be broken up into double $HO^{\bullet}$ radicals by virtue of the catalysis of gold nanoparticles, and the generated hydroxyl radicals might be stabilized by gold nanoparticles via partial electron exchange interactions. Further electron-transfer processes between $L^{\bullet-}$ and $O_2^{\bullet-}$ radicals on the surface of gold nanoparticles would take place to produce the key intermediate hydroxy hydroperoxide as indicated in Figure 2.11., leading to the enhancement of the CL.

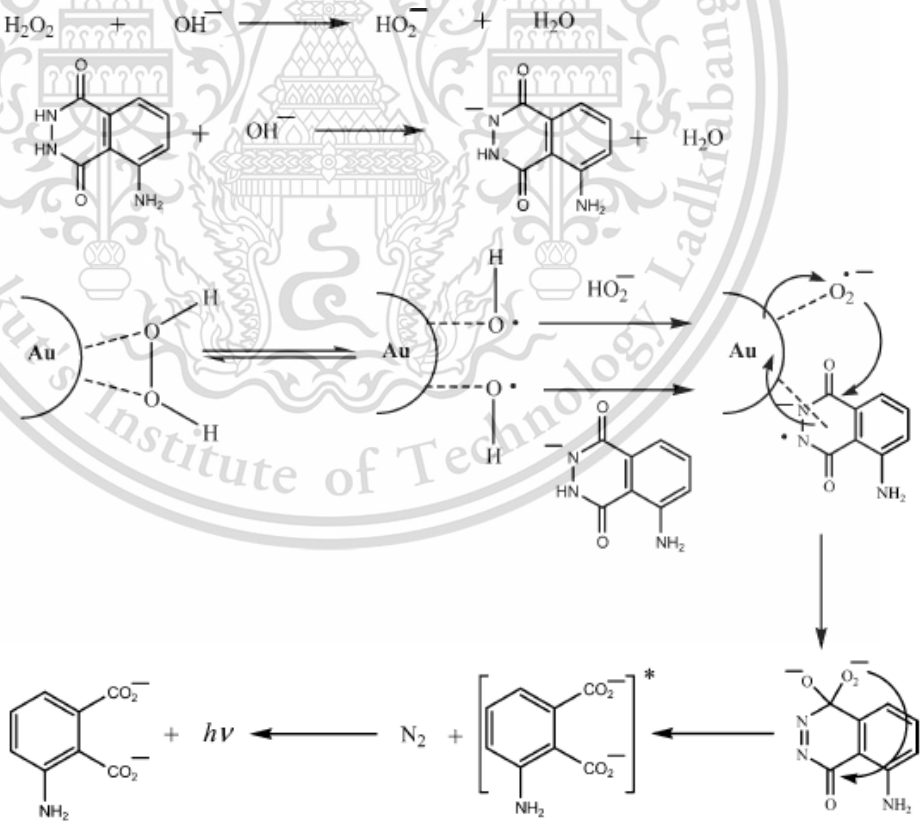

Figure 2.11. Mechanism for the Luminol-H_2O_2-Gold Colloids CL System [10].

2.4.3 Chemistry of detection principles

2.4.3.1 Detection principle for the GABA measurement

The detection reaction for GABA is presented as the following this mechanism which was shown in Figure 2.12.

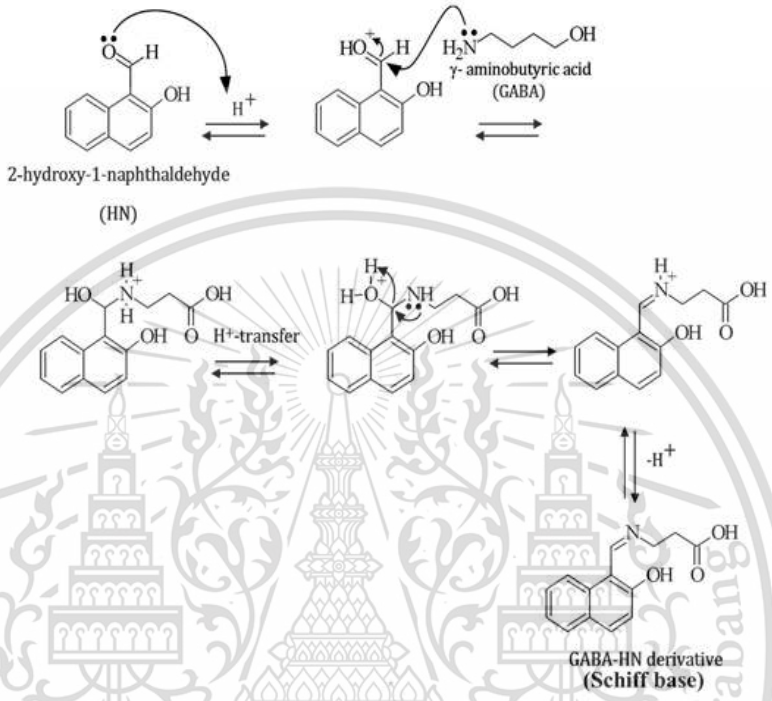

Figure 2.12. Reaction between GABA and 2-hydroxy-1-naphthaldehyde (HN).

The method for derivatization with subsequent colorimetric determination of γ-aminobutyric acid (GABA) is presented. GABA was derivatized with 2-hydroxy-1-naphthaldehyde (6% w/v) in the presence of borate buffer (pH 8.0) and acetonitrile. A maximum absorption wavelength of the derivative was located at 425 nm, this wavelength was employed as a detection wavelength.

2.4.3.2 Detection principle for the albumin measurement

The principle for the determination of albumin is based on chemiluminescence (CL) detection. Gold nanoparticles (AuNPs)-catalyzed luminol chemiluminescence [10] were employed as detection reaction. In the presence of albumin, aggregation of the AuNPs was induced and this inhibited the CL light caused

by the luminol-H_2O_2 system. The proposed mechanism of the interaction between the AuNPs and creatinine is illustrated in Figure 2.13.

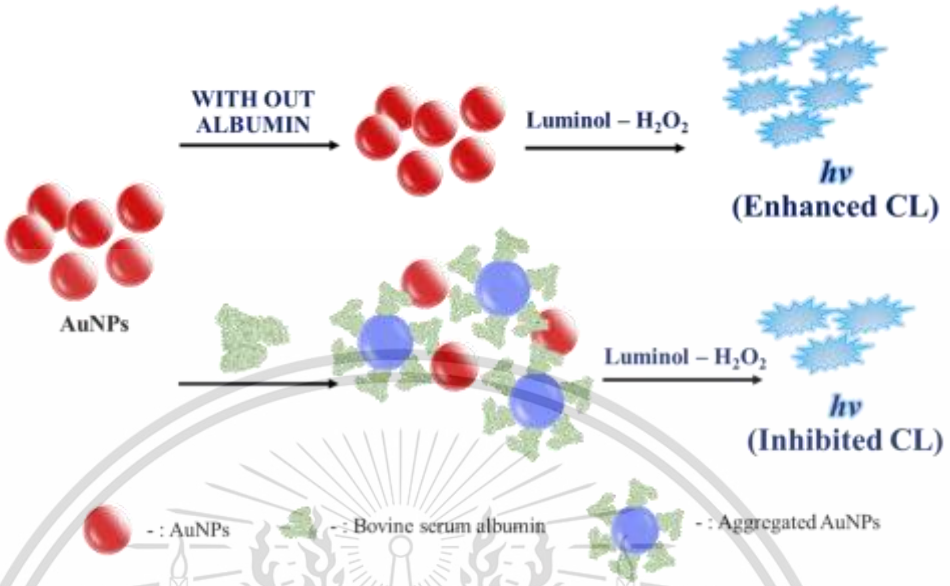

Figure 2.13. Schematic illustration of the proposed mechanism using AuNPs as sensor for the detection of albumin by luminol-H_2O_2 system.

2.5 Literature Reviews

2.5.1 Quantitative analysis of GABA

Khuhawar *et al.* [7] described a method for determination of gamma aminobutyric acid (GABA) in cerebral spinal fluid (CSF) samples with pre-column derivative formation, which used 2-hydroxynaphthaldehyde as a reagent. This method used Phenomenex C_{18}, 5 mm column with methanol: water (62:38 v/v) as the mobile phase and with UV detection at 330 nm. The results showed that all amines and amino acids in the mixture samples did not interfere with the response of GABA. The method provided a linear calibration curve for GABA in the range of 1.2–28.0 mg mL^{-1} with a detection limit of 2.8 ng mL^{-1}.

Hayat *et al.* [28] developed a selective and sensitive HPLC method for separation and quantification of GABA and lysine simultaneously in food samples, especially in cereal seeds. The analytes were determined through a post-column derivatization with 2-hydroxynaphthaldehyde followed by an HPLC analysis. This

technique operated in a reverse phase C-18 column with diode array detector (DAD) at 254 nm. The proposed method provided a linear range of 3.83-34.58 μg mL^{-1} for GABA and 5.16-48.68 μg mL^{-1} for lysine with a correlation coefficient of 0.998 for both standards.

Hayat *et al.* [29] proposed a simultaneous method for separation and quantification of gamma amino butyric acid (GABA) and biogenic amines (BAs) by high performance liquid chromatographic (HPLC). The pre-column derivatization step for both analytes used 2-hydroxynaphthaldehyde as a derivatizing reagent. The derivative was separated in a reversed phase C-8 column with diode-array detection at 230 nm. The method provided a good linear range of 2.25-34.5 mg mL^{-1} for standard GABA and DOP, of 1.15-28.5 mg mL^{-1} for standard PUT, CAD, HIST, and of 2.50-48.5 mg mL^{-1} for standard TYRA, SPD, SPM with a correlation coefficient in the range of 0.997- 0.998.

Tsukatani *et al.* [8] proposed a flow-injection system with immobilized-enzyme reactors to quantify the concentration of γ-aminobutyrate (GABA) and l-glutamate. A co-immobilized glutamate oxidase (l-GOD), a catalase (CAT) reactor, and an immobilized GABase reactor were introduced into the flow-line in series. The concept of this method was to make use of immobilized-enzyme reactors in a single line; the NADPH produced being monitored fluorometrically at 455 nm (excitation at 340 nm). The linear detection range for GABA was 5.0×10^{-6}–5.0×10^{-4} mol L^{-1} and that for l-glutamate was 1.0×10^{-5}–5.0×10^{-4} mol L^{-1}. Ten injections resulted in a relative standard deviation of less than 2% at 0.5 mmol L^{-1} level. The concentrations of both analytes monitored by the developed method agreed well with those obtained by liquid chromatography.

Jinnarak *et al.* [9] developed a sequential injection incorporated with second order scattering (SOS) detection for determination of GABA. The detection relied on the electrostatic attraction between positively charged GABA and negatively charged citrate-capped silver nanoparticles in acetate buffer (pH 3.8) in which the nanoparticles are readily aggregated. When the particle size of agglomerated nanoparticles increases, SOS intensity is enhanced. Concentration of GABA can be quantified by monitoring the relative change in SOS intensity using a

spectrofluorometer. The linear detection range was 100– 400 mg L^{-1} GABA. The detection limit of the method was 39.6 mg L^{-1}.

Horanni *et al.* [30] presented a precise and sensitive HPLC method for the determination of both primary and secondary amino acids in tea including GABA. The separation procedure was performed on a Kinetex C 18 column at 40 °C and 262 nm detection wavelength. The developed method was validated, showing an excellent linearity ($R^2 \geq 0.999$), a high recovery rate (>91%), and low detection and quantification limits (LOD: 0.057-0.534 μg mL^{-1}; LOQ: 0.235-1.849 μg mL^{-1}).

Even though the above-mentioned methods provide high specificity and high accuracy for determination of GABA, those methods require a batchwise procedure for sample preparation which is not practical for analyzing a large number of samples. Therefore, many methods have been developed for solving this problem by on-line sample clean–up for liquid samples. This solution enables a direct analysis of GABA for a large number of samples. These on-line sample clean-up methods are described in the next section.

2.5.2 On-line sample clean-up methods

Nagul *et al.* [31] introduced a flow analysis system for determination of trace-level reactive phosphate in natural water by spectrophotometry. This developed method utilized a polymer inclusion membrane (PIM) for on-line analyte separation and preconcentration. Under optimal FI conditions, the method provided a linear detection range of 0.5 – 1000 μg L^{-1} with a 0.5 μg L^{-1} limit of detection.

G. Giakisikli *et al.* [32] proposed a fully automated sequential injection system for on–line column preconcentration and determination of trace metal ions in biological samples with polyamino-polycarboxylic acid chelating resin (Nobias chelate PA-1) as adsorbent material. This system was successfully demonstrated for vanadium (V (V)), cadmium (Cd (II)) and lead (Pb (II)) determination by electrothermal atomic absorption spectrometry. The chelate complexes of analytes were kept at pH 6.0, while the highest elution effectiveness was observed with 1.0 mol L^{-1} HNO_3 in the revers phase. The detection limits of V (V), Cd (II) and Pb (II) were found to be 3.0, 0.06, and 2.0 ng L^{-1}, respectively, with relative standard deviations ranging from 1.9-3.7%.

In addition, numerous methods employing dialysis membrane as part of a flow system have been reported. A piece of membrane was used to separate low-molecular weight analytes from interfering macromolecules, colloids, and suspended particles in a sample matrix. J.F. van Staden. [1] developed a fully automated flow injection analysis (FIA) procedure for simultaneous determination of sodium, potassium and chloride in blood serum using a single sample injection (100 μL blood serum), where two dialyzers were used in series and the dialyzed components were detected with a flame photometer and UV-vis spectrophotometer (at 485 nm). The presented method provided a high sample throughput of 106 samples per hour.

Silva *et al*. [2] employed an automated sequential injection (SI) system with conductimetric detection for determination of chloride in milk. This system employed a dialysis unit for on-line sample pretreatment, and a sample addition method was used for monitoring the concentration of the analyte in the samples. The linear range of the developed method was $5x10^{-3}$–$1x10^{-2}$ mol L^{-1}, and the detection limit was 2.16 $0.71x10^{-3}$ mol L^{-1} with a relative standard deviation of less than 1.0%.

Staden [33] developed an automated flow injection system for direct measurement of chloride content in milk samples. The on-line sample preparation step utilized a dialysis unit to eliminate interference. The dialysate was monitored with a coated tubular chloride-selective electrode. Under optimal FI conditions, the developed method provided a sample throughput of 120 samples per hour. The calibration curve was linear in the range of 250 – 5000 mg L^{-1} with a 0.50% coefficient of variation or better.

Nacapricha *et al*. [3] developed a simple flow injection (FI) system using iodine-starch reaction to determine iodide concentration in pharmaceutical samples. The idea of the method was that iodide in a sample would be oxidized into iodine, then a gas diffusion unit enabled selective permeation of iodine through a hydrophobic membrane. Finally, detection of iodine exploited the formation of I_3^--starch complex. The method provided a linear curve in the range of 6000–10000 mg L^{-1} and a detection limit of 200 mg L^{-1} with a relative standard deviation of less than 1.44%.

Morais *et al*. [4] evaluated the dialysing yield of membranes with different chemical compositions employed in a sample pre-treatment procedure in a flow

injection system for determination of chloride content in fruit juices. Polyetherimide-composed membranes were selected because they provided high yield, strong analytical signal, low blank signal, and absence of membrane clogging. Under optimal conditions, this method provided a linear calibration curve in the range of 20-250 mg L^{-1} with a relative standard deviation of 1.1 %. The percentage recovery was 102.2.

2.5.3 Quantitative analysis of albumin

Qin *et al.* [34] developed a spectrometric method for determination of total protein in cow milk powder samples. The method utilized nitrophenylfluorone–Mo (VI) as derivatizing agent for reacts with proteins in a Tween 20 microemulsion medium. The linear range for BSA was 0–16 μg mL^{-1}. The recoveries were between 97.6% and 105.8%, and the standard relative deviations were less than 4.3%.

Zhong *et al.* [35] developed a new technique based on enhancement and spectrum change of Rayleigh light scattering (RLS). The technique employed 1,2-dihydroxyanthraquinone-3-sulfonate (Alizarin Red S) at pH = 3.6 as a derivatizing agent that reacted with proteins in samples. The derivative was monitored at wavelength 505 nm. The linear range was 0.20–24.9 μg mL^{-1} for BSA and 0.20–15.5 μg mL^{-1} for HSA. The detection limit (S/N = 3) was 9.59 ng mL^{-1} for BSA and 9.51 ng mL^{-1} for HAS.

Devi *et al.* [36] demonstrated a successful determination of albumin concentration with a voltammetry method, which is a label-free detection of proteins using BSA in the presence of electrochemically formed silver nanostructure (AgNs) on Au substrate modified by a self-assembled monolayer (SAM) of thioctic acid (TA). The linear range was 10^{-4} to 10^{-11} g mL^{-1} with a limit of detection of 50 pg mL^{-1}.

Deftereos *et al.* [37] proposed a flow injection (FI) system for determination of albumin. The developed method was based on a Chemiluminescence (CL) reaction of albumin with potassium permanganate in the presence of polyphosphoric acid (PPA). The calibration curve was linear in the range of 5.00–300 mg mL^{-1} with a detection limit of 4 mg mL^{-1}.

Moreover, nowadays, gold nanoparticles (AuNPs) are the most outstanding metal nanoparticles because of their chemical inertness, easy modification, simple control of particle size, and high extinction coefficient. Many works have investigated conjugation of AuNPs to albumin. Furthermore, some works applied AuNPs as catalyst

for chemiluminescence (CL). Interesting publications on this aspect are briefly described below.

Brewer *et al.* [11] studied the interaction of gold colloids surface with bovine serum albumin (BSA). This reaction was monitored by ζ-potential (surface charge and charge coverage) and quartz crystal microbalance (QCM) measurements. The combination of these two kinds of measurements suggested that BSA binding to gold nanoparticles and gold surface was due to an electrostatic mechanism in the presence of citrate.

Y. Wang and Y. ni [38] studied an interaction between a protein and nanomaterials to better understand protein nanoconjugate. Human serum albumin (HSA) and citrate-capped gold nanoparticles (AuNPs) were utilized as a representative of protein and nanomaterial interaction, which was monitored by UV–vis spectroscopy. HAS molecules were attached to AuNPs surface predominantly as a flat monolayer, forming a stable AuNPs–HSA conjugate with a core–shell structure, the binding process took place mainly through electrostatic and hydrogen-bond interactions between the positive amino acid residues of HAS and the negative carboxyl group of citrate on AuNPs surface.

Iosin *et al.* [39] evaluated the influences of pH and temperature on induction of conformation between Bovine Serum Albumin (BSA) and the surface of gold nanoparticles (AuNPs), which was monitored by UV–vis and fluorescence spectroscopy. the results show that pH had a major impact on the AuNPs–albumin interface, influencing the values of binding and quenching constants as well as the number of binding sites.

Zhang *et al.* [10] reported that different sizes of gold nanoparticles (AuNPs) affected the CL reaction of a luminol-H_2O_2 system differently. The most intensive CL signals were obtained with 38-nm gold nanoparticles. In addition, Organic compounds containing OH, NH_2, and SH groups were found to inhibit the CL signal of luminol-H_2O_2-gold colloids system, which made it applicable for determination of those compounds.

Chapter 3
Research methodology

3.1 Chemicals and apparatus

3.1.1 Chemical

Name	Chemical formula	Purity (%)	Suppliers
γ-aminobutyric acid	$C_4H_9NO_2$	99.0	Aldrich, USA
2-hydroxy-1-naphthaldehyde	$C_{11}H_8O_2$	98.0	Aldrich, USA
Acetonitrile	C_2H_3N	99.5	RCI Labscan, Thailand
Sodium hydroxide	NaOH	98.0	Sigma Aldrich, USA
Glacial acetic acid	$C_2H_4O_2$	99.8	Carlo Erba, Italy
Phosphoric acid	H_3PO_4	85.0	Sigma-Aldrich, USA
Boric acid	BH_3O_3	99.8	Sigma-Aldrich, USA
Trisodium citrate	$Na_3C_6H_5O_7$	-	Sigma-Aldrich, Japan
Tetrachloroauric (III) acid trihydrate	$HAuCl_4.\ 3H_2O$	99.9	Sigma-Aldrich, USA
Hydrochloric acid	HCl	37.0	Carlo Erba, Italy
Nitric acid	HNO_3		Carlo Erba, Italy
Bovine serum albumin	-	-	Thermo Fisher Scientific, USA
5-Amino-2,3-dihydrophthalazine-1,4-dione	$C_8H_7N_3O_2$	97.0	Sigma, USA
Hydrogen peroxide	H_2O_2	-	Merck, Germany

Bis-acylphosphine oxide	$C_{26}H_{27}O_3P$	97.0	Sigma-Aldrich, USA
Acrylonitrile butadiene styrene	$(C_8H_8{\cdot}C_4H_6{\cdot}C_3H_3N)_n$	-	Dynalon, USA
Acetic acid	CH_3COOH	99.8	RCI Labscan, Thailand
Methanol	CH_3OH	99.9	RCI Labscan, Thailand
Vitamin B12	$C_{63}H_{88}CoN_{14}O_{14}P$	98.0	Merck, Germany
Lysine	$C_3H_7NO_3$	90.0	Hidedia, India
Glutamic acid	$C_5H_9NO_4$	99.0	Hidedia, India
Valine	$C_5H_{11}NO_2$	99.0	Hidedia, India
Leucine	$C_6H_{13}NO_2$	99.0	Merck, Germany
Histidine	$C_6H_9N_3O_2$	99.0	Hidedia, India
Arginine	$C_6H_{14}N_4O_2$	99.0	Hidedia, India
Tryptophan	$C_{11}H_{12}N_2O_2$	98.0	Hidedia, India
Phenylalanine	$C_9H_{11}NO_2$	99.0	Hidedia, India
Threonine	$C_4H_9NO_3$	99.0	Hidedia, India
Serine	$C_6H_{14}N_2O_2$	99.0	Hidedia, India
Isoleucine	$C_6H_{13}NO_2$	99.0	Hidedia, India
Aspartic acid	$C_4H_7NO_3$	98.5	Hidedia, India

3.1.2 Apparatus

1) Volumetric flask
2) Erlenmeyer flask
3) Micropipette
4) Beaker
5) Test tube
6) pH meter – FiveEasyPlus™ FEP20, USA
7) Hotplate – IKA® C-MAG HS7, Malaysia
8) Magnetic stirrer - Heidolph, Schwabach, Germany)

9) UV - visible spectrophotometer – Jasco FP-8000, USA

10) 3D printer - KINGS600, China.

11) Deionized water system - ZENEER UP 900, Human Corporation, Korea

13) Centrifuge - Spectrafuge™ Model 6C, USA

14) Cellulose acetate membrane - Metrohm™, UAS

15) High performance liquid chromatograph- Waters, model 486, Italy

17) Transmission electron microscope - FEI-TECNAI T20 G^2, Netherlands

17) Vortex - Scientific Industries, Genie 2, USA

18) Centrifuge - Kubota 3700 micro refrigerated centrifuge, Japan

19) Spectrofluorometer - Jasco, FP-8200, Japan

20) Sequential Injection system

20.1 8-port multi-selection valve - Reno, Nevada, USA

20.2 PSD-4 syringe pump - Reno, Nevada, USA

20.3 Flow cell - Phillips, USA

20.4 PTFE tubing - AG International, JR-T6807-M 25, Switzerland

20.5 Auto-Pret™software - MKG Company, Japan

21) Flow injection system

21.2 6-Port valves - model V-450, USA

21.3 Peristaltic pump – Ismatec®, IS7610, Switzerland

21.4 PTFE tubing - Cole Parmer, USA

21.5 Pump Tubing, 3-Stop - Ismatec®, USA

3.2 Research methodology

3.2.1 Determination of gamma-aminobutyric acid in foodstuff and beverages exploiting a 3D printed dialysis unit and sequential injection

All standards and reagents used were of analytical reagent grade. Deionized-distilled water was used throughout all the experiments.

3.2.1.1 Chemical preparation

1) 2000 mg L^{-1} of GABA standard stock solution

2000 mg L^{-1} of GABA standard stock solution was prepared by dissolving 0.0508 g of solid powder of GABA in 25.00 mL of Britton-Robinson buffer (pH 5.0).

2) Working GABA standard solution

10 mg L^{-1} of albumin standard solution was freshly prepared by pipetting 0.125 mL of the albumin standard stock solution into 25.00 mL volumetric flask and diluting to the mark with Britton-Robinson buffer (pH 5.0). The concentrations of 50, 100, 300, 500, 700, and 1,000 mg L^{-1} were prepared by pipetting 0.625, 1.250, 3.750, 6.250, and 12.500 mL of the albumin standard stock solution, respectively.

3) 3% w/v of 2-hydroxy-1-naphthaldehyde (HN)

3% w/v of 2-hydroxy-1-naphthaldehyde (HN) was prepared by dissolving 0.7508 g of solid powder of HN in 25.00 mL of acetonitrile solution.

4) Britton-Robinson buffer (pH 5.0)

Britton-Robinson buffer (pH 5.0) was prepared by mixing 0.05 mol L^{-1} sodium hydroxide, 0.03 mol L^{-1} acetic acid, 0.03 mol L^{-1} phosphoric acid, and 0.03 mol L^{-1} boric acid. This solution was adjusted to a final pH of 5.0 by using either 0.1 mol L^{-1} of HCl or NaOH.

5) GABA foodstuff and beverages sample

Nine samples of GABA- supplemented tablets/ capsules, germinated brown rice, instant green tea powder and GABA- enriched milk were employed for the method validation. All samples were commercially available in local drug stores and supermarkets in Bangkok, Thailand. These samples were chosen to demonstrate the suitability of the developed method for direct analysis of both solid and turbid liquid samples. The samples were directly transferred into the donor chamber without any sample preparation except for grinding the tablets and rice grains.

3.2.1.2 Experiment

1) Study on detection reaction of GABA using UV - visible spectrophotometer

Aliquot of 1.00 mL of the standard GABA in Britton-Robinson buffer (pH 5.0) was transferred to a 10 mL-volumetric flask. Then, 2 mL of 3% (w/v) HN was added. Acetonitrile was used as diluent to adjust the volume to mark. This solution was incubated overnight in dark at ambient temperature. The derivative was detected at 425 nm via UV-visible spectrophotometer.

2) Fabrication of the 3D printed dialysis unit

The fabrication of the 3D printed dialysis unit is started by a computer-aided design (CAD) was utilized to design this unit, which was shown in Figure 3.1. by SketchUp 8™ software. Then, this image file was converted to an STL file and digitally sliced into multiple 2D layers prior to its export for fabrication by the 3D printer. The 3D printing step, poly (methyl methacrylate) (PMMA), bis-acylphosphine oxide and acrylonitrile butadiene styrene were used as photo-initiator and additive, respectively. After that, curing step an Nd: YVO_4 solid-state laser (355 nm) as the light source and a fixed scanning speed of 10.0 m s^{-1} was employed.

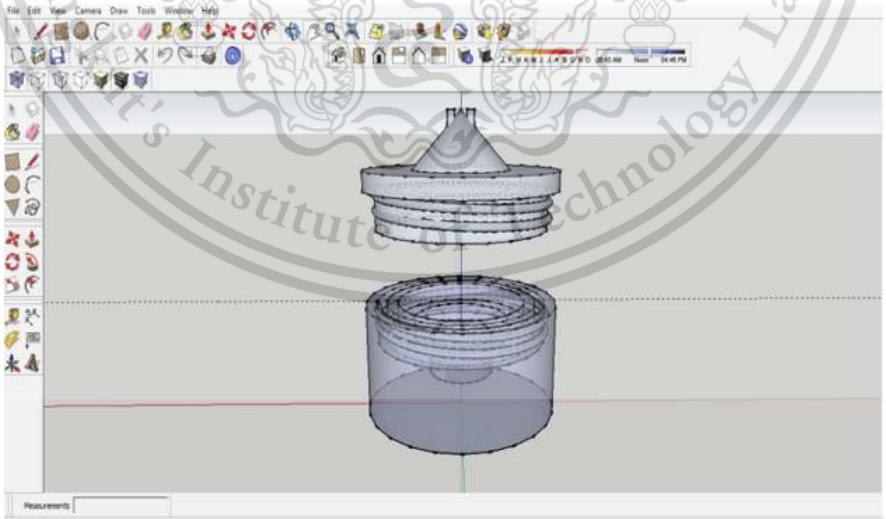

Figure 3.1. Photograph of the screen capture represented the drawing of the 3D printed dialysis unit which is designed by SketchUp 8™ software.

3) The SI system and working flow

The SI system for the automated on-line derivatization and determination of GABA is presented in Figure 3.2. A. PTFE tubing (1.0 mm i.d.) was employed to construct the manifold. The lengths of the holding and the mixing coils were 25 cm and 50 cm, respectively. The SI assembly comprised a PSD-4 syringe pump, equipped with a 12.5-mL glass syringe and an 8-port multi-selection valve. Spectrophotometric detection at 425 nm was carried out using a UV-visible spectrophotometer, which was equipped with a 10-mm flow cell.

The 3D printed dialysis units were integrated into the SI system (see Figure 3.2. A). While dialysis in DU#1 was proceeding, the dialysis procedure for samples in dialysis units, DU#2 to DU#5, was consecutively conducted. This strategy provides more rapid analysis for routine work with a large number of samples.

All the operational sequences of the SI method were controlled using the Auto-Pret™software. Details of the sequence are given in Table 3.1 and Figure 3.2. B. Briefly, the system was prefilled with the carrier (acetonitrile). Aliquots of 25 μL of the dialysate and 30 μL of HN were sequentially aspirated into the holding coil. By reversing the pump flow and selecting the appropriate position of the MV port, the zone of the reaction mixture was propelled to the mixing coil and subsequently to the flow-cell of the spectrophotometer. The absorbance of the derivative was monitored at 425 nm. The entire sequence for the on-line derivatization and absorbance measurement were completed in less than 1.0 min.

Table 3.1 Operational sequence of the SI method for one complete measurement cycle.

Step	SP		Flow rate ($\mu L\ sec^{-1}$)	MV port	Volume (μL)	Action description
	Piston Position	T-way Connection				
1	down	left	400	-	1000	Suction of the carrier into the syringe
2	down	right	10	3[a]	25	Aspiration of the dialysate from the dialysis unit no. 1, (DU#1 in Figure 3.2. A) into the holding coil
3	down	right	10	2	30	Aspiration of the derivatizing solution (HN) into the holding coil
4	up	right	150	1	1055	Propelling the reacted zone through the mixing coil into the detector

[a] the port was consecutively switched to No. 4-7 when the following dialysis units (Figure 3.2. A) were employed.

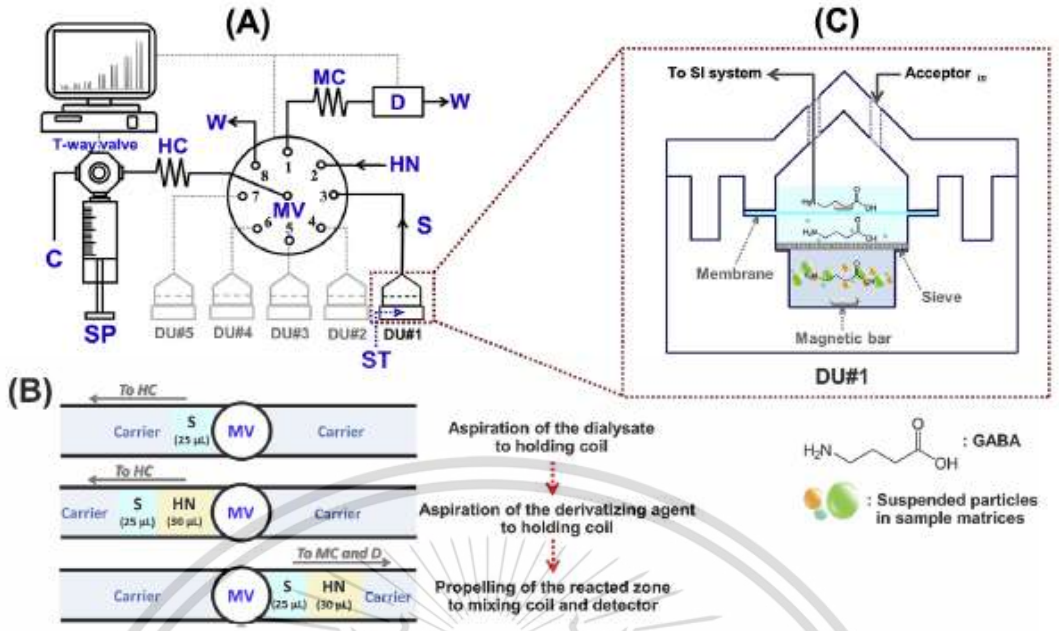

Figure 3.2. (A) The SI system with the 3D printed dialysis unit for automated on-line derivatization and absorbance measurement of derivatized GABA. SP: Syringe pump, MV: 8-port multi-selection valve, D: UV-visible spectrophotometer (λ = 425 nm), ST: Magnetic stirrer, HC: Holding coil (25 cm), MC: Mixing coil (50 cm), DU: an homemade 3D printed dialysis unit, C: Carrier (acetonitrile), S: Dialysate, HN: 3% (w/v) of 2 hydroxy-1-naphthaldehyde in acetonitrile, W: Waste. (B) Schematic of the sequence of the multi-selection valve, direction of carrier flow and the resulting zones of dialysate sample (S) and derivatizing reagent (HN). (C) Schematic drawing of the closed 3D printed dialysis unit showing the position of the stainless steel sieve, the cellulose dialysis membrane, the two magnetic stirring bars, the sample and dialysate solutions and the two narrow vertical vents in the conical section of the lid.

4) Dialysis procedure

The dialysis procedure is started by transferring an accurate weight of the sample powder into the donor chamber and then the small magnetic bar, followed by the stainless steel sieve (30 mm i.d., 0.33 mm thickness). An aliquot of 6.0 mL of Britton-Robinson buffer (pH 5.0) was then added. A cellulose acetate membrane (Metrohm™, 0.2 μm pore size, 30 mm i.d. and 115 μm thickness) was placed between the donor and acceptor chambers. A smaller magnetic bar was placed onto the

membrane (Figure 3.2. C) for homogeneous mixing of the dialysate. The top lid was then screwed on to the body. An aliquot of 1.5 mL of the acceptor solution (Britton-Robinson buffer, pH 5.0) was pipetted into the assembled unit via 'Hole-2' in the lid (Figure 3.2. C). Finally, the dialysis unit was fixed firmly on a magnetic stirrer and connected to the SI system. At exactly 5.0 min after the start of the dialysis process, 25 μL of the dialysate was aspirated into the SI flow-line for on-line derivatization and absorbance measurement. For the milk sample, the experimental procedure is the same as for the solid, but an aliquot of 6.0 mL of a sample solution was pipetted into the donor chamber instead.

5) Optimization of dialysis process conditions

Optimization of the conditions of the dialysis process was performed. The dialysate was processed through the developed SI system and monitored with a spectrophotometer, as shown in Figure 3.2. The sequence of the dialysis process is described in 3.2.1.2 (4), and the measurement procedure is described in section 3.2.1.2 (3).

- Volume of acceptor solution

In this study, standard solutions of GABA (50-1000 mg L^{-1}) and Britton-Robinson buffer (pH 5.0) were employed as the donor and the acceptor solutions, respectively. The effect of the volume of the acceptor was studied with the donor volume kept constant at 6.0 mL (the maximum volume in the donor chamber). This volume of the donor solution allows the donor solution to reach the surface of the hydrophilic membrane in order for dialysis to take place. The investigated acceptor solution volumes were 1.5, 2.0, 3.0, 4.0, 5.0, and 6.0 mL.

- Dialysis time

The dialysis time is defined as the time interval from the start of stirring of the sample solution in the donor chamber until it is stopped. The effect of dialysis time was studied using 6.0 mL of calibrators (50-1000 mg L^{-1} GABA) and 1.5 mL of Britton-Robinson buffer (pH 5.0) as the donor and acceptor solutions, respectively. The investigated dialysis times were 1, 3, 5, 8, and 10 min.

- Stirring speed

The effect of stirring speed was examined using 6.0 mL of 200 mg L^{-1} GABA, 1.5 mL of Britton-Robinson buffer (pH 5.0) acceptor solutions, and 3 min of dialysis time. The investigated stirring speed were 440, 880, 1320, 1760, and 2200 min.

6) Factors affecting the derivatization reaction

Factors affecting the derivatization reaction in a dialysis unit were optimized. The dialysate was processed through the developed SI system and monitored with a spectrophotometer, as shown in Figure 3.2. The sequence of the dialysis process is described in 3.2.1.2 (4), and the measurement procedure is described in section 3.2.1.2 (3).

- Effect of pH of acceptor solution

Since the reaction between GABA (a primary amine) and HN (an aldehyde) is a pH dependent reaction, the dependence needed to be studied. Therefore, the acceptor solution was adjusted to various pH: 1, 2, 3, 4, 5, 6, 8, and 10 and investigated under the following conditions: 6.0 mL of calibrator at various concentrations (50-1000 mg L^{-1} GABA), 3 min of dialysis time, 1.5 mL of acceptor solution, and 1760 rpm of stirring speed.

- Concentration of 2-hydroxy-1-naphthaldehyde (HN)

The effect of concentration of 2-hydroxy-1-naphthaldehyde (HN) on sensitivity was studied using 6.0 mL of calibrator at various concentrations (50-1000 mg L^{-1} GABA), 1.5 mL of Britton-Robinson buffer (pH 5.0) as donor and acceptor solutions, 3 min of dialysis time, and 1760 rpm of stirring speed. The investigated concentrations of HN were 0.3, 0.6, 1.5, 3.0, 4.5, and 6% w/v.

7) Optimization of the SI system

Optimization of the SI system was performed. The dialysate was processed through the developed SI system and monitored with a spectrophotometer,

as shown in Figure 3.3. The sequence of dialysis process is described in section 3.2.1.2 (4), and the measurement procedure is described in section 3.2.1.2 (3).

- Aspirated volume

The effect of aspirated volume of the dialysate on sensitivity was studied using 6.0 mL of calibrator at various concentrations (50-1000 mg L^{-1} GABA), 1.5 mL of Britton-Robinson buffer (pH 5.0) as donor and acceptor solutions, 3 min of dialysis time, and 1760 rpm of stirring speed, while the volume of 3% w/v HN in the flow-line was kept fixed at 30 μL.

- Mixing coil length

The effect of mixing coil length on sensitivity was studied using 6.0 mL of calibrator at various concentrations (50-1000 mg L^{-1} GABA), 1.5 mL of Britton-Robinson buffer (pH 5.0) as donor and acceptor solutions, 3 min of dialysis time, 1760 rpm of stirring speed, 3% w/v of HN, and 25 μL of dialysate. The investigated mixing coil lengths were 0, 50, 100, 200, 300, and 400 cm.

- Dispensing flow rate

The effects of dispensing flow rate on sensitivity and sample throughput was studied using 6.0 mL of calibrator at various concentrations (50-1000 mg L^{-1} GABA), 1.5 mL of Britton-Robinson buffer (pH 5.0) as donor and acceptor solutions, 3 min of dialysis time, 1760 rpm of stirring speed, 3% w/v of HN, and 25 μL of dialysate. The investigated dispensing flow rates were 25, 50, 75, 100, 120, and 150 μL sec^{-1}.

8) Effects of coexisting interfering species

Some compounds that were found in the samples, including milk, rice, and tea that might cause interference with this method were selected and studied using 50 mg L^{-1} GABA. The tolerance limit was the maximum concentration of the spiked compound, i.e., the maximum concentration that would result in a measured GABA absorbance that did not lie outside the range of mean± 3SD of the absorbance value of the standard 50 mg L^{-1} GABA. The investigated compounds were vitamin B12,

lysine, glutamic acid, valine, leucine, histidine, arginine, tryptophan, phenylalanine, threonine, serine, isoleucine, and aspartic acid. Those were studied in a dialysis unit. The dialysate was processed through the developed SI system and monitored with a spectrophotometer, as shown in Figure 3.2. The sequence of dialysis process is described in section 3.2.1.2 (4), and the measurement procedure is described in section 3.2.1.2 (3).

9) Validation

- Accuracy

Accuracy was determined as percentage analytical recovery (%). Percentage recovery was calculated by equation 3.1.

$$\%\, recovery = \frac{spiked\ sample - sample}{standard} \times 100 \quad (3.1)$$

Where: Spiked sample is the concentration of GABA found in sample that spiked with the standard of GABA solution of 50 mg L^{-1} by adding into the donor chamber of 3D printed dialysis unit. Sample is the concentration of the GABA samples, including GABA-supplemented tablets/capsules, grains of germinated brown rice, instant green tea powder and GABA-enriched milk. Standard is the standard of GABA solution of 50 mg L^{-1}.

- Precision

% RSD was considered for precision of the method. The reproducibility was studied by a series of ten repetitive measurements of 500 mg L^{-1} of standard GABA. Calculation of *% RSD was done according* to equation 3.2 below,

$$\%\, RSD = \frac{SD}{\bar{X}} \times 100 \quad (3.2)$$

where SD is the standard deviation of ten replicates,

$\bar{x}$ is the mean of ten replicates.

10) HPLC measurement

A reversed-phase HPLC method [7] was employed as a comparison method. Nylon membrane filter (0.45-μm) was used throughout. The steps for the sample preparation were as follows:

1) GABA-supplemented powder: 0.3182 g of GABA-supplemented powder was dissolved in 25.0 mL of DI water. The solution was centrifuged at 1500 rpm for 10 min and the supernatant was filtered.

2) Germinated brown rice [40]: the germinated brown rice, 0.2534 g of ground sample was added to 800 mL of 70 % (v/v) ethanol. The solution was vortexed mixed for 1 min at ambient temperature and then centrifuged at 14000 rpm (4 ^{o}C) for 10 min and the supernatant was filtered.

3) Instant green tea powder: instant green tea powder, 3.0823 g of sample was infused with 100.0 mL of water (60 ^{o}C). The solution was cooled down to the ambient temperature prior to being was filtered.

4) GABA-enriched milk [41]: GABA-enriched milk, 4.0 mL of the sample was acidified by adding 2.5 mL of 3% (v/v) acetic acid. The solution was vortexed and kept for 15 min before centrifuging at 1500 rpm for 10 min, and the supernatant filtered.

Batchwise derivatization was performed by pipetting either 1.0 mL of GABA standard solution or the final filtered supernatant of a sample into a 5.0-mL glass vial. Aliquots of 0.6 mL of borate buffer (pH 8.0) and 2.0 mL of HN (0.3 % w/v in methanol) were added. The solution was vortexed and heated at 80 ^{o}C for 10 min using a heated bath. The mixture was cooled down before adjusting to the final volume of 10.0 mL with methanol. The solution was injected into the HPLC system using the following conditions: injection volume of 5 μL, guard column (C18, 20 mm x 3.9 mm i.d.), analytical column (Phenomenex C18, 150 mm x 4.6 mm i.d., 5 μm particle), mobile phase of methanol-water at 60:40 (v/v) at flow rate of 1.0 mL min^{-1} (isocratic elution) and detection wavelength of 330 nm.

3.2.2 Flow-based systems with 3D printed flow cells for quantitative measurement of Albumin in urine based on using the AuNPs-catalyzed chemiluminescence detection

All standards and reagents used were of analytical reagent grade. Deionized-distilled water was used throughout all the experiments. All glassware in the experiments were soaked in 10 % (v/v) of nitric acid and rinsed thoroughly with distilled water prior to use.

3.2.2.1 Chemical preparation

1) 100 mg L^{-1} of Albumin standard stock solution

100 mg L^{-1} of albumin standard stock solution was prepared by dissolving 0.0250 g of solid powder of albumin in 250.00 mL of water which was adjusted pH to 6.0 with 0.01 mol L^{-1} HCl then standard stock solution was kept at 4°C.

2) Working Albumin standard solution

0.1 mg L^{-1} of albumin standard solution was freshly prepared by pipetting 0.025 mL of the albumin standard stock solution into 25.00 mL volumetric flask and diluting to the mark with water (pH 6.0). The concentrations of 1, 10, 30, 50, and 70 mg L^{-1} were prepared by pipetting 0.25, 2.50, 7.50, 12.50, and 17.50 mL of the albumin standard stock solution, respectively.

3) 0.1 mol L^{-1} of sodium hydroxide

0.1 mol L^{-1} of sodium hydroxide was prepared by dissolving 1.00 g of sodium hydroxide in 250.00 mL of DI water.

4) 1.0×10^{-2} mol L^{-1} of luminol

A 1.0×10^{-2} mol L^{-1} stock solution of luminol sodium salt (3-Aminophthalhydrazide) was prepared by dissolving 0.17716 g of luminol in 100.0 mL of 0.10 mol L^{-1} sodium hydroxide solution.

5) 0.15 mol L^{-1} of hydrogen peroxide

0.15 mol L^{-1} of H_2O_2 was daily prepared by dilution 3.83 mL of 30% (v/v) H_2O_2 then made up with water to 250.0 mL.

6) 1.0 mmol L^{-1} of standard tetrachloroauric acid

1.0 mmol L^{-1} of tetrachloroauric acid solution was prepared by dissolving 0.0394 g of tetrachloroauric (III) acid trihydrate in 100.00 mL of DI water.

7) 38.8 mmol L^{-1} of trisodium citrate

38.8 mmol L^{-1} of sodium citrate was prepared by dissolving 0.5706 g of trisodium citrate dehydrate in 50.00 mL of DI water.

8) Urine sample Urine sample

Urine samples were collected from healthy volunteers. After filtration through a 0.45-μm cellulose membrane filter, 5 mL of sample was pipetted into a 10.0 mL volumetric flask and then made up with water.

3.2.2.2 Experiment

1) Synthesis of gold nanoparticle

AuNPs were prepared by modified procedure of Turkevich's method [42]. 100.0 mL of 1 mmol L^{-1} chloroauric acid ($HAuCl_4 \cdot H_2O$) was heated to 95^{o}C and stirred vigorously. Then, 7 mL of 38.8 mmol L^{-1} of trisodium citrate solution was immediately added. The color of the solution was changed from pale yellow to deep red. This mixture was further boiled for 10 min and was cooled to room temperature. The as-prepared AuNPs colloidal was kept at 4^{o}C overnight before using.

2) Characterization of AuNPs

- UV-vis spectroscopy

Two mL of AuNPs was transferred into a quartz cuvette, then the absorption spectrum was scanned with a UV-vis spectrophotometer in the wavelength range of 400 - 800 nm

- **Transmission electron microscopy**

Ten μL of AuNPs was dropped onto a copper grid and the excess was wiped off, and the grid was then left to dry overnight. Then, the morphology of the prepared copper grid was observed under a transmission electron microscope.

3) Fabrication of the 3D printed flow cell

The 3D printed flow cell was designed in two different types for two different options, namely flow cell prototype I and II. Prototype I was used as detection flow cell as shown in Figure 3.3 and prototype II was utilized for on-line detection of albumin as presented in figure 3.4.

A computer-aided design (CAD) was utilized to design the flow cell by SketchUp 8™ software, as shown in Figure 3.3 (A) and 3.4 (A). This image file was converted to an STL file and digitally sliced into multiple 2D layers prior to its export for fabrication by the 3D printer. Poly (methyl methacrylate) (PMMA), bis-acylphosphine oxide and acrylonitrile butadiene styrene were used as photo-initiator and additive, respectively. For curing step an Nd: YVO_4 solid-state laser (355 nm) was used as the light source and a fixed scanning speed of 10.0 m s^{-1} was employed. The design and the photograph of the 3D printed flow cell are depicted in Figure 3.3. and 3.4, respectively.

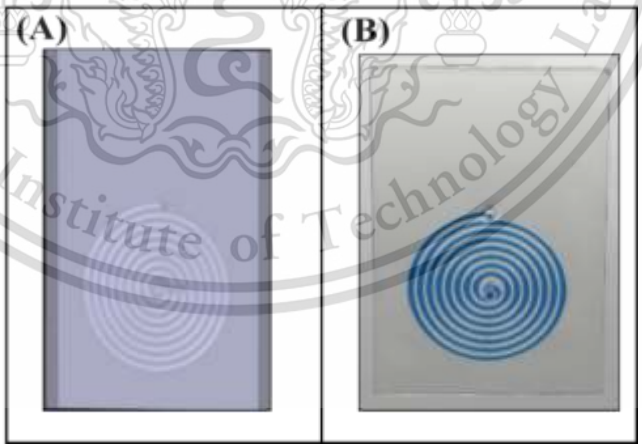

Figure 3.3. The flow cell prototype I: (A) photograph of the screen capture represented the drawing of the flow cell which is designed by SketchUp 8™ software and (B)

Photograph of the homemade 3D printed flow cell. Note: In Figure 3.4 (B), the flow cell was filled with blue dye solution.

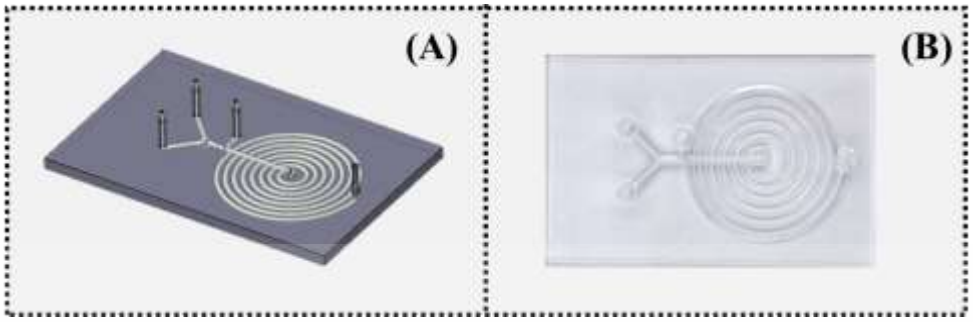

Figure 3.4. The flow cell prototype II: (A) photograph of the screen capture represented the drawing of the flow cell which is designed by SketchUp 8^{TM} software and (B) Photograph of the homemade 3D printed flow cell.

4) Study on aggregation of AuNPs by albumin using UV - visible spectrophotometer

Aliquot of 2.00 mL of the AuNPs was transferred into a 10-mm pathlength quartz cuvette. Then, 0.2 mL of 0.1 mg L^{-1} of standard albumin was added. This solution was shacked for 5 min. The spectrum of mixture was monitored from 400 to 800 nm. Other standard albumin concentrations (1, 10, 30, 50, and, 70 mg L^{-1}) were monitored with the same procedure.

5) Effect of incubation time on AuNPs aggregation by albumin

Incubation time was defined as the period of time that the solution was kept after standard albumin and AuNPs were mixed and before albumin detection. This effect was investigated with various concentrations of AuNPs: 1.42, 2.57, 4.30, and 8.38 nmol L^{-1}, while the standard albumin concentration was fixed at 10 mg L^{-1}. The procedure started by transferring an aliquot of 2.00 mL of 1.42 nmol L^{-1} AuNPs into a quartz cuvette. Then, 0.2 mL of 10 mg L^{-1} standard albumin was added. The mixture was incubated from 1 to 60 min. The absorption spectra from 400 to 800 nm was scanned every 1 min for 1 to 30 min of incubation time, then the measurement frequency was changed to every 5 min for incubation time from 30 to 60 minutes. This procedure was applied with all other investigated AuNPs concentrations.

6) The FI system and working flow

- FI system and working flow of flow cell prototype I

The FI system for determination of albumin in urine using 3D printed flow cell prototype I is presented in Figure 3.5. PTFE tubing (1.0 mm i.d.) was used throughout. An Ismatec peristaltic pump was used for driving reagents. Two 6-Port valves, depicted as V_1 and V_2, were used for injection of luminol and mixture solution between AuNPs and std. albumin/urine, respectively. The 3D-printed spiral flow cell was attached in front of PMT in a Jasco spectrofluorometer for monitoring of the light intensity (425 nm). 1 x 10^{-2} mol L^{-1} luminol was injected via V_1 into the stream of 0.1 mol L^{-1} of NaOH. The injectate was merged with the H_2O_2 steam. The standard albumin or sample was off-line mixed with AuNPs (10 min) before injection through V_2.

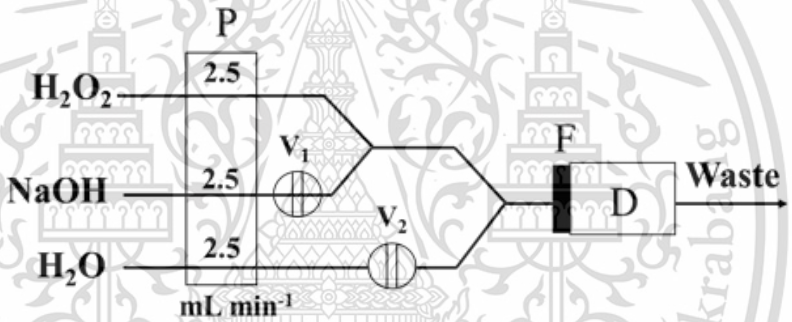

Figure 3.5. A schematic diagram of the FI system for determination of albumin based on the AuNPs-catalyzed reaction between luminol-H_2O_2. P; peristaltic pump, V; 6-Port injection valves, F; the 3D-printed spiral flow cell, D; spectrofluorometer

- Flow-based system and working flow of flow cell prototype II

The developed FI system is combined with flow injection system and sequential injection system for on-line detection of albumin. This developed FI system was presented in figure 3.6.

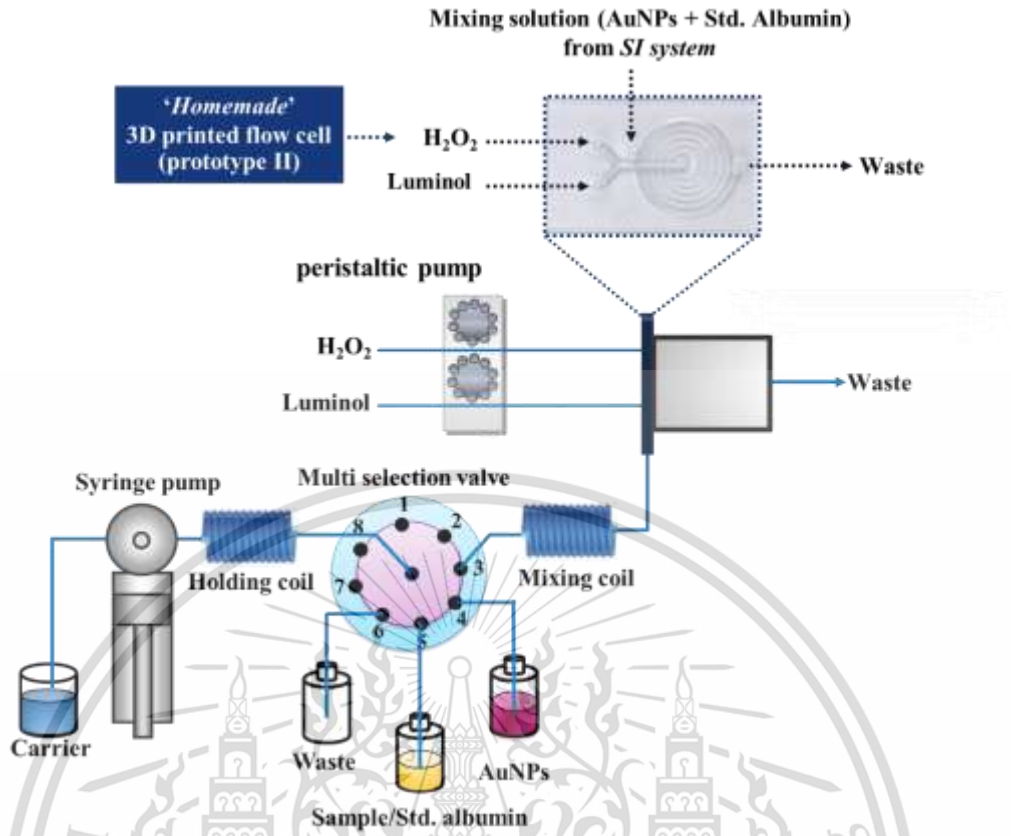

Figure 3.6. The developed flow-based system was combined with FI and SI system for automated on-line derivatization and chemiluminescence (CL) detection using the 3D printed detection flow cell prototype II.

The developed flow system was presented in Figure 3.6. In flow injection part, the PTFE tubing (1.0 mm i.d.) was used throughout. An Ismatec peristaltic pump was used for driving luminol and H_2O_2 solution through the 3D-printed flow cell prototype II, which was attached in front of PMT in a Jasco spectrofluorometer for monitoring of the light intensity (425 nm). The steam of 1 x 10^{-2} mol L^{-1} luminol in 0.1 mol L^{-1} of NaOH was merged with the H_2O_2 steam in flow cell and reacted with on-line mixing solution of standard albumin or sample with AuNPs from SI system.

The SI system was utilized for the automated on-line derivatization of albumin and AuNPs. In Figure 3.6., the PTFE tubing (1.0 mm i.d.) was employed to construct the manifold. The lengths of the holding and the mixing coils were 25 cm and 250 cm, respectively. The SI assembly comprised a PSD-4 syringe pump, equipped with a 12.5 mL glass syringe and an 8-port multi-selection valve. All

the operational sequences of the SI method were controlled using the Auto-Pret™software. Details of the sequence are given in Table 3.2 and Figure 3.6. Briefly, the system was prefilled with the carrier (water). Aliquots of 1000 μL of the AuNPs solution and 100 μL of sample/std. albumin were sequentially aspirated into the holding coil and incubated for 3 min. By reversing the pump flow and selecting the appropriate position of the MV port, the zone of the reaction mixture was propelled to the mixing coil and subsequently to the 3D printed flow cell.

Table 3.2 Operational sequence of the SI system for one complete measurement cycle.

Step	SP		Flow rate ($\mu L\ sec^{-1}$)	MV port	Volume (μL)	Action description
	Piston Position	T-way Connection				
1	down	left	400	-	1000	Suction of the carrier into the syringe
2	down	right	10	4	1000	Aspiration of the AuNPs solution
3	down	right	10	5	100	Aspiration of the sample / std. albumin into the holding coil
4	-	-	-	-	-	Incubated the mixing solution in holding coil for 3 min
4	up	right	25	3	2100	Propelling the reacted zone through the mixing coil into 3D printed flow cell

[a] the port was consecutively switched to No. 1,2,7 and 8 for other samples/Std. albumin.

7) Optimization of flow system

Optimization of the FI system was performed, as shown in Figure 3.5. The sequence of measurement is described in section 3.2.2.2 (6).

- Effect of sample volume

Sample volume was defined as the volume of a mixture of AuNPs and standard albumin. Various sample volumes were investigated: 100, 200, 300, 400, 500, 550, and 600 μL, while the volume of luminol was fixed at 400 μL.

- Effect of flow rate

The effects of flow rate on sample throughput and sensitivity were investigated. The investigated flow rates were 1, 1.5, 2, 2.5, and 3 mL min^{-1}, while the volume of luminol was fixed at 400 μL, and the volume of sample was fixed at 500 μL.

- Effect of concentration of AuNPs

The effect of AuNPs concentration on sensitivity was investigated. The investigated AuNPs concentrations were $5.88x10^{-10}$, $1.42x10^{-9}$, $2.57x10^{-9}$, $4.30x10^{-9}$, $8.38x10^{-9}$, and $9.72x10^{-9}$ mol L^{-1}, while the volume of luminol was fixed at 400 μL and the sample volume was fixed at 500 μL. The flow rate of every line stream in this FI system was 2.5 mL min^{-1}.

- Effect of concentration of luminol

The effect of AuNPs concentration on sensitivity was investigated. The investigated luminol concentrations were 0.1, 1, 10, 100 and 1000 mmol L^{-1}, while the volume of luminol was fixed at 400 μL, the concentration of AuNPs was fixed at 1.42 nmol L^{-1} and the sample volume was fixed at 500 μL. The flow rate of every line stream in this FI system was 2.5 mL min^{-1}.

8) Effect of flow cell design

The effect of regarded in term of flow cell was investigated. Both designs were utilized for determination of the std. albumin in range of 0.1-70 mg L^{-1} and the sensitivity of each design will be compared.

- Flow cell prototype I

The optimization of the FI system was performed, as shown in Figure 3.5. The sequence of measurement is described in section 3.2.2.2 (6), while the concentration of luminal was fixed at 0.01 mol L^{-1}, the volume of luminol was fixed at 400 μL, the concentration of AuNPs was fixed at 1.42 nmol L^{-1} and the sample volume was fixed at 500 μL. The flow rate of every line stream in this FI system was 2.5 mL min^{-1}.

- Flow cell prototype II

The developed FI system was performed, as shown in Figure 3.6. The sequence of measurement is described in section 3.2.2.2 (6), while the concentration of luminal was fixed at 0.01 mol L^{-1} in 0.1 mol L^{-1} of NaOH, the concentration of AuNPs was fixed at 1.42 nmol L^{-1} and the concentration of H_2O_2 was fixed at 0.15 mol L^{-1}.

9) Validation

- Accuracy

Accuracy was regarded in term of percentage analytical recovery. A spiked sample solution was prepared by pipetting 9.00 mL of urine sample into a 10.00 mL volumetric flask, followed by an addition of 1 mL of 100 mg L^{-1} albumin standard solution. A sample solution was prepared by pipetting 9.00 mL of urine sample into a 10.00 mL volumetric flask and diluted it to the mark with DI water. Standard albumin concentrations of 1, 10, 30, 50, and 70 mg L^{-1} were prepared by pipetting 0.1, 1.00, 3.00, 5.00, and 7.00 mL of the albumin standard stock solution into a 10-ml volumetric flask and diluted it to the mark with DI water. The detection process of all prepared solutions is described in section 3.2.2.2 (6).

- Precision

% RSD was considered for precision of the method. The reproducibility was studied by a series of ten repetitive measurements of 30 mg L^{-1} albumin. Calculation of *% RSD was done according* to equation 3.2

- LOD and LOQ [43]

The limit of detection (LOD) and the limit of quantitation (LOQ) were calculated by calibration curve method using the following equations:

$$LOD = y_B + 3S_B \quad (3.3)$$

$$LOQ = y_B + 10S_B \quad (3.4)$$

Where y_B is intercepts of regression line and S_B is standard deviation of intercepts of regression line.

Chapter 4
Results and Discussion

4.1 Determination of gamma-aminobutyric acid in foodstuff and beverages exploiting a 3D printed dialysis unit and sequential injection

In this work, a direct analysis method using a newly designed 3D printed dialysis unit and sequential injection analysis (SIA) for spectrophotometric determination for determination of GABA in both liquid and solid samples was developed. In this chapter shown the results of optimization conditions, method validation, and the application of the developed system to GABA supplemented products and beverages.

4.1.1 Study on detection reaction of GABA using UV–visible spectrophotometer

In this study, the association reaction between gamma-aminobutyric acid (GABA) in Britton-Robinson buffer (pH 5.0) and 2-hydroxy-1-naphthaldehyde was chosen as detection reaction. The chemical reactions can be written as the following equations, which was presented in Figure 4.1.

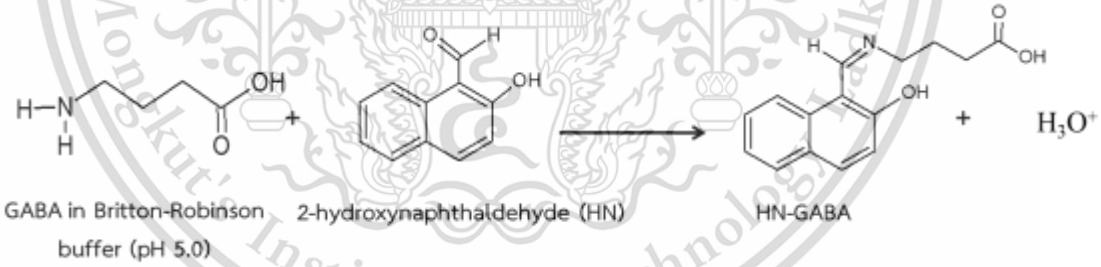

Figure 4.1. Imine reaction between GABA and HN was exploited as derivatization reaction.

The derivatization process is also carried out under mild condition without heating. The problem risen from air bubble produced by heating which has been always found in flow analysis is therefore ignorable. We also found by the batchwise experiment that the sensitivity obtained by our derivatization method is greater than that of the other derivatization conditions as employed by the other works in literatures [7] (See Figure 4.2.).

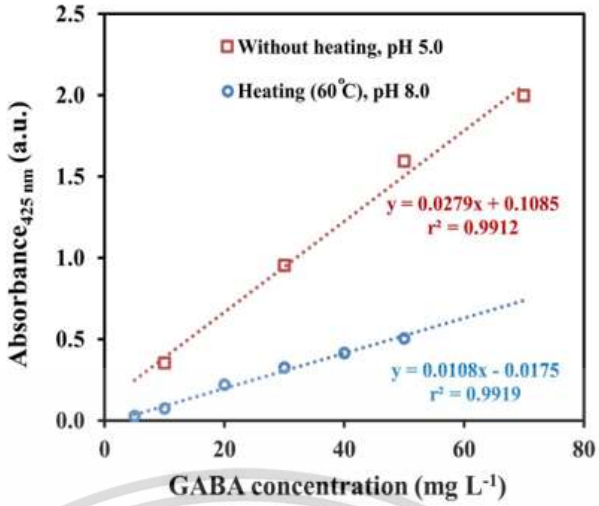

Figure 4.2. Calibration plots of the standard GABA solutions (from 5.0 to 70 mg L^{-1}) obtained by the different derivatization conditions. our method and another method [7].

After derivatization the mixture is changed from colorless to yellow, that demonstrates the HN-GABA derivative product can be monitored using UV – visible spectrophotometer. The absorption spectra of derivatives were monitored in range of 400 to 500 nm. The studied solutions were prepared by mixing of the 1 mL of standard working solutions of GABA (0, 50, 100, 200, 300, and 400 mg L^{-1}) in buffer pH 5 with 2 mL of 3% (w/v) HN. This solution was incubated overnight in dark at ambient temperature. Results were shown in Figure 4.3.

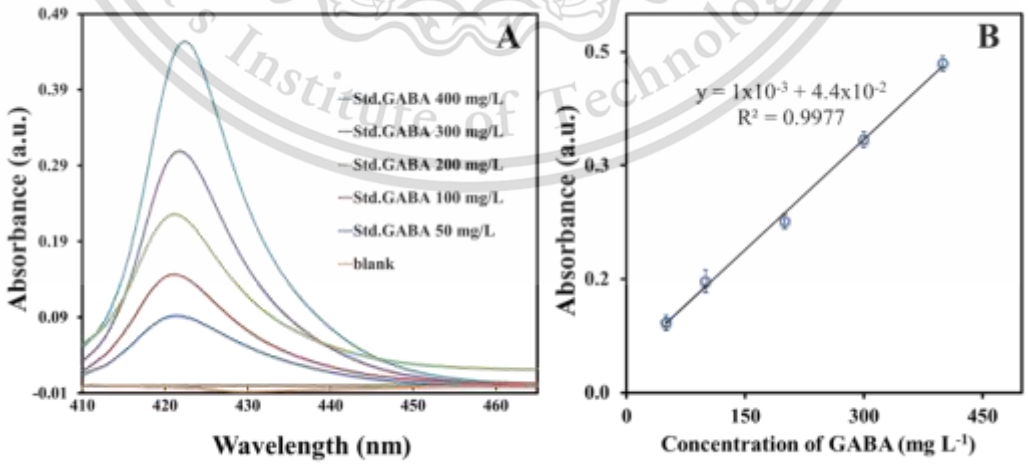

Figure 4.3. (A) Absorption spectra and (B) calibration line of the standard GABA solution (from 50 – 400 mg L^{-1}) were obtained.

The absorption spectra in Figure 4.3A show that the maximum absorption wavelength (λ_{max}) located at 425 nm. When the concentration of standard GABA in buffer pH 5 is increased, the absorbance reading is increased in the concentration range of 50 to 400 mg L^{-1} GABA. The linear calibration curve that plotted between the absorbance values at λ_{max} and the concentrations of standard GABA (Figure 4.3B) also showed good linearity (r^2 = 0.9977).

4.1.2 Design of the homemade 3D printed dialysis unit

Figure 4.4A and B are the photograph and schematic drawing of the homemade 3D printed dialysis unit, respectively. The unit is composed of four key components (from bottom to top): (i) the unit body, (ii) the stainless steel sieve, (iii) the dialysis membrane and (iv) the unit lid. The lid is screwed on to the body for rapid opening and closing. This design allows for easy addition of solid or liquid sample into the unit. The unit body comprises the cylindrical-shaped donor and acceptor chambers. The donor chamber is designed as having two 'bathtubs', as shown in Figures 4.4B and 4.5. 'Bathtub-1' and 'Bathtub-2' are employed for placing the stainless steel sieve and the dialysis membrane, respectively. This stainless steel sieve is an important component that allows for direct analysis of solids since it prevents macromolecules in sample matrices from contacting the membrane. This is confirmed by the SEM images in Figure 4.6A and B that clearly show that, without the sieve, clogged membrane surface is observed. This strongly affects the function of the membrane resulting in decreased efficiency of mass transfer during dialysis.

The unit lid is designed in a cylindrical configuration to screw on to the unit body but with a cone at the top (Figure 4.4B). There are two small holes in the cone section of the lid. 'Hole-1' is used for inserting a PTFE tube (0.1 mm i.d., 100 mm length) for withdrawing the dialysate into the SI system. 'Hole-2' serves two purposes: (i) as a ventilator for preventing excessive build-up of pressure inside the unit during the dialysis process and (ii) as the channel for pipetting the acceptor solution into the unit (Figure 3.2C). Beneath the cone section of the lid, there is a cylindrical wall (Figures 4.4B and 4.5). This wall gives tight fitting of the lid into the groove of the unit body and to press the membrane on to 'Bathtub-2'. This keeps the membrane taut and rigid.

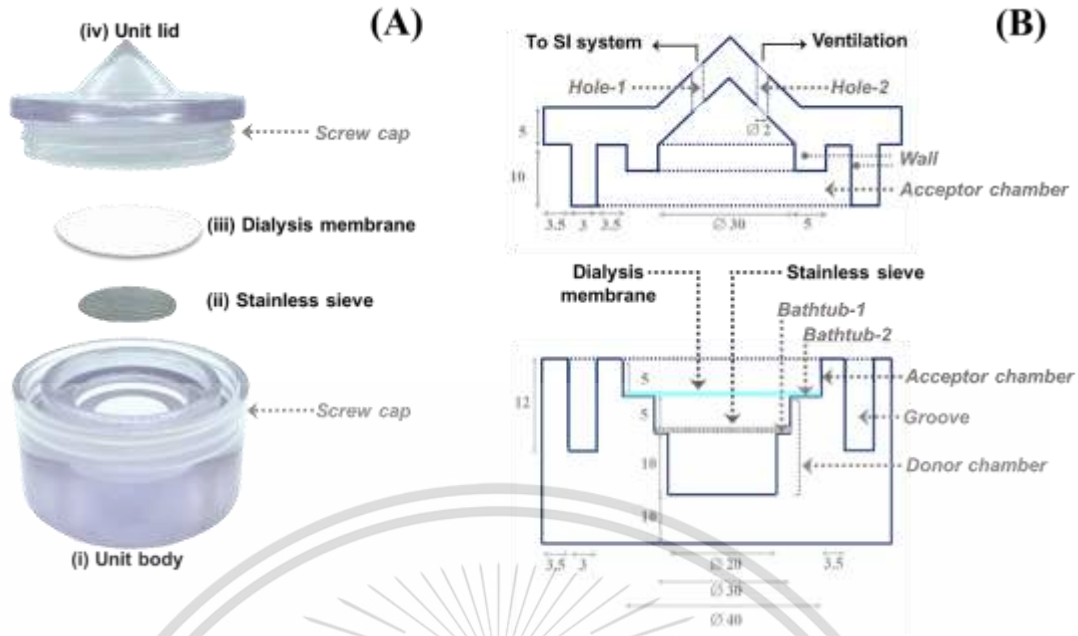

Figure 4.4. (A) Photograph and (B) Schematic drawing of the exploded view of the 'in-house' 3D printed dialysis unit for direct analysis of solid and liquid samples. Note: All dimensions as illustrated in Figure 4.4(B) are presented in 'mm'.

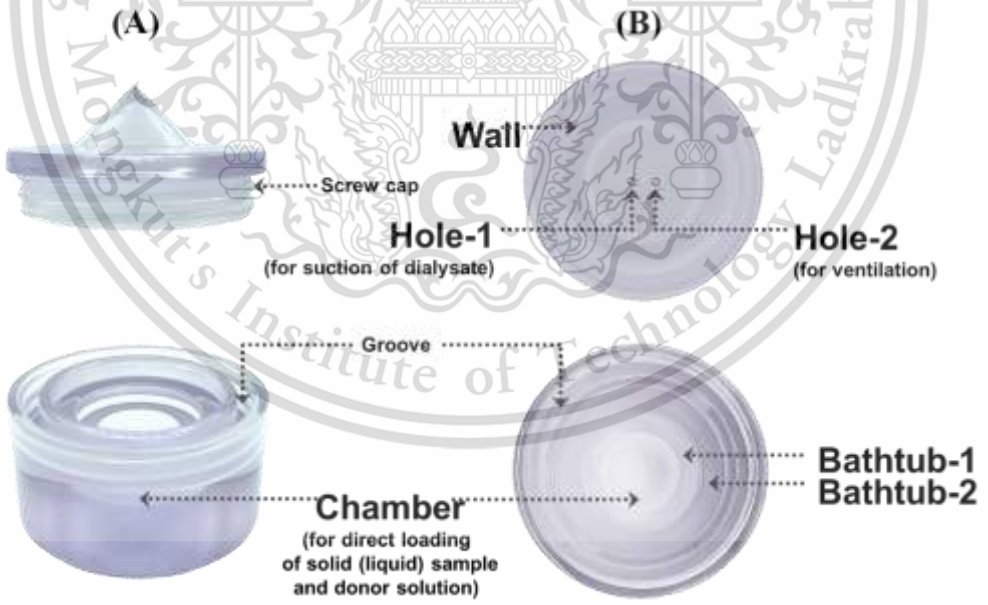

Figure 4.5. (A) Side-view and (B) faced-up view of the photographs of the 3D printed dialysis unit body and its lid.

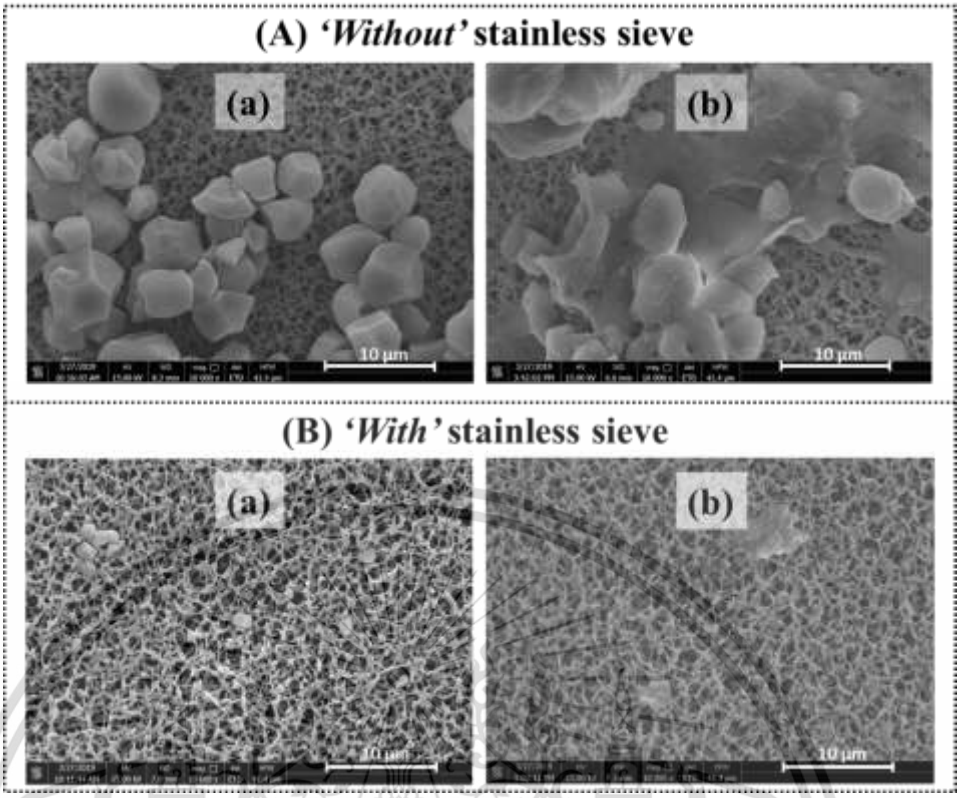

Figure 4.6. SEM images of the cellulose dialysis membrane: (A) without and (B) with the stainless steel sieve after analyses of ground (a) GABA-supplemented tablet and (b) germinated-brown rice.

4.1.3 Optimization of conditions of dialysis process

4.1.3.1 Volume of acceptor solution

In this study, standard solutions of GABA (50-1000 mg L^{-1}) and Britton-Robinson buffer (pH 5.0) were employed as the donor and the acceptor solutions, respectively. The effect of the volume of the acceptor was studied with the donor volume kept constant at 6.0 mL (the maximum volume in the donor chamber). This volume of the donor solution allows the donor solution to reach the surface of the hydrophilic membrane in order for dialysis to take place. The results were shown in Figure 4.7.

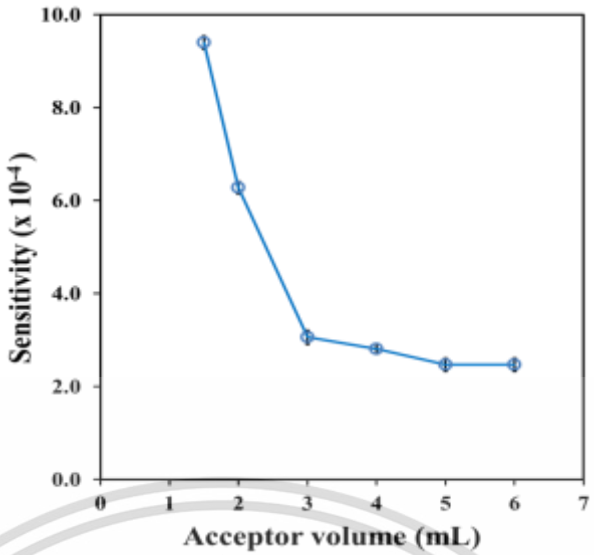

Figure 4.7. Volume of acceptor solution affecting the dialysis procedure.

Figure 4.7. demonstrate that the sensitivity (slope of the calibration line) rapidly decreases with increasing acceptor volume due to dilution effect. The highest sensitivity is obtained at 1.5 mL, and this volume was selected. An acceptor volume of 1.0 mL was also employed. However, the level of the acceptor solution was very small, resulting in air bubbles being drawn into the SI flow line when the dialysate was aspirated leading to disturbance to the derivatization and absorbance measurement. In principle the acceptor volume of 1.5 mL gives a 4-fold pre-concentration factor. This is very useful for the analysis of the samples containing very low GABA content.

4.1.3.2 Dialysis time

The dialysis time is defined as the time interval from the start of stirring of the sample solution in the donor chamber until it is stopped. The effect of dialysis time was studied using 6.0 mL of calibrators (50-1000 mg L^{-1} GABA) and 1.5 mL of Britton-Robinson buffer (pH 5.0) as the donor and acceptor solutions, respectively. The results in Figure 4.8. was presented below.

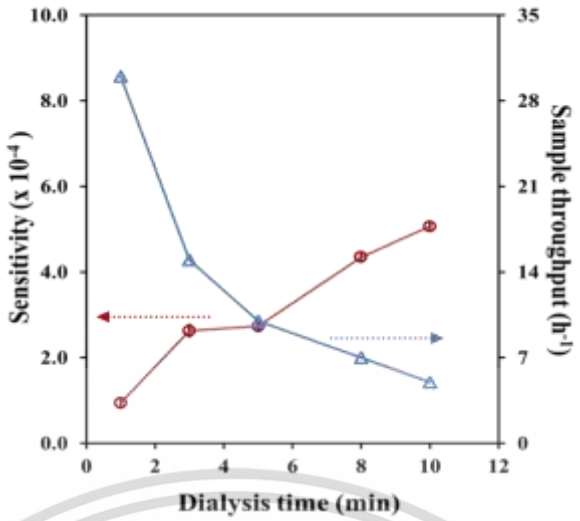

Figure 4.8. Effect of dialysis time on sensitivity and sample throughput.

The results in Figure 4.8. show that the sensitivity is improved as the dialysis time is increased. However, sample throughput is reduced. As a compromise between sensitivity and throughput, a dialysis time of 5.0 min was chosen.

4.1.3.3 Stirring speed

The effect of stirring speed was examined using 6.0 mL of 200 mg L^{-1} GABA. The results were presented in Figure 4.9.

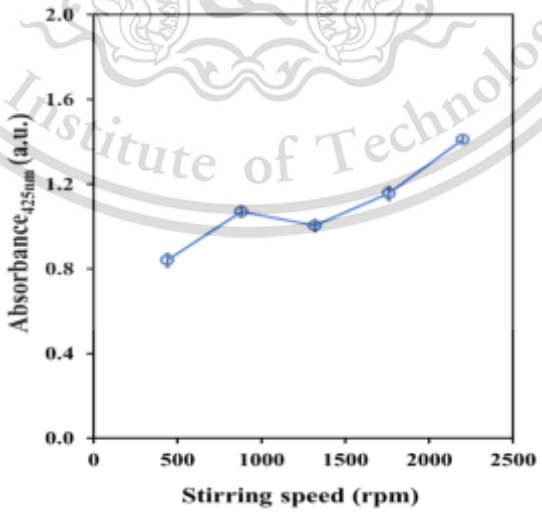

Figure 4.9. Effect of stirring speed on sensitivity of dialysis process.

Those results in Figure 4.9. show that increasing the stirring speed enhances the absorbance reading. This is because the efficiency of the dialysis process is typically enhanced by mechanical stirring to promote the convective-controlled mass transport. However at the highest setting (2200 rpm), there was turbulence of donor solution and also the magnetic bar was unstable and collided with the metal sieve. The speed of 1700 rpm was therefore chosen.

4.1.4 Factors affecting the derivatization reaction

4.1.4.1 Effect of pH of the acceptor solution

Since the reaction between GABA (a primary amine) and HN (an aldehyde) is a pH dependent process, a pH range of 1-10 of the acceptor buffer solution was investigated, at unit pH interval. The results were depicted in Figure 4.10.

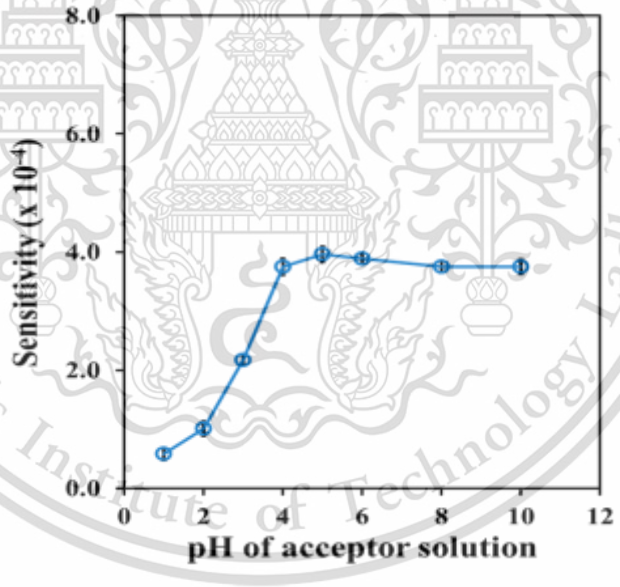

Figure 4.10. Effect of pH on sensitivity of imine reaction between GABA and HN.

The results in figure 4.10 show that sensitivity increases sharply from pH of 1-4 and then remaining unchanged from pH 5 to 10. At low pH, the amine group of GABA is converted to the ammonium ion and becomes non-nucleophilic. At higher pH, there is not enough acid to protonate the hydroxyl group of the intermediate to allow

for the removal of water (see the reaction mechanism in Figure 2.12. for more details). Therefore, a pH of 5 was considered suitable.

4.1.4.2 Study on kinetic of the reaction

Kinetics of the detection reaction was studied for 500 min at the fixed wavelength (425 nm). The results are shown in Figure 4.11.

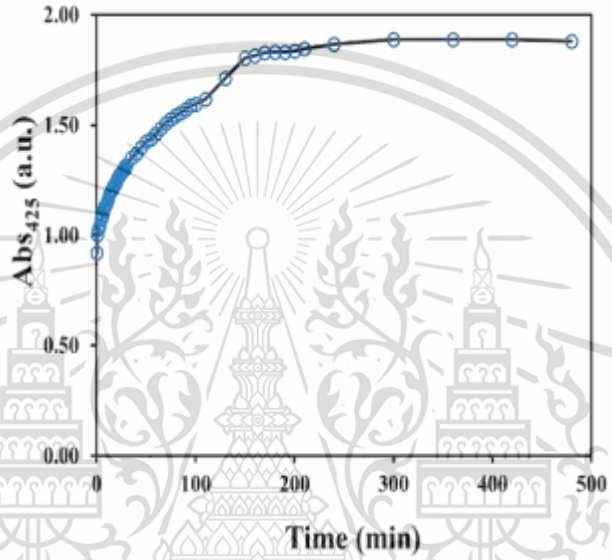

Figure 4.11. The kinetic curves of the reaction between GABA and HN when standard GABA solution (400 mg L^{-1}) were studied.

The results in Figure 4.11. show that the absorbance of the standard GABA solutions in buffer pH 5 (400 mg L^{-1}) after mixing with HN reached equilibrium within 120 min. It is clearly observed that the reaction is quite slow. Therefore, we try optimizing the other parameter such as pH value in order to improve the reaction rate and the sensitivity of the method.

4.1.4.3 Concentration of 2-hydroxy-1-naphthaldehyde (HN)

2-hydroxy-1-naphthaldehyde (HN) was employed as the derivatizing agent. The concentrations of HN were studied from 0.3-6% (w/v), the results were demonstrated in Figure 4.12.

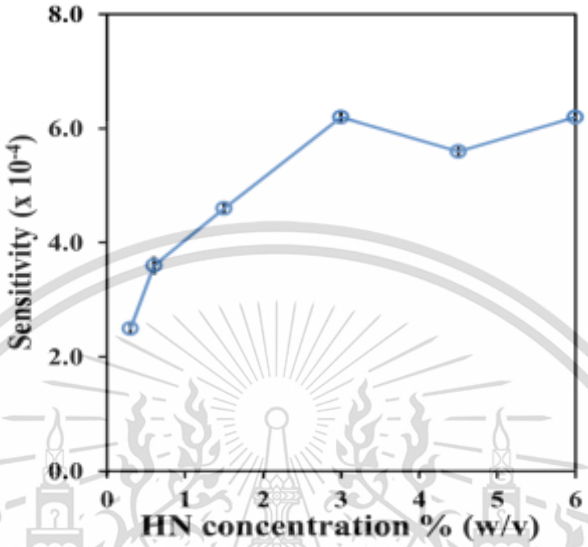

Figure 4.12. Effect of concentration of the derivatization solution (2-hydroxy-1-naphthaldehyde or HN).

The results in Figure 4.12. show that the sensitivity is considerably enhanced by increasing the concentration of HN from 0.3 to 3.0% (w/v) but does not differ from 3.0 to 6.0% (w/v), respectively. As a compromise between the sensitivity and the reagent consumption, the concentration of 3.0% (w/v) was selected.

4.1.5 Optimization of the SI system

4.1.5.1 Aspirated volume

The effect of the aspirated volume of the dialysate was studied while keeping the volume of HN in the flow-line fixed at 30 μL. The results were shown in Figure 4.13.

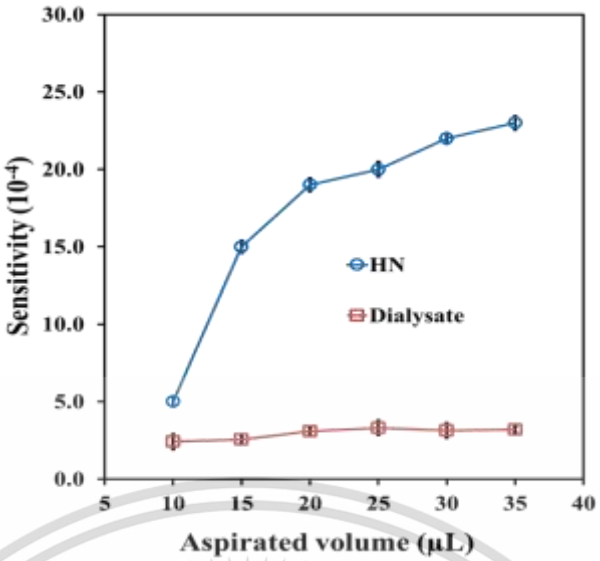

Figure 4.13. Effects of the physical parameters of the SI system of aspirated volume of the dialysate and derivatizing solutions.

The Figure 4.13. indicate that the sensitivity increases slightly before reaching a plateau value at 25 μL. This may be because of insufficient amount of the derivatizing agent when using higher volume of the dialysate. The aspirated volume of the dialysate of 25 μL was therefore selected and employed in the following study. As expected, the sensitivity significantly increases with increasing volume of the derivatizing solution (Figure 4.13). However, the baseline shifts due to a layer of the sample zone remaining on the window of the flow-through cell was observed at high volume (35 and 40 μL). Therefore, the aspirated volume of the HN solution was set at 30 μL (with the aspirated volume of the dialysate of 25 μL).

4.1.5.2 Mixing coil length

The effect of mixing coil length on sensitivity was studied using 6.0 mL of calibrator at various concentrations (50-1000 mg L^{-1} GABA). The investigated mixing coil length were 0, 50, 100, 200, 300, and 400 cm. The results were demonstrated in Figure 4.14.

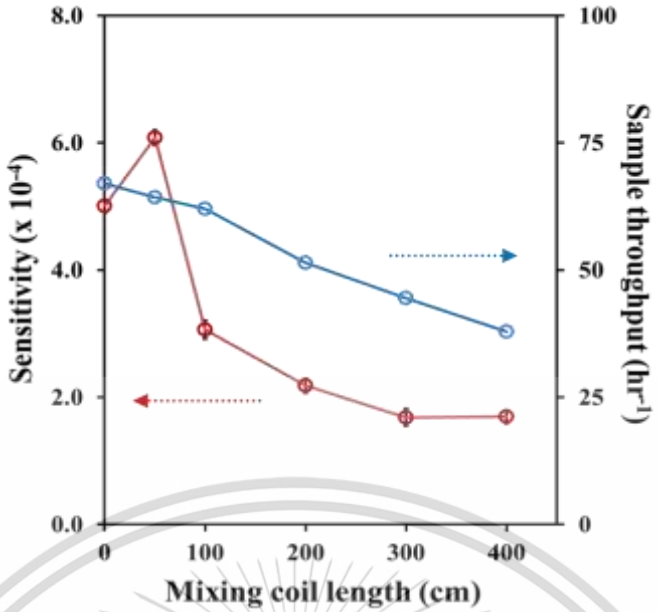

Figure 4.14. Effects of the physical parameters of the SI system; Length of mixing coil.

The results in Figure 4.14. show that the use of the mixing coil (50 cm), as compared to having no coil, gives higher sensitivity as the mixing process is more efficient. However the sensitivity decreases when the length of the length was increased due to dispersion effect; also a longer coil results in a lower sample throughput. Thus the mixing coil of 50 cm length was employed in the final system.

4.1.5.3 Dispensing flow rate

The effects of dispensing flow rate on sensitivity and sample throughput was studied using calibrator at various concentrations (50-1000 mg L^{-1} GABA), 1.5 mL of Britton-Robinson buffer (pH 5.0) as donor and acceptor solutions, 3 min of dialysis time, 1760 rpm of stirring speed, 3% w/v of HN, and 25 μL of dialysate. The investigated dispensing flow rates were 25, 50, 75, 100, 120, and 150 μL sec^{-1}. The results were shown in Figure 4.15.

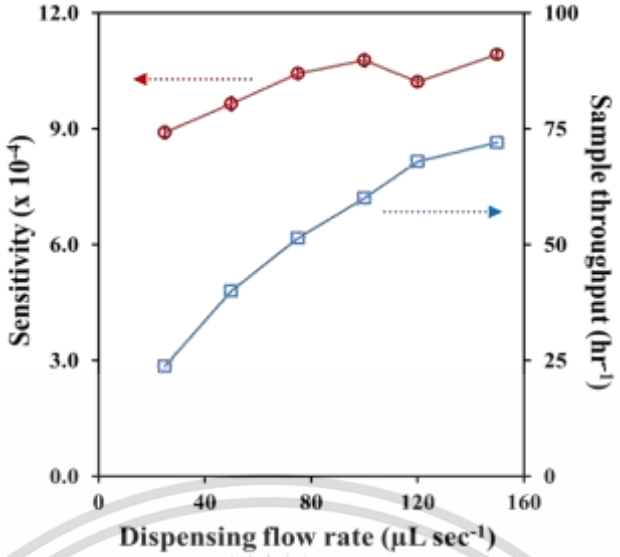

Figure 4.15. Effects of the physical parameters of the SI system for aspirated volume of dispensing flow rate.

The results in figure 4.15. show that at faster flow rates sensitivity only gradually increases whilst the sample throughput increases in proportion with the flow rate. The flow rate of 150 µL s^{-1} was selected since it offers the highest sensitivity and sample throughput. At this flow rate, the sample throughput of 64 samples h^{-1} is achieved.

4.1.6 Analytical performance

Under the optimal conditions listed in Table 4.1, a linearity range of 10-1000 mg L^{-1} GABA was obtained with reproducible signal profiles (Figure 4.16). The detection limit (3SD of blank) is 0.14 mg L^{-1} which is sensitive enough to determine the GABA content in dietary supplements and beverages. However the colorimetric detection might not be sufficiently sensitive to analyze low concentrations of GABA found in biological samples [7,8,42]. In order to employ this developed method for these kinds of samples, a pre-concentration step may be required.

Using the SI system, rapid and repeatable measurements were achieved (<1.0 min $sample^{-1}$) with high precision of 1.2 %RSD, 15 injections of 10 mg L^{-1} GABA (see Figure 4.17.). Furthermore, the SI system allows simultaneous dialysis of many

samples. This strategy provides rapid measurements, which is necessary for routine application.

Comparison of this method with other analytical methods in the literature is shown in Table 4.2. In Table 4.2 the methods are categorized as non-derivatization and derivatization methods. For the non-derivatization methods, it was necessary to use either an enzyme reactor [8] or modified heavy metal nanoparticles (chemosensors) [9] to improve the selectivity. Amongst the derivatization methods which employed HN as the derivatizing reagent [7, 28-19], our analytical procedure was simpler and faster. This is because the SI system offers automated on-line derivatization and measurement. The derivatization reaction was carried out under mild condition without heating eliminating the problem of air bubbles being generated.

The unique feature of this method is that with our design of the 3D printed dialysis unit, direct analysis of solid and liquid samples is possible without sample preparation, except grinding of the solid samples. This is because installing the stainless steel sieve inside the donor chamber prevents clogging of the dialysis membrane by colloidal matters. Turbid and coloured liquid samples can also be directly analysed.

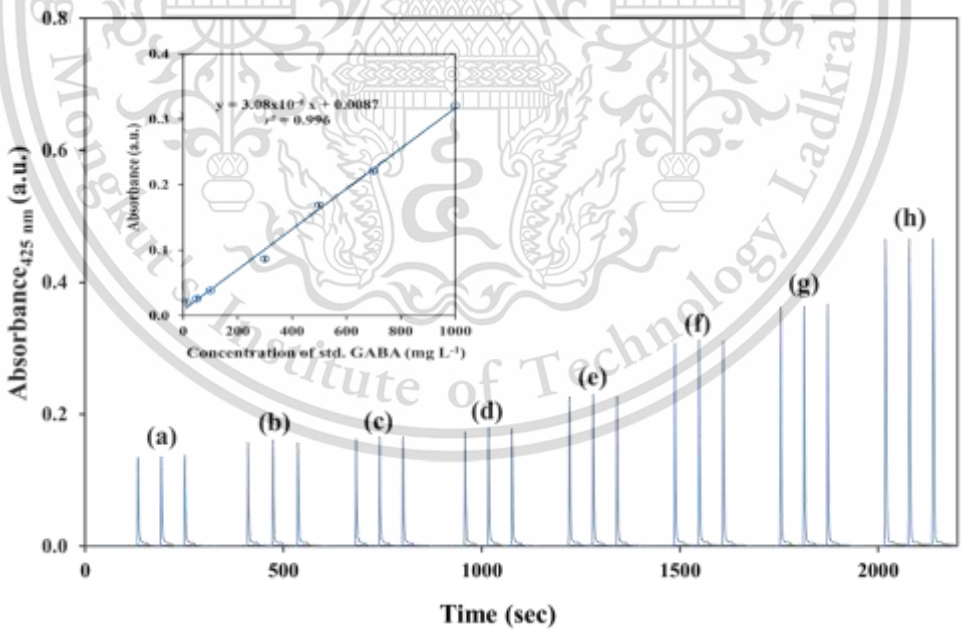

Figure 4.16. Examples of the signal profiles of the standard GABA solutions and the corresponded calibration graph. Form (a) to (h) are 0, 10, 50, 100, 300, 500, 700, and 1,000 mg L^{-1} of standard GABA. Inset is the corresponded linear calibration plot.

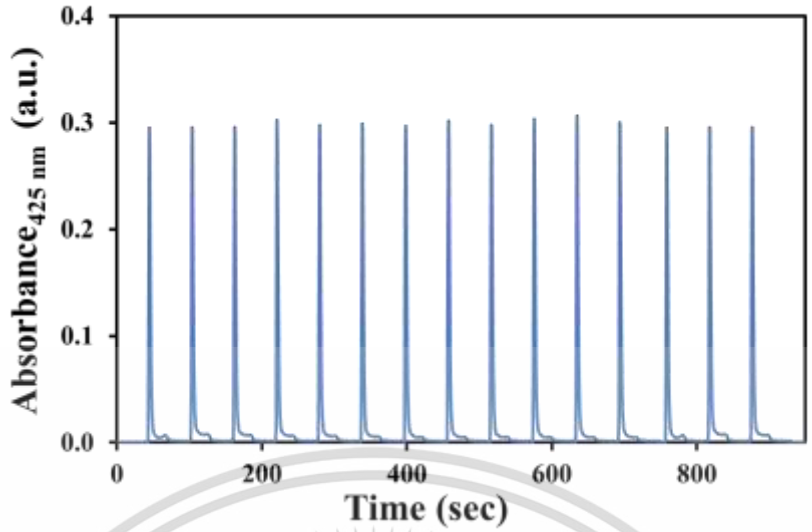

Figure 4.17. Examples of the reproducibility of signal profiles at 10 mg L^{-1} GABA, 15 injection.

Table 4.1 Summary on the optimization study and the selected conditions for the dialysis procedure and for automated derivatization with subsequent determination of GABA by the SI system incorporation with the 3D printed dialysis unit.

Parameters	Studied range	Selected value
(1) *The dialysis procedure*		
(1.1) Acceptor volume (mL)	1.5 – 6.0	1.5
(1.2) Dialysis time (min)	1.0 – 10	5.0
(1.3) Stirring speed (rpm)	440 – 2,200	1,700
(2) *The SI system*		
(2.1) pH of the derivatizing agent	1.0 – 10	5.0
(2.2) Concentration of the derivatizing agent (% w/v)	0.3 – 6.0	3.0
(2.3) Aspirated volume of dialysate (μL)	10 – 35	25
(2.4) Aspirated volume of the derivatizing agent (μL)	10 – 35	30
(2.5) Length of mixing coil (cm)	Without - 400	50
(2.6) Dispensed flow rate (μL sec^{-1})	25 - 150	150

Table 4.2 Comparison of the analytical characteristics of the proposed method with the other methods in literatures for determination of GABA.

No	Analytical technique/ Detection	Analytical characteristics			Direct analysis of sample	Sample (Preparation)	Derivatization (Condition)	Ref
		Working range ($mg\ L^{-1}$)	RSD (%)	Detection time ($min\ sample^{-1}$)				
Non-derivatization methods								
1	FI + Enzyme reactor /Fluorescence	Up to 4.8 x 10-3	> 2.0	3	No	Culture medium/ (Dilution + Filtration)	-	[8]
2	SI/ Light scattering	100 - 400	< 3.3	2.4	No	Green tea/ (Centrifugation + Filtration)	-	[9]
Derivatization methods								
3	HPLC/ UV	1.2 - 28	2.4	2	No	Human CFS (Centrifugation + Filtration)	Batchwise [a] (80 °C, pH 8.0, 10 min)	[7]
4	HPLC/ UV	3.83 – 34.58	1.25	8	No	Rice (Centrifugation + Filtration)	Batchwise [a] (80 °C, pH 8.0, 10 min)	[28]
5	HPLC/ UV	2.25 – 34.5	2.19	5	No	Rice (Centrifugation + Filtration)	Batchwise [a] (85 °C, pH 8.5, 15 min)	[29]
6	SI + HPLC/ UV	0.01 – 3	3.2 - 5	12	No	Human CFS/ Urine (Centrifugation + Filtration)	On-line [b] (Without heating, pH 9.4, < 1 min)	[32]
7	SI/ Colorimetry	10-2,000	1.2	1	Yes	Food stuffs/ beverages (without preparation)	On-line [a] (Without heating, pH 5.0, < 1 min)	This work

***Note*:** The derivatizing agents are: [a] 2-hydroxy-1-naphthaldehyde and [b] o-phthalaldehyde.

4.1.7 Effects of coexisting interferences

In this work, compounds that are found in the samples [22-24], including milk, rice and tea, and which may cause interference with this method, were selected and investigated using 50 mg L^{-1} GABA. The tolerance limit is the maximum concentration of the spiked compound giving the measured absorbance for GABA which does not lie outside the range of mean± 3SD of the absorbance value for the standard 50 mg L^{-1} GABA. As shown in Table 4.3, the tolerance limits for all investigated interferences are higher than the concentrations that may exist in samples [22-24]. This suggests that the developed method is not affected by these compounds.

Table 4.3 Tolerance limit of the interfering compounds.

Foreign species	Tolerance limit (mg L^{-1})
Isoleucine, Methionine, Serine, Threonine	100
Phenylalanine, Tryptophan, Arginine, Histidine	200
Leucine, Valine, Glutamic acid, B12	300
Lysine	500
Aspartic acid	1,000

4.1.8 Application to sample and validation

To verify that developed method is fit for the purpose, it was applied to analysis of nine samples, including GABA-supplemented tablets/capsules, grains of germinated brown rice, instant green tea powder and GABA-enriched milk. Recovery study was first carried out. Standard solution of GABS was added to the sample in the donor chamber to give the spiked concentration of 50 mg L^{-1}. It is observed in Table 4.4 that the recoveries ranged from 97.4 to 102.2% (mean recovery: 99.8% ± 1.5). This result demonstrates that the method is free from sample matrix effect.

The GABA contents determined using the developed method and the reversed-phase HPLC, were compared and the results are listed in Table 4.5. The results are not significantly different using the Pearson linear regression test (r^2 = 0.9999) [25]. The GABA contents are compared to the label values and they are in good agreement.

Table 4.4 Percentage recovery of spiked GABA using the developed SI system.

Sample	GABA content, as mg L^{-1} (Mean + SD, n =3)			Recovery (%)
	Original	Added	Found	
GABA supplement-1(Tablet)	99.5 ± 0.30	50	149.3 ± 0.47	99.6
GABA supplement-2 (Capsule)	201.4 ± 0.98	50	251.3 ± 0.28	99.7
GABA supplement-3 (Capsule)	502.7 ± 0.52	50	552.3 ± 0.17	99.3
GABA supplement-4 (Capsule)	500.3 ± 0.08	50	549.9 ± 0.07	99.1
GABA supplement-5 (Capsule)	750.9 ± 0.62	50	801.7 ± 0.45	101.7
GABA-enriched milk-1	14.7 ± 0.31	50	63.4 ± 0.07	97.3
GABA-enriched milk-2	11.5 ± 0.07	50	61.0 ± 0.50	99.1
Germinated-brown rice	20.7 ± 0.50	50	71.8 ± 0.29	102.2

Table 4.5 Comparison of the GABA contents in foodstuffs and beverages, determined by the developed SI system and the validating HPLC method.

Sample	GABA content, as mg L^{-1} (Mean + SD, n =3)		Label value
	This work	HPLC method	
GABA supplement-1(Tablet)	99.5 ± 1.3	100.8 ± 0.03	100[a]
GABA supplement-2 (Capsule)	202.4 ± 2.0	202.9 ± 0.5	200[b]
GABA supplement-3 (Capsule)	502.7 ± 1.5	499.9 ± 1.4	500[b]
GABA supplement-4 (Capsule)	500.3 ± 2.1	498.6 ± 2.4	500[b]
GABA supplement-5 (Capsule)	743.4 ± 1.6	751.9 ± 0.2	750[b]
GABA-enriched milk-1	3383.5 ± 0.3	3519.0 ± 0.01	3,412[c]
GABA-enriched milk-2	2637.3 ± 0.1	2645.0 ± 0.02	2,656[c]
Germinated-brown rice	31.6 ± 0.5	30.4 ± 0.04	30.5[d]
Instant green tea powder	20.1 ± 0.1	20.7 ± 0.6	20[e]

Note: The GABA contents are. [a]: mg $tablet^{-1}$, [b]: mg $capsule^{-1}$, [c]: mg $carton^{-1}$, [d]: mg 100 g^{-1} and, and [e]: mg $pack^{-1}$.

4.2 Flow-based systems with 3D printed flow cells for quantitative measurement of Albumin in urine based on using the AuNPs-catalyzed chemiluminescence detection.

4.2.1 Characterization of the AuNPs

AuNPs were prepared by modified procedure of Turkevich's method [42]. The color of the solution was changed from pale yellow to deep red. The as-prepared AuNPs colloidal was kept at 4°C overnight before using. The Characterization of AuNPs is carried out and the results are shown in Figure 4.18.

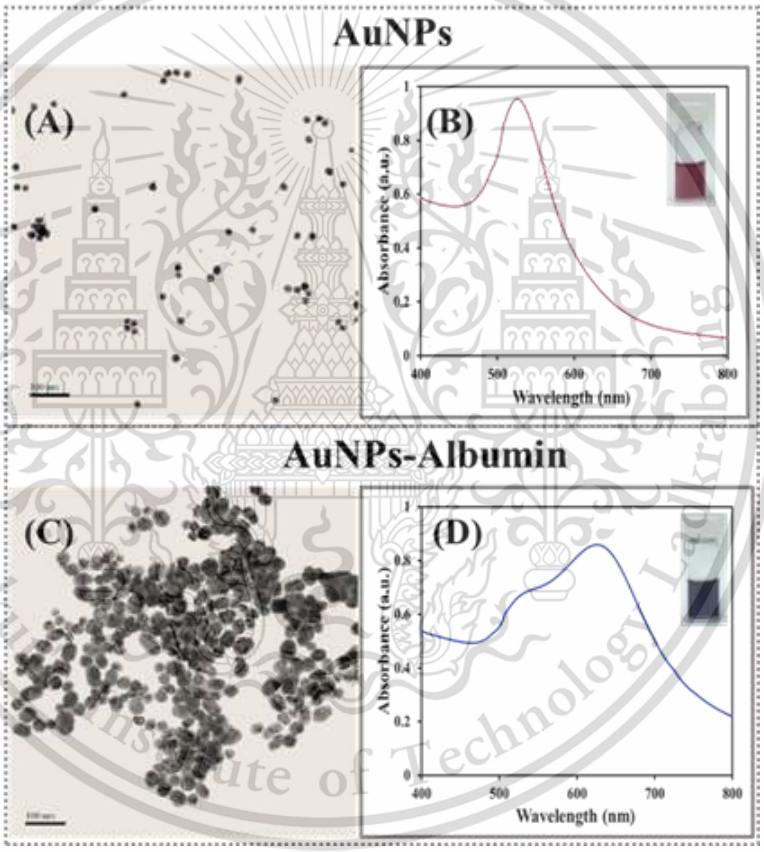

Figure 4.18. (A) and (B) are TEM image and absorption spectra of the prepared AuNPs, respectively. (C) and (D) are TEM image and absorption spectra of AuNPs in the presence of standard albumin (50 mg L^{-1}), respectively. The inset pictures of (B) and (D) are the observed colors of the AuNPs solutions.

Transmission electron microscopy (TEM) image in Figure 4.18A show that the monodispersed and spherical nanoparticles are observed (average size: 18.4 ± 0.04 nm). Maximum absorption wavelength of the as-prepared AuNPs is located at 520 nm (Figure 4.18B). These results are agreed with the literature report [42]. TEM image in Figure 4.18C reveals that aggregation of AuNPs in the presence of albumin is occurred. This results in red shift of the absorption spectrum of the AuNPs as shown in Figure 4.18D.

4.2.2 Study on aggregation of AuNPs by albumin using spectrophotometer

Albumin can simply bind on the AuNPs surface through the displacement mechanism, where the stabilized citrate ion around the nanoparticles can be displaced by BSA upon adsorption, with the amino acids (functional groups), lysine (amine), histidine (imidazole), and cysteine (thiol) [43]. After binding, the AuNPs became aggregate. Then the absorption spectra and the color change of the AuNPs in the presence of various concentrations of albumin is presented in Figure 4.19.

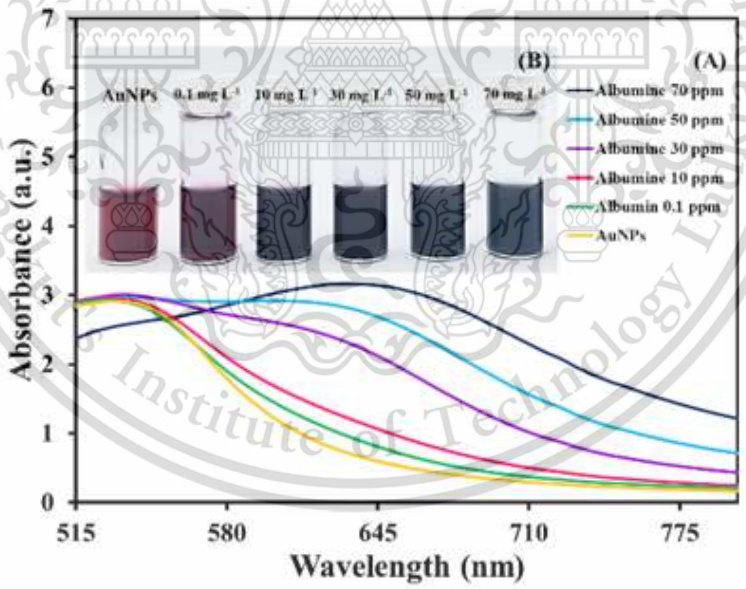

Figure 4.19. (A) Absorption spectra and (B) the color of the AuNPs (8.38 nmol L^{-1}) with various concentrations of standard albumin (0.1 to 70 mg L^{-1}).

Figure 4.19A indicates that increasing in the concentration of albumin, induce aggregation of the AuNPs. The color of the AuNPs solutions are changed from

red to dark blue (Figure 4.19B). This confirm that the formation of AuNPs-albumin conjugate is occurred.

4.2.3 Catalytic effect of AuNPs on the CL reaction between luminol and H_2O_2

This effect was studied in the absence of albumin. Results in Figure 4.20 indicate that when the concentration of AuNPs is increased, the CL intensity is also increased. This is an evidence that the as-prepared AuNPs can catalyze the CL reaction of luminol and H_2O_2.

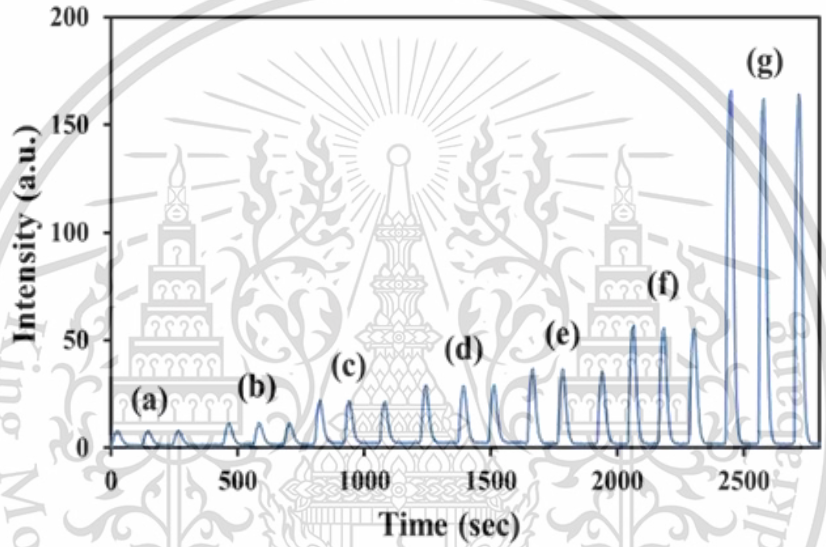

Figure 4.20 Signal profiles, obtained by injection of various concentrations of AuNPs into the developed FI: (a) 0, (b) 0.59 x 10^{-9}, (c) 1.42 x 10^{-9}, (d) 2.57 x 10^{-9}, (e)4.30 x 10^{-9} , (f) 8.38 x 10^{-9} and (g) 9.72 x 10^{-9} mol L^{-1}.

4.2.4 Study on detection reaction of albumin using spectrofluorometer

Schematic illustration of the detection principle is shown in Figure 4.21. Gold nanoparticles (AuNPs)-catalyzed luminol chemiluminescence [10] is employed as detection reaction. In the presence of albumin, aggregation of the AuNPs is induced and this inhibited the CL light caused by the luminol-H_2O_2 system. The mechanism of the interaction between the AuNPs and albumin is proposed in Figure 4.21.

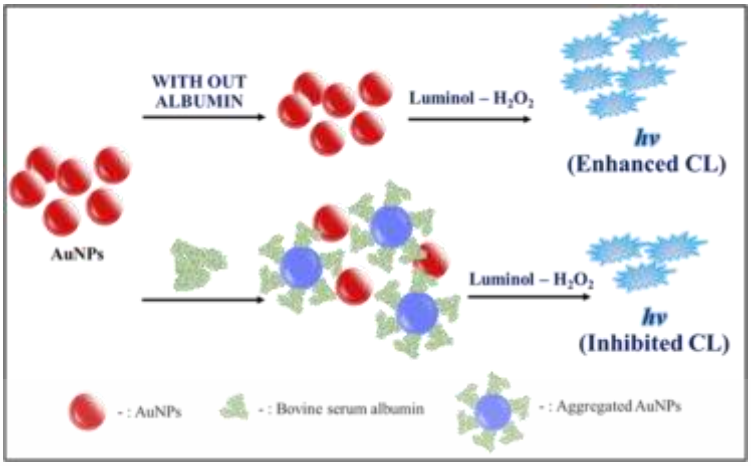

Figure 4.21. Schematic illustration of the AuNPs sensor to detect albumin in the luminol-H_2O_2 system.

Results in Figure 4.22A show that, gold nanoparticles (AuNPs) can catalyze luminol chemiluminescence. The intensity of luminol-H_2O_2 system was increased in the presence of AuNPs. In the other hand, the intensity of (AuNPs)-catalyzed luminol chemiluminescence is decreased when, the albumin concentration is increased. Because albumin bound to the AuNPs, the AuNPs became aggregate. The results in minimizing in free AuNPs for catalysis of the luminol-H_2O_2 chemiluminescence system. The inset pictures of (A) and (B) are the observed colors of the AuNPs solutions.

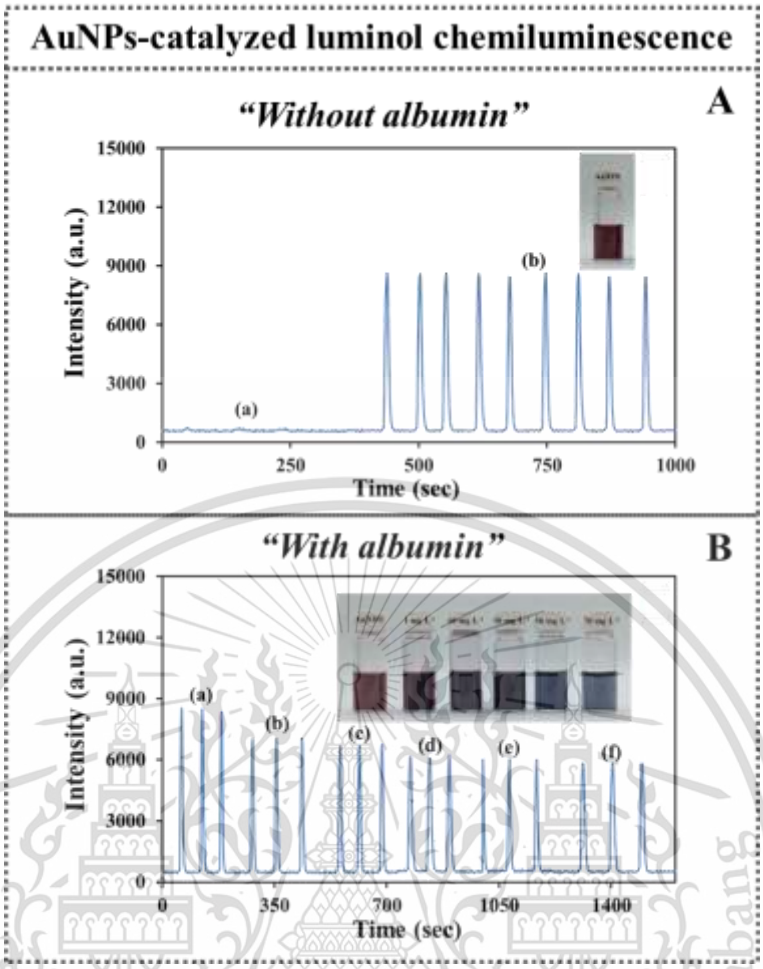

Figure 4.22 A: The signal profiles of (a) luminol-H_2O_2 and (b) AuNPs catalyzed luminol-H_2O_2, B: AuNPs-catalyzed luminol chemiluminescence in the presence of standard albumin concentrations of (a)-(f); 0, 10, 30, 50, and 70 mg L^{-1}.

4.2.5 Design of the homemade 3D printed spiral flow cell

The 3D printed flow cell was designed in two different configurations. The flow cell prototype I was used as detection flow cell (Figure 4.23.) and the flow cell prototype II was utilized for on-line mixing with subsequent detection of albumin. There pictures are presented in Figure 4.24.

Both flow cell was designed as spiral and fabricated quickly and easily using three-dimensional (3D) printing technology. This cell was attached in front of the photomultiplier tube inside the spectrofluorometer.

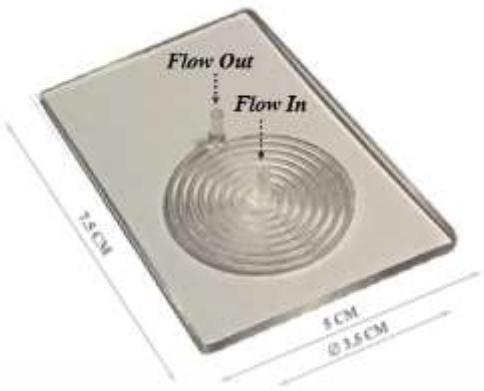

Figure 4.23. The picture of 3D printed spiral flow cell prototype I.

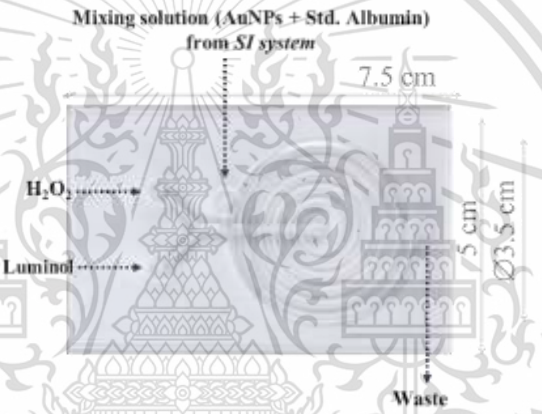

Figure 4.24. The picture of 3D printed spiral flow cell prototype II.

4.2.6 Batchwise study on the reaction between albumin and the AuNPs using spectrophotometer

Reaction time (or incubation time) is defined as the period of time that the solution was kept after mixing between standard albumin and AuNPs. This effect was investigated by various concentrations of AuNPs from 1.42 to 8.38 nmol L^{-1} (standard albumin was fixed at 10 mg L^{-1}). The results are shown in Figure 4.25. When incubation time is increased, the absorbance ratio (A_{620}/A_{520}) is also increased. The ratio is slightly difference after 10 min. Therefore, 10 min is selected.

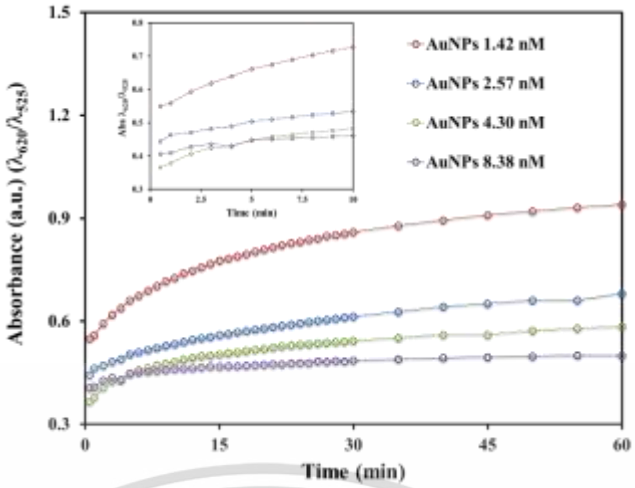

Figure 4.25. Effect of incubation time

.

4.2.7 Optimization of FI system

4.2.7.1 Effect of sample volume

The effect of the sample volume (the mixture between AuNPs and standard albumin/urine) was studied while the volume of luminol was fixed at 400 μL. The results are shown in Figure 4.26. The sensitivities are increased when the volumes are increased from 100 to 500 μL. The sensitivity is decreased at higher volume. This was due to the doublet peak was observed. The injection volume of 500 μL is therefore chosen.

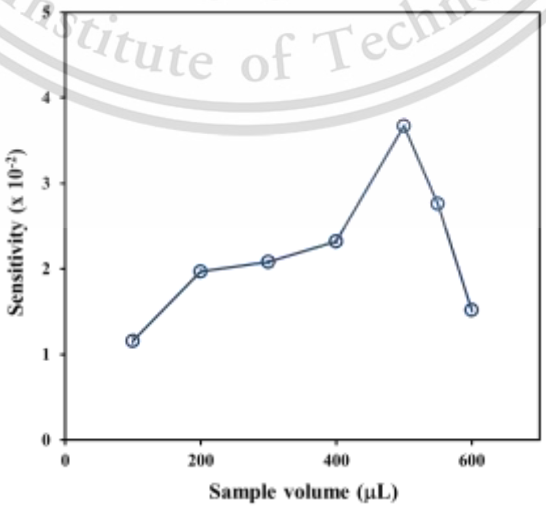

Figure 4.26. Effect of sample volume

4.2.7.2 Effect of flow rate

Effect of flow rates were studied from 1 to 3 mL min^{-1}. The results are presented in Figure 4.27. Increasing in the flow rate results in increasing in the sensitivity and the throughput. However, at 3.0 ml min^{-1}, the sensitivity is decreased. The flow rate of 2.5 mL min^{-1} is selected as compromising between the sensitivity and the throughput. By this flow rate the throughput of 66 samples h^{-1} was achieved.

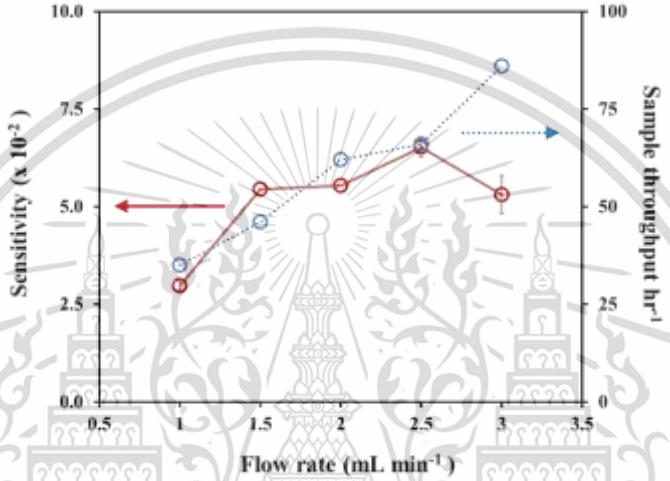

Figure 4.27. Effect of flow rate

4.2.7.3 Effect of concentration of the AuNPs

Effect of the concentration of the AuNPs was studied from 0.59 to 9.72 nmol L^{-1}. Results are shown in Figure 4.28. As the concentrations are increased, the sensitivities are decreased. Because when the concentrations of AuNPs increased, this caused the intensity of luminol-H_2O_2 CL increased. This is more difficult to investigate the slightly decrease of intensity from quenching mechanism of albumin. Hence, AuNPs 1.42 nmol L^{-1} was chosen as the suitable concentration of AuNPs for further studies.

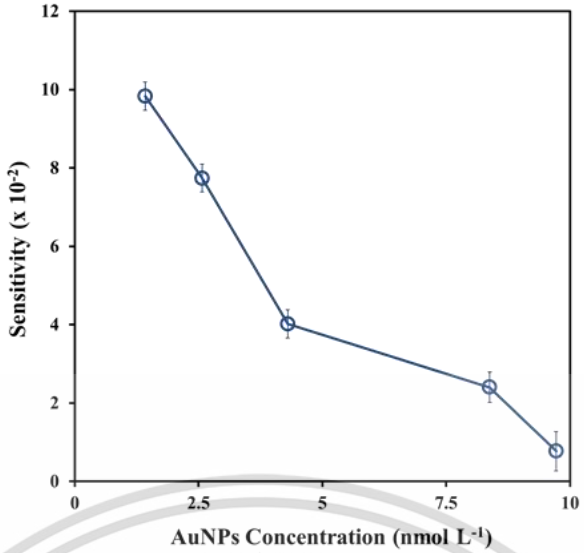

Figure 4.28. Effect of AuNPs concentration

4.2.7.4 Effect of concentration of Luminol

The concentration of luminol was studied from 0.1 to 1000 mmol L^{-1}. Results are shown in Figure 4.29. The sensitivity is considerably enhanced by increasing in the concentration of luminol from 0.1 to 10 mmol L^{-1}. The sensitivity become slightly increase but slightly increase from 10 to 1000 mmol L^{-1}. As a compromise between the sensitivity and the reagent consumption, the concentration of 10 mmol L^{-1} is selected.

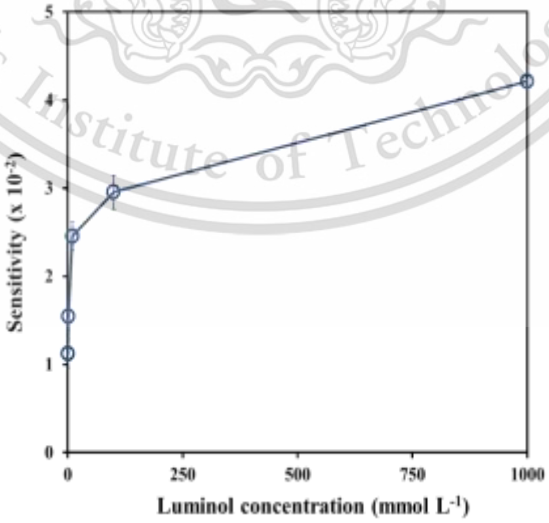

Figure 4.29. Effect of luminol concentration

4.2.8 Effect of flow cell design

Figure 4.30. demonstrate the signal profiles and linearity ranges of standard albumin (0.1-70 mgL^{-1}). These signal profiles were detected with using 3D printed flow cells prototype I and II. The sensitivities of both systems were compared and shown in Figure 4.31.

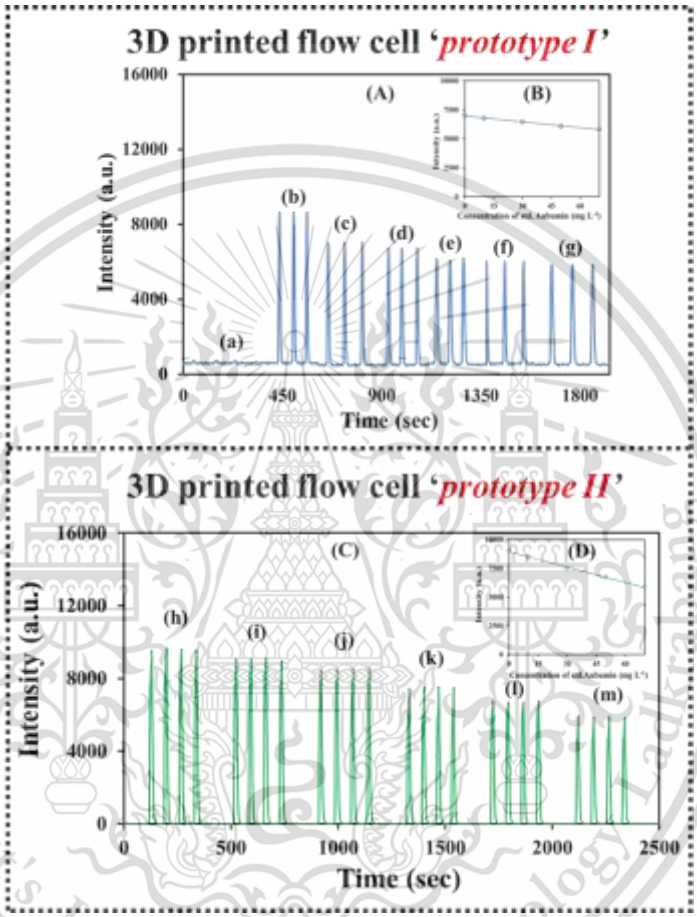

Figure 4.30. (A) Signal profiles of luminol-H_2O_2 CL using flow cell prototype I : (a), luminol-H_2O_2 without AuNPs and (b)-(g), (AuNPs)-catalyzed luminol-H_2O_2 CL in the presence of standard albumin concentration of 0, 0.1, 10, 30, 50, and 70 mg L^{-1}, respectively and (B) linear calibration curve. (C) Signal profiles of luminol-H_2O_2 CL using flow cell prototype II: (h)-(g), (AuNPs)-catalyzed luminol-H_2O_2 CL in the presence of standard albumin concentration of 0, 0.1, 10, 30, 50, and 70 mg L^{-1}, respectively and (D) linear calibration curve.

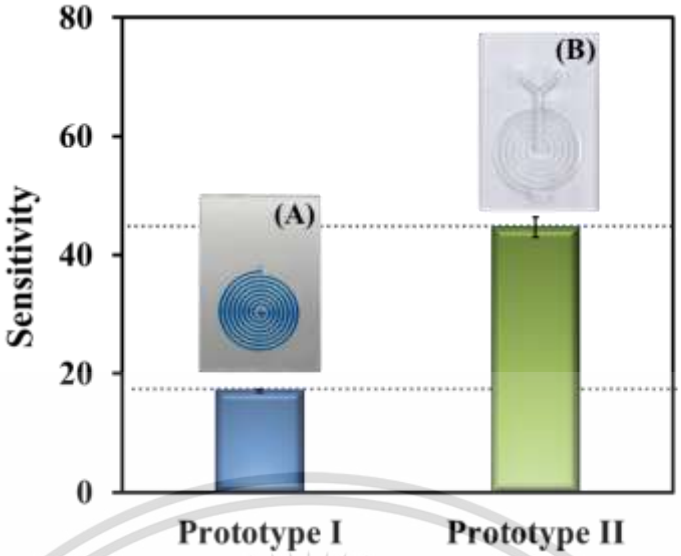

Figure 4.31. Effect of flow cell design on sensitivity, (A) is the picture of 3D printed spiral flow cell prototype I, which was filled with blue dye, (B) is the picture of 3D printed spiral flow cell prototype II.

Results in Figure 4.30. and 4.31. clearly indicate that the sensitivity obtain by the flow cell prototype II provides better sensitivity. It is because the flow cell allows on-line mixing with subsequent detection. Dispersion of the reacted zone as occurred in flow cell prototype I was eliminated.

4.2.9 Analytical performances

Under the optimal conditions, Figure 4.32(B) demonstrated a linearity range of 0.1 to 70 mg L^{-1} albumin (Intensity = -44.665[Albumin] + 8956.3, r^2 = 0.996). The results were good reproducibility (RSD < 1.0 % at 30 mg L^{-1} of standard albumin). The signal profiles were shown in Figure 4.32(A). Limit of detection (3SD/slop) was obtained at 0.01 mg L^{-1}.

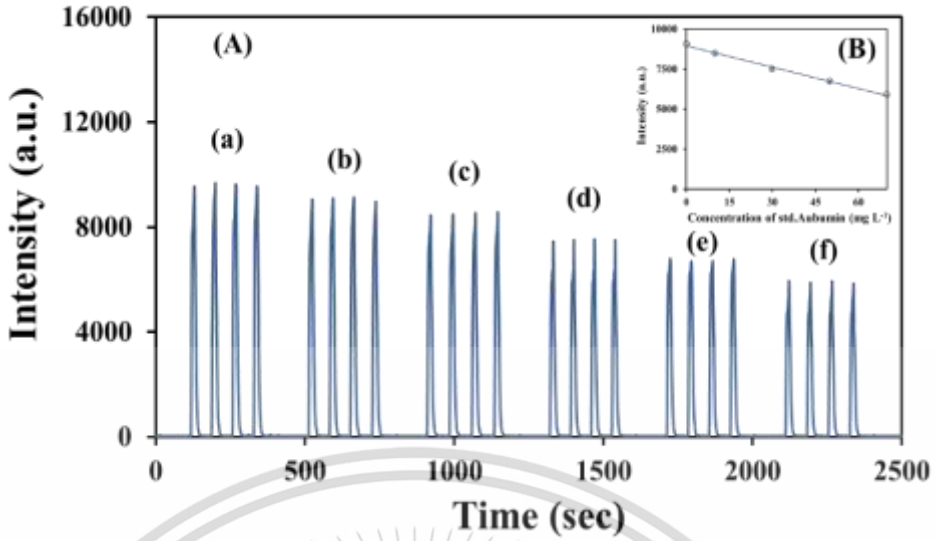

Figure 4.32. (A) Signal profiles of luminol-H_2O_2 CL: (a)-(f), (AuNPs)-catalyzed luminol-H_2O_2 CL in the presence of standard albumin concentration of 0, 0.1, 10, 30, 50, and 70 mg L^{-1}, respectively and (B) linear calibration curve.

4.2.10 Application to urine sample

The developed FI system was applied to determine the albumin content in the spiked urine, collected from normal volunteers. The results are shown in Table 4.6. It was observed that good recovery was obtained (95.7 to 101.1 %). These results can guarantee that the method was free from the sample matrix effect.

Table 4.6 Percentage recovery of albumin in urine samples, evaluated by the developed method

sample	Albumin concentration (mg L^{-1})			%
	Original	Added	Found	Recovery
1	13.1±0.02	10	23.4±0.47	101.1
2	8.7±0.02	10	18.5±0.28	98.1
3	1.3±0.01	10	22.9±0.17	95.7
4	15.2±0.02	10	25.0±0.07	98.2

Chapter 5
Conclusions and Suggestions

5.1 Conclusions

5.1.1 Determination of gamma-aminobutyric acid in foodstuff and beverages exploiting a 3D printed dialysis unit and sequential injection system

The 3D printed dialysis unit was applied for the direct analysis of solid and liquid samples. The homemade dialysis unit was easily and rapidly fabricated. By adding a stainless-steel sieve inside the donor chamber, the problem of the clogging of the dialysis membrane by suspended particulates or macromolecules in the sample matrices was eliminated. More than one 3D printed dialysis unit can be incorporated with the SI system for simultaneous dialysis of many samples. The dialysate from each dialysis unit is consecutively aspirated into the SI flow-line for automated on-line derivatization and absorbance measurement of the derivatized GABA. The developed method provides rapid analysis with high precision and accuracy. Successful validation of the developed method against HPLC was achieved.

5.1.2 Flow-based systems with 3D printed flow cells for quantitative measurement of Albumin in urine based on using the AuNPs-catalyzed chemiluminescence detection.

The flow-based system for the determination of albumin based on chemiluminescence (CL) detection using 3D printed spiral flow cell was successfully developed. The method was possible for on-line determination of urinary albumin and also gave high precision and high accuracy with high throughput.

References

[1] Staden, J.F.V. 1991. "Simultaneous flow-injection analysis of three components with no-line dialyzers in series. Determination of sodium, potassium and chloride in blood serum." **Talanta**. 38(9): 1033–1039.

[2] Silva, F.V., Souza, G.B., Ferraz, L.F.M. and Nogurira, A.R.A. 1999. "Determination of chloride in milk using sequential injection automated conductimetry." **Food Chemistry**. 67: 317–322.

[3] Nacapricha, D., Uraisin, K., Ratanawimarnworng, N. and Grudpan, K. 2004. "Simple and selective method for determination of iodide in pharmaceutical products by flow injection analysis using the iodine–starch reaction." **Analytical and Bioanalytical Chemistry**. 378: 816–821.

[4] Morais, S., Alcaina-Miranda, M.I., Liizaro, F., Planta, M., Maquieira, A. and Puchades, R. 1997. "Evaluation of the dialysing yield of membranes with different composition. Application to the analysis of chloride in fruit juices by flow injection." **Analytica Chimica Acta**. 353: 245–254.

[5] Miro, M. and Frenzel, w. 2003. "A novel flow-through microdialysis separation unit with integrated differential potentiometric detection for the determination of chloride in soil samples." **The Analyst**. 128: 1291–1297.

[6] Miro, M. and Frenzel, w. 2004. "Automated membrane-based sampling and sample preparation exploiting flow-injection analysis." **Trends in Analytical Chemistry**. 23(9): 624–636.

[7] Khuhawar, M.Y. and Rajper, A.D. 2003. "Liquid chromatographic determination of γ-aminobutyric acid in cerebrospinal fluid using 2-hydroxynaphthaldehyde as derivatizing reagent." **Journal of Chromatography B**. 788: 413–418.

[8] Tsukatani, T. and Matsumoto, K. 2005. "Sequential fluorometric quantification of γ-aminobutyrate and L-glutamate using a single line flow-injection system with immobilized-enzyme reactors." **Analytica Chimica Acta**. 546: 154–160.

[9] Jinnarak, A., Anantavichian, P., Intanin, A., Fungladda, S., Choengchan, N., Wilairat, P., Nacapricha, D. and Teerasong, s. 2016. "Sequential injection for determination of gamma-aminobutyric acid based on its effect on second order light scattering of silver nanoparticles." **Journal of Food Composition and Analysis**. 51: 69–75.

[10] Zhang, ZF., Cui, H., Lai, CZ. and Liu, LJ. 2005. "Gold nanoparticle-catalyzed luminol chemiluminescence and its analytical applications." **Analytical Chemistry**. 77: 3324–3329.

[11] Brewer, S.H., Glomm, W.R., Johnson, M.C., Knag, M.K. and Franzen, S. 2005. "Probing BSA binding to citrate-coated gold nanoparticles and surfaces." **Langmuir**. 21: 9303–9307.

[12] Online available: https://en.wikipedia.org/wiki/Gamma-Aminobutyric_acid. Search 21 January 2020.

[13] Ngo, DH. And Vo, T.S. 2019. "An updated review on pharmaceutical properties of gamma-aminobutyric acid." **Molecules**. 24 (15): 2678–2681.

[14] Quinlan, G.J., Martin, G.S. and Evans, T.W. 2005. "Albumin: biochemical properties and therapeutic potential." **Wiley-Interscience**. 41(6): 1211–1219.

[15] Lakshmi, P., Mondal, M., Ramadas, K. and Natarajan, S. 2017. "Molecular interaction of 2,4-diacetylphloroglucinol (DAPG) with human serum albumin (HSA): The spectroscopic, calorimetric and computational investigation." **Spectrochimica Acta Part A: Molecular and Biomolecular Spectroscopy**. 183: 90–102.

[16] Busher, J.T. 1990. "Serum albumin and globulin." Chapter 101. 497-499 in Walker, H.K., Hall. W.D., Hurst, J.W. **Clinical Methods: The History, Physical, and Laboratory Examinations.** 3rd edition. Boston: Butterworths.

[17] National Kidney Foundation. 2007. "KDOQI Clinical practice guidelines and clinical practice recommendations for diabetes and chronic kidney disease." **American Journal of Kidney Diseases.** 49(2): 850-886.

[18] Low, Z.X., Chua, Y.T., Ray, B.M., Mattia, D., Metcalfe, I.S. and Pattersona, D.A. 2017. "Perspective on 3D printing of separation membranes and comparison to related unconventional fabrication techniques." **Journal of Membrane Science**. 523: 596–613.

[19] Waheed, S., Cabot, J.M., Macdonald, N.P., Lewis, T., Guijt, R.M., Paull, B. and Breadmore, M.C. 2016. "3D printed microfluidic devices: enablers and barriers." **Lab on a Chip**. 16: 1993–2013.

[20] Aldstadt, J.H., Olson, D.C., Wolcott, D.K., Marshall, G.D. and Stieg, S.W. 2006. "Flow and sequential injection analysis techniques in process analysis." **Encyclopedia of Analytical Chemistry**. 0: 1–24.

[21] Perkampus, H.H. 1992. "The Bouguer-Lambert-Beer law and its practical application." Chapter 2. 1-3 in **UV-VIS and its applications**. Springer-Verlag.

[22] Online available: https://chem.libretexts.org/Bookshelves/Spectrophotometry. Search: 22 December 2019

[23] Valeur, B. and Berberan-Santos, M.N. 2013. "A brief history of fluorescence and phosphorescence." Chapter 1. 2-17 in **Molecular fluorescence**. Wiley-VCH.

[24] Online available: https://www.shsu.edu/chm_tgc/chemilumdir/JABLONSKI. Html. Search: 11 December 2019

[25] "An Introduction to Fluorescence Spectroscopy." 2000. 1-36 PerkinElmer, Inc.

[26] Online available: http://namrataheda.blogspot.com/spectrofluorimetry.html. Search: 11 June 2019

[27] Garcıa-Campana, A.M., Baeyens, W.R.G. and Zhang, X. 2001. "General principles." Chapter 2. 42-61 in **Chemiluminescence in analytical chemistry**. Marcel Dekker, Inc.

[28] Hayat, A., Jahangir, T.M., Khuhawar, M.Y., Alamgir, M., Siddiqui, A.J. and Musharraf, S.G. 2014. "Simultaneous HPLC determination of gamma amino butyric acid (GABA) and lysine in selected Pakistani rice varieties by pre-column derivatization with 2-Hydroxynaphthaldehyde." **Journal of Cereal Science**. 60 (2): 356–360.

[29] Hayat, A., Jahangir, T.M., Khuhawar, M.Y., Alamgir, M., Hussain, Z., Haq, F.U. and Musharraf, S.G. 2015. "HPLC determination of gamma amino butyric acid (GABA) and some biogenic amines (BAs) in controlled, germinated, and fermented brown rice by pre-column derivatization." **Journal of Cereal Science**. 64: 56–62.

[30] Horanni, R. and Engelhardt, U.H. 2013. "Determination of amino acids in white, green, black, oolong, pu-erh teas and tea products." **Journal of Food Composition and Analysis**. 31(1): 94–100.

[31] Nagul, E.A., Fontàs, C., McKelvie, I.D., Cattrall, R.W. and Kolev, S.D. 2013. "The use of a polymer inclusion membrane for separation and preconcentration of orthophosphate in flow analysis." **Analytica Chimica Acta**. 803: 82–90.

[32] Giakisikli, G., Quezada, A.A., Tanaka, J., Anthemidis, A.N., Murakami, H., Teshima, N. and Sakai, T. 2015. "Automatic on-line solid-phase extraction-electrothermal atomic absorption spectrometry exploiting sequential injection analysis for trace vanadium, cadmium and lead determination in human urine Samples." **Analytical Sciences**. 31: 383–389.

[33] Staden, J.F.V. 2006. "Flow-injection analysis of chloride in milk with a dialyzer and a coated tubular inorganic chloride-selective electrode." **Analytical Letters**. 19(13-14): 1407–1419.

[34] Qin, W., Dan, W., Bin, D., Zaijun, L. and Yanqiang, H. 2006. "A spectrophotometric method for determination of total proteins in cow milk powder samples using the o-nitrophenylfluorone/Mo (VI) complex." **Journal of Food Composition and Analysis**. 19: 76–82.

[35] Zhong, H., Li, N., Zhao, F. and Li, K.A. 2004. "Determination of proteins with Alizarin Red S by Rayleigh light scattering technique." **Talanta**. 62: 37–42.

[36] Devi, L.B., Berchmans, S. and Mandal, A.B. 2012. "Highly sensitive detection of proteins using voltammetric assay in the presence of silver nanostructures." **Journal of Electroanalytical Chemistry**. 665: 20–25.

[37] Deftereos, N.T., Grekas, N. and Calokerinos, A.C. 1999. "Flow injection chemiluminometric determination of albumin." **Analytica Chimica Acta**. 403: 137–143.

[38] Wang, Y. and Ni, Y. 1999. "Combination of UV–vis spectroscopy and chemometrics to understand protein–nanomaterial conjugate: A case study on human serum albumin and gold nanoparticles." **Talanta**. 119: 320–330.

[39] Iosin, M., Canpean, V. and Astilean, S. 2011. "Spectroscopic studies on pH- and thermally induced conformational changes of Bovine Serum Albumin adsorbed onto gold nanoparticles." **Journal of Photochemistry and Photobiology A: Chemistry**. 217: 395–401.

[40] Kimling, J., Maier, M., Okenve, B., Kotaidis, V., Ballot, H. and Plech, A. 2006. "Turkevich Method for Gold Nanoparticle Synthesis Revisited." **The Journal of Physical Chemistry B**. 110: 15700–15707.

[41] Miller, J.N. and Miller, J. C. 1993. **Statistics and chemometrics for analytical chemistry**. 4th edition. London: Pearson Education.

[42] Zhao, P., Li, N. and Astruc D. 2013 “State of the art in gold nanoparticle synthesis.” **Coordination Chemistry Reviews**. 257: 638-665.

[43] Brewer, S.H., Glomm, W.R., Johnson, M.C., Knag, M.K. and Franzen, S. 2005. “Probing BSA binding to citrate-coated gold nanoparticles and Surfaces.” **Langmuir**. 21: 9303-9307.

Appendix

Appendix A1

International publication

Analytica Chimica Acta 1097 (2020) 103–109

Contents lists available at ScienceDirect

Analytica Chimica Acta

journal homepage: www.elsevier.com/locate/aca

Towards direct analysis of solid and liquid samples exploiting a 3D printed dialysis unit and sequential injection: Application for automated derivatization and determination of gamma-aminobutyric acid in foodstuff and beverages

Bhoonnarasa Kasetsoontorn [a, b], Nathawut Choengchan [a, b, *]

[a] Flow Innovation-Research for Science and Technology Laboratories (FIRST Labs), Bangkok, Thailand
[b] Department of Chemistry and Applied Analytical Chemistry Research Unit, Faculty of Science, King Mongkut's Institute of Technology Ladkrabang, Chalongkrung Road, Ladkrabang, Bangkok, 10520, Thailand

HIGHLIGHTS

- A new design of a 3D printed dialysis unit was successfully applied for direct analysis of gamma-aminobutyric acid (GABA) in solid foodstuffs and beverages.
- A stainless steel sieve placed inside the donor chamber effectively prevents clogging of the dialysis membrane by the sample matrices.
- Multiple dialysis units were integrated to the sequential injection (SI) system so that consecutive dialysis of samples could be achieved.
- The dialysate was aspirated into the SI system for automated derivatization and spectrophotometric measurement within less than 1.0 min.

ARTICLE INFO

Article history:
Received 14 May 2019
Received in revised form
30 October 2019
Accepted 31 October 2019
Available online 2 November 2019

Keywords:
3D printing
Dialysis
Direct analysis
Automated derivatization
Sequential injection
GABA

ABSTRACT

In this work, a new design of a dialysis unit for direct analysis of solid and liquid samples is presented. The homemade unit was constructed using a 3D printer due to its simple and fast fabrication ability. The dialysis unit is composed of cylindrical-shaped donor and acceptor chambers. A stainless steel sieve is installed inside the donor chamber. SEM images clearly showed that the sieve prevented membrane blockage by suspension particles in the sample. Multiple dialysis units were connected to a sequential injection (SI) system for serial determination of gamma-aminobutyric acid (GABA) in solid and liquid samples. The dialysate from each dialysis unit was consecutively aspirated into the SI flow line for on-line derivatization of GABA with 2-hydroxy-1-naphthaldehyde (3.0% w/v). The derivative was detected spectrophotometrically at 425 nm. The linear calibration range extended to 1000 mg L^{-1} GABA ($r^2 > 0.99$) with high precision (1.2 %RSD). The developed system was applied to analysis of dietary supplements, grains of germinated brown rice and milk. The samples were directly introduced into the donor chamber either as powder or liquids. The measured GABA content using the developed method was compared using high performance liquid chromatography, with good agreement using Pearson's correlation ($r^2 = 0.9999$). The method has high accuracy based on recovery studies (99.8 ± 1.5%) and high sample throughput (64 samples h^{-1}).

1. Introduction

The direct analysis of samples has always been a challenge for analytical chemists. Usually a pre-treatment/preparation step is required to achieve the desired selectivity [1–3]. Dialysis using membrane is one of the sample clean-up methods for separating low-molecular weight analytes from interfering macromolecules, colloids and suspended particles in the sample matrix [1].

Various designs of dialysis units have been reported. With regards to flow analysis, the majority of the dialysis units have the sandwich design with rectangular geometry [4,5]. A flat sheet of

* Corresponding author. Flow Innovation-Research for Science and Technology Laboratories (FIRST Labs), Bangkok, Thailand.
E-mail address: nchoengchan@gmail.com (N. Choengchan).

https://doi.org/10.1016/j.aca.2019.10.074
0003-2670/

hydrophilic membrane is placed between the upper and the lower plates. The use of this sandwich-type dialysis unit as part of the flow system was shown to be very effective for removing particulate matter in liquid samples, such as serum [6], milk [7,8], pharmaceutical products [9] and fruit juices [10]. Some study employed a concentric-type dialysis unit [5] or a microdialyser [11] for analysis of solids. However, the devices were not suitable for direct analysis. Prior sample preparation was necessary before the devices could be applied. Therefore, in this work, we designed a new dialysis unit suitable for direct analysis of solids. The unit comprises cylindrical-shaped donor and acceptor chambers. In contrast to the other dialysis units, this unit incorporates a stainless steel sieve inside the donor chamber. Using this feature, clogging of the membrane by macromolecules in sample matrices was eliminated. The dialysis unit was constructed using 3D printing based on stereolithography [12–14]. The advantage of 3D printing is its capability to construct components that cannot be easily manufactured using conventional means [14]. It is a one-step production process suitable for producing prototypes with low running costs.

Gamma-aminobutyric acid (GABA) has been considered as a health promoting substance that can reduce anxiety and promote relaxation [15]. Various analytical methods have been employed for the quantitative analysis of GABA, including high performance liquid chromatography (HPLC) [16–19], flow injection (FI) [20] and sequential injection (SI) [21]. The chromatographic techniques provide high selectivity but the flow-based methods offer rapid determination. Nevertheless, all these methods are not applicable for the direct analysis of samples. Sample preparation protocols with extensive time and labour are required. In this work, samples are directly transferred into the dialysis unit as powder or liquids. The unit was integrated with a SI system for on-line derivatization of GABA using 2-hydroxy-1-naphthaldehyde (HN) as the derivatizing reagent. The derivative was monitored at 425 nm. Application to solid samples, including GABA-supplemented tablets/capsules, grains of germinated brown rice and green tea powder were studied and also GABA-enriched milk as an example of turbid coloured liquid.

2. Experimental

2.1. Reagents and samples

All chemicals were of analytical reagent grade. Deionized-distilled water (18 MΩ cm) was from a Zeneer UP 900 water purification system (Human Corporation, Seoul, Korea). The derivanzing solution (3% w/v) was prepared by dissolving 0.75 g of 2-hydroxy-1-naphthaldehyde (Sigma Aldrich, USA) in 25.00 mL of acetonitrile (RCI Labscan, Thailand). A stock standard solution of 2000 mg L^{-1} GABA was prepared by dissolving 0.0508 g of GABA (Sigma Aldrich, USA) in 25.00 mL of Britton-Robinson buffer (pH 5.0). The buffer was prepared by mixing 0.05 mol L^{-1} sodium hydroxide (Sigma Aldrich, USA), 0.03 mol L^{-1} acetic acid (RCI Labscan, Thailand), 0.03 mol L^{-1} phosphoric acid (Sigma Aldrich, USA) and 0.03 mol L^{-1} boric acid (Sigma Aldrich, USA). The working standard solutions were freshly prepared using appropriate dilution of the stock GABA solution with the buffer solution.

Nine samples of GABA-supplemented tablets/capsules, germinated brown rice, instant green tea powder and GABA-enriched milk were employed for the method validation. All samples were commercially available in local drug stores and supermarkets in Bangkok, Thailand. These samples were chosen to demonstrate the suitability of the developed method for direct analysis of both solid and turbid liquid samples. The samples were directly transferred into the donor chamber without any sample preparation except for grinding the tablets and rice grains.

2.2. Fabrication of the 3D printed dialysis unit

The photograph and schematic drawing of the homemade 3D printed dialysis unit for the direct analysis of the samples are depicted in Fig. 1A and B, respectively. The unit was made from poly(methyl methacrylate) (PMMA), using bis-acylphosphine oxide (Sigma-Aldrich, USA) and acrylonitrile butadiene styrene (Dynalon, USA) as the photo-initiator and additive, respectively. The unit was fabricated using a computer-aided design (CAD) (Fig. 1S, SketchUp 8™ software). This image file was converted to an STL file and digitally sliced into multiple 2D layers prior to its export for fabrication by the 3D printer (KINGS600, China.) The printer uses an Nd:YVO4 solid-state laser (355 nm) as the light source and a fixed scanning speed of 10.0 m s^{-1}.

2.3. The SI system and working flow

The SI system for the automated on-line derivatization and determination of GABA is presented in Fig. 2A. PTFE tubing (1.0 mm i.d.) was employed to construct the manifold. The lengths of the holding and the mixing coils were 25 cm and 50 cm, respectively. The SI assembly comprised a PSD-4 syringe pump (SP), equipped with a 12.5-mL glass syringe and an 8-port multi-selection valve (MV). Both the SP and MV were purchased from Hamilton Company (Reno, Nevada, USA). Spectrophotometric detection at 425 nm was carried out using a Jasco V630 UV–visible spectrophotometer (D) (Tokyo, Japan), which was equipped with a 10-mm flow cell (18-μL, Phillips, USA). The 3D printed dialysis units (DU) were integrated into the SI system (see Fig. 2A). While dialysis in DU#1 was proceeding, the dialysis procedure for samples in dialysis units, DU#2 to DU#5, was consecutively conducted. This strategy provides more rapid analysis for routine work with a large number of samples.

All the operational sequences of the SI method were controlled using the Auto-Pret™ software (MKC Company, Japan). Details of the sequence are given in Table 1 and Fig. 2B. Briefly, the system was prefilled with the carrier, C (acetonitrile). Aliquots of 25 μL of the dialysate and 30 μL of HN were sequentially aspirated into the holding coil (HC). By reversing the pump flow and selecting the appropriate position of the MV port, the zone of the reaction mixture was propelled to the mixing coil (MC) and subsequently to the flow-cell of the spectrophotometer (D). The absorbance of the derivative was monitored at 425 nm. The entire sequence for the on-line derivatization and absorbance measurement were completed in less than 1.0 min.

2.4. Dialysis procedure

The dialysis procedure is started by transferring an accurate weight of the sample powder into the donor chamber and then the small magnetic bar, followed by the stainless steel sieve (30 mm i.d., 0.33 mm thickness) (Fig. 1). An aliquot of 6.0 mL of Britton-Robinson buffer (pH 5.0) was then added. A cellulose acetate membrane (Metrohm™, 0.2 μm pore size, 30 mm i.d. and 115 μm thickness) was placed between the donor and acceptor chambers. A smaller magnetic bar was placed onto the membrane (Fig. 2C) for homogeneous mixing of the dialysate. The top lid was then screwed on to the body. An aliquot of 1.5 mL of the acceptor solution (Britton-Robinson buffer, pH 5.0) was pipetted into the assembled unit via 'Hole-2' in the lid (Fig. 2C). Finally, the dialysis unit was fixed firmly on a magnetic stirrer (Heidolph, Schwabach, Germany) and connected to the SI system. At exactly 5.0 min after the start of the dialysis process, 25 μL of the dialysate was aspirated into the SI flow-line for on-line derivatization and absorbance measurement. For the milk sample, the experimental procedure is the same as for the solid, but an aliquot of 6.0 mL of a sample solution was pipetted into the donor chamber instead.

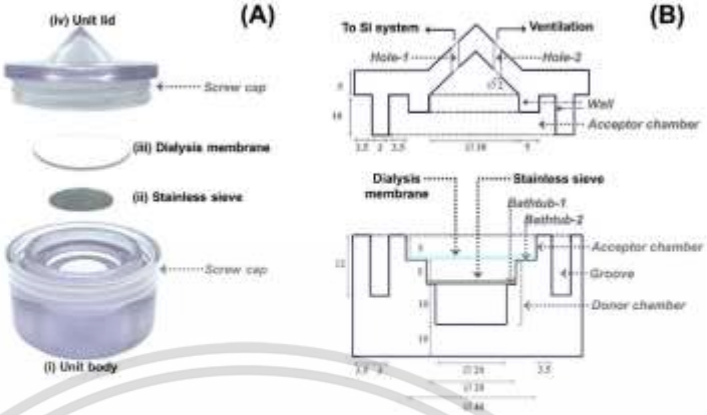

Fig. 1. (A) Photograph and (B) schematic drawing of the homemade 3D printed dialysis unit for direct analysis of samples. Note: All dimensions in Fig. 1(B) are in unit of mm.

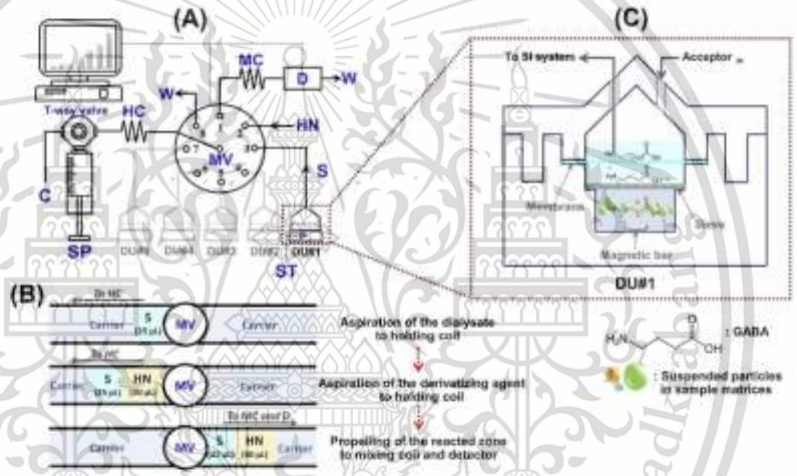

Fig. 2. (A) The SI system with the 3D printed dialysis unit for automated on-line derivatization and absorbance measurement of derivatized GABA. SP: Syringe pump, MV: 8-port multi-selection valve, D: UV–visible spectrophotometer (λ = 425 nm), ST: Magnetic stirrer, HC: Holding coil (25 cm), MC: Mixing coil (50 cm), DU: an homemade 3D printed dialysis unit, C: Carrier (acetonitrile), S: Dialysate, HN: 3% (w/v) of 2-hydroxy-1-naphthaldehyde in acetonitrile, W: Waste. (B) Schematic of the sequence of the multi-selection valve, direction of carrier flow and the resulting zones of dialysate sample (S) and derivatizing reagent (HN). (C) Schematic drawing of the closed 3D printed dialysis unit showing the position of the stainless steel sieve, the cellulose dialysis membrane, the two magnetic stirring bars, the sample and dialysate solutions and the two narrow vertical vents in the central section of the lid.

Table 1
Operational sequence of the SI method for one complete measurement cycle.

Step	SP		Flow rate (μL s^{-1})	MV port	Volume (μL)	Action
	Piston Position	T-way Connection				
1	down	left	400	–	1000	Suction of the carrier into the syringe
2	down	right	10	3[a]	25	Aspiration of the dialysate from the dialysis unit No.1 (DU#1 in Fig. 2A) into the holding coil
3	down	right	10	2	30	Aspiration of the derivatizing solution (HN) into the holding coil
4	up	right	150	1	1055	Propelling of the reacted zone through the mixing coil (MC) into the detector (D)

[a] The port was consecutively switched to No. 4–7 when the following dialysis units (Fig. 2A) were employed.

2.5. HPLC measurements

A reversed-phase HPLC method [16] was employed as a comparison method. Nylon membrane filter (0.45-μm, Sigma-Aldrich, USA) was used throughout. The steps for the sample preparation were as follows: 0.3182 g of GABA-supplemented powder was dissolved in 25.0 mL of DI water. The solution was centrifuged at 1500 rpm for 10 min (Spectrafuge™ Model 6C, Labnet International Inc., NJ, USA) and the supernatant filtered. For the germinated brown rice, 0.2534 g of ground sample was added to 800 μL of 70% (v/v) ethanol. The solution was vortexed mixed (Vortex Genie 2, Scientific Industries, Inc., NY, USA) for 1 min at ambient temperature and then centrifuged at 14000 rpm (4 °C) for 10 min (Kubota 3700 micro refrigerated centrifuge, Tokyo, Japan) and the supernatant filtered. For instant green tea powder, 3.0823 g of sample was infused with 100.0 mL of water (60 °C). The solution was cooled down to the ambient temperature prior to being filtered. For GABA-enriched milk, 4.0 mL of the sample was acidified by adding 2.5 mL of 3% (v/v) acetic acid (RCI Labscan, Thailand). The solution was vortexed and kept for 15 min before centrifuging at 1500 rpm for 10 min, and the supernatant filtered.

Batch wise derivatization was performed by pipetting either 1.0 mL of GABA standard solution or the final filtered supernatant of a sample into a 5.0-mL glass vial. Aliquots of 0.6 mL of borate buffer (pH 8.0) and 2.0 mL of HN (0.3% w/v in methanol) were added. The solution was vortexed and heated at 80 °C for 10 min using a heated bath (IKA®, C-MAG, HS7, KL, Malaysia). The mixture was cooled down before adjusting to the final volume of 10.0 mL with methanol. The solution was injected into the HPLC system (Waters, model 486 with UV detector) using the following conditions: injection volume of 5 μL, guard column (C18, 20 mm × 3.9 mm i.d.), analytical column (Phenomenex C18, 150 mm × 4.6 mm i.d., 5 μm particle), mobile phase of methanol-water at 60:40 (v/v) at flow rate of 1.0 mL min^{-1} (isocratic elution) and detection wavelength of 330 nm.

3. Results and discussion

3.1. Design of the homemade 3D printed dialysis unit

Fig. 1A and B are the photograph and schematic drawing of the homemade 3D printed dialysis unit, respectively. The unit is composed of four key components (from bottom to top): (i) the unit body, (ii) the stainless steel sieve, (iii) the dialysis membrane and (iv) the unit lid. The lid is screwed on to the body for rapid opening and closing. This design allows for easy addition of solid or liquid sample into the unit.

The unit body comprises the cylindrical-shaped donor and acceptor chambers. The donor chamber is designed as having two 'bathtubs', as shown in Figs. 1B and 2S. 'Bathtub-1' and 'Bathtub-2' are employed for placing the stainless steel sieve and the dialysis membrane, respectively. This stainless steel sieve is an important component that allows for direct analysis of solids since it prevents macromolecules in sample matrices from contacting the membrane. This is confirmed by the SEM images in Fig. 3A and B that clearly show that, without the sieve, clogged membrane surface is observed. This strongly affects the function of the membrane resulting in decreased efficiency of mass transfer during dialysis.

The unit lid is designed in a cylindrical configuration to screw on to the unit body but with a cone at the top (Fig. 1B). There are two small holes in the cone section of the lid. 'Hole-1' is used for inserting a PTFE tube (0.1 mm i.d., 100 mm length) for withdrawing the dialysate into the SI system. 'Hole-2' serves two purposes: (i) as a ventilator for preventing excessive build-up of pressure inside the unit during the dialysis process and (ii) as the channel for pipetting the acceptor solution into the unit (Fig. 2C). Beneath the cone section of the lid, there is a cylindrical wall (Figs. 1B and 2S). This wall gives tight fitting of the lid into the groove of the unit body and to press the membrane on to 'Bathtub-2'. This keeps the membrane taut and rigid.

3.2. Optimization of conditions of dialysis process

3.2.1. Volume of acceptor solution

In this study, standard solutions of GABA (50–1000 mg L^{-1}) and Britton-Robinson buffer (pH 5.0) were employed as the donor and the acceptor solutions, respectively. The effect of the volume of the acceptor was studied with the donor volume kept constant at 6.0 mL (the maximum volume in the donor chamber). This volume of the donor solution allows the donor solution to reach the surface of the hydrophilic membrane in order for dialysis to take place. Fig. 3S(A) shows that the sensitivity (slope of the calibration line) rapidly decreases with increasing acceptor volume due to dilution effect. The highest sensitivity is obtained at 1.5 mL, and this volume was selected. An acceptor volume of 1.0 mL was also employed. However the level of the acceptor solution was very small, resulting in air bubbles being drawn into the SI flow line when the dialysate was aspirated leading to disturbance to the derivatization and absorbance measurement. In principle the acceptor volume of 1.5 mL gives a 4-fold pre-concentration factor. This is very useful for the analysis of the samples containing very low GABA content.

3.2.2. Dialysis time and stirring speed

The dialysis time is defined as the time interval from the start of stirring of the sample solution in the donor chamber until it is stopped. The effect of dialysis time was studied using 6.0 mL of calibrators (50–1000 mg L^{-1} GABA) and 1.5 mL of Britton-Robinson buffer (pH 5.0) as the donor and acceptor solutions, respectively. The results in Fig. 3S(B) show that the sensitivity is improved as the dialysis time is increased. However sample throughput is reduced. As a compromise between sensitivity and throughput, a dialysis time of 3.0 min was chosen.

The effect of stirring speed was examined using 6.0 mL of 200 mg L^{-1} GABA. The results in Fig. 3S(C) show that increasing the stirring speed enhances the absorbance reading. This is because the efficiency of the dialysis process is typically enhanced by mechanical stirring to promote the convective-controlled mass transport. However at the highest setting (2200 rpm), there was turbulence of donor solution and also the magnetic bar was unstable and collided with the metal sieve. The speed of 1700 rpm was therefore chosen.

3.3. Factors affecting the derivatization reaction

3.3.1. Effect of pH of the acceptor solution

Since the reaction between GABA (a primary amine) and HN (an aldehyde) is a pH dependent process, a pH range of 1–10 of the acceptor buffer solution was investigated, at unit pH interval. The results in Fig. 4S(A) show that sensitivity increases sharply from pH of 1–4 and then remaining unchanged from pH 5 to 10. At low pH, the amine group of GABA is converted to the ammonium ion and becomes non-nucleophilic. At higher pH, there is not enough acid to protonate the hydroxyl group of the intermediate to allow for the removal of water (see the reaction mechanism in Fig. 5S for more details). Therefore, a pH of 5 was considered suitable.

3.3.2. Concentration of 2-hydroxy-1-naphthaldehyde (HN)

The results in Fig. 4S(B) show that the sensitivity is considerably enhanced by increasing the concentration of HN from 0.3 to 3.0% (w/v) but does not differ from 3.0 to 6.0% (w/v), respectively. As a

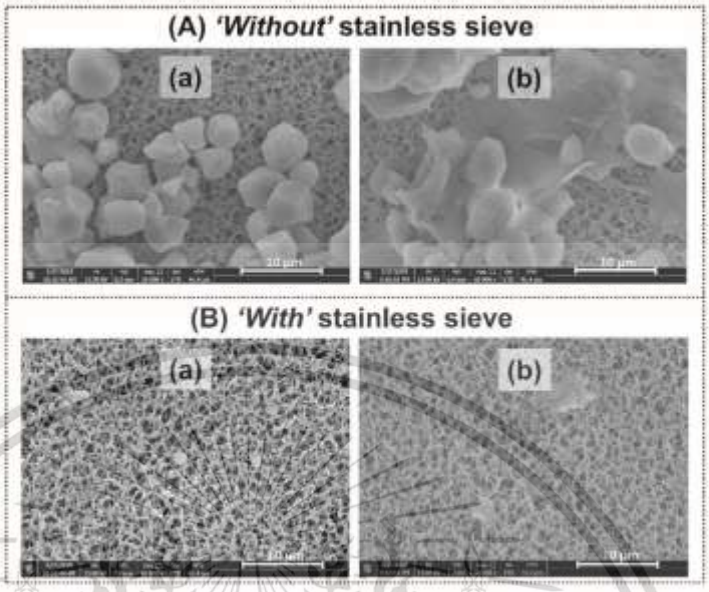

Fig. 3. SEM images of the cellulose dialysis membrane; (A) without and (B) with the stainless steel sieve after analyses of ground (a) GABA-supplemented tablet and (b) germinated-brown rice.

compromise between the sensitivity and the reagent consumption, the concentration of 3.0% (w/v) was selected.

3.4. Optimization of the SI system

3.4.1. Aspirated volume

The effect of the aspirated volume of the dialysate was studied while keeping the volume of HN in the flow-line fixed at 30 μL. The results in Fig. 6S(A) indicate that the sensitivity increases slightly before reaching a plateau value at 25 μL. This may be because of insufficient amount of the derivatizing agent when using higher volume of the dialysate. The aspirated volume of the dialysate of 25 μL was therefore selected and employed in the following study. As expected, the sensitivity significantly increases with increasing volume of the derivatizing solution (Fig. 6S(A)). However the baseline shift due to a layer of the sample zone remaining on the window of the flow-through cell was observed at high volume (35 and 40 μL). Therefore, the aspirated volume of the HN solution was set at 30 μL (with the aspirated volume of the dialysate of 25 μL).

3.4.2. Mixing coil length

The results in Fig. 6S(B) shows that the use of the mixing coil (50 cm), as compared to having no coil, gives higher sensitivity as the mixing process is more efficient. However the sensitivity decreases when the length of the length was increased due to dispersion effect; also a longer coil results in a lower sample throughput. Thus the mixing coil of 50 cm length was employed in the final system.

3.4.3. Dispensing flow rate

The results in Fig. 6S(C) show that at faster flow rates sensitivity only gradually increases whilst the sample throughput increases in proportion with the flow rate. The flow rate of 150 μL s^{-1} was selected since it offers the highest sensitivity and sample throughput. At this flow rate, the sample throughput of 64 samples h^{-1} is achieved.

3.5. Analytical performance

Under the optimal conditions listed in Table 2, a linearity range of 10–1000 mg L^{-1} GABA was obtained with reproducible signal profiles (Fig. 7S). The detection limit (3SD of blank) is 0.14 mg L^{-1} which is sensitive enough to determine the GABA content in dietary supplements and beverages. However the colorimetric detection might not be sufficiently sensitive to analyze low concentrations of GABA found in biological samples [16,19,20]. In order to employ this developed method for these kinds of samples, a pre-concentration step may be required.

Using the SI system, rapid and repeatable measurements were achieved (<1.0 min $sample^{-1}$) with high precision (1.2 %RSD, 15 injections of 10 mg L^{-1} GABA). Furthermore, the SI system allows simultaneous dialysis of many samples. This strategy provides rapid measurements, which is necessary for routine application.

Comparison of this method with other analytical methods in the literature is shown in Table 1S. In Table 1S the methods are categorized as non-derivatization and derivatization methods. For the non-derivatization methods, it was necessary to use either an enzyme reactor [20] or modified heavy metal nanoparticles (chemosensors) [21] to improve the selectivity. Amongst the derivatization methods which employed HN as the derivatizing reagent [16–18], our analytical procedure was simpler and faster. This is because the SI system offers automated on-line derivatization and measurement. The derivatization reaction was carried out under mild condition without heating eliminating the problem of air bubbles being generated.

The unique feature of this method is that with our design of the

Table 2
Summary of the optimization study and the selected parameter value.

Parameter		Studied range	Selected value
(1)	The dialysis procedure		
	(1.1) Acceptor volume (mL)	1.5–6.0	1.5
	(1.2) Dialysis time (min)	1.0–10	5.0
	(1.3) Stirring speed (rpm)	440–2200	1700
(2)	Factors affecting derivatization reaction		
	(2.1) pH of the derivatizing reagent	1.0–10.0	5.0
	(2.2) Concentration of the derivatizing reagent (% w/v)	0.3–6.0	3.0
(3)	The SI system		
	(3.1) Aspirated volume of dialysate (μL)	10–35	25
	(3.2) Aspirated volume of the derivatizing reagent (μL)	10–35	30
	(3.3) Length of mixing coil (cm)	0–400	90
	(3.4) Dispensing flow rate (μL sec $^{-1}$)	25–150	150

3D printed dialysis unit, direct analysis of solid and liquid samples is possible without sample preparation, except grinding of the solid samples. This is because installing the stainless steel sieve inside the donor chamber prevents clogging of the dialysis membrane by colloidal matters. Turbid and coloured liquid samples can also be directly analysed.

3.6. Effects of coexisting interferences

In this work, compounds that are found in the samples [22–24], including milk, rice and tea, and which may cause interference with this method, were selected and investigated using 50 mg L $^{-1}$ GABA. The tolerance limit is the maximum concentration of the spiked compound giving the measured absorbance for GABA which does not lie outside the range of mean ± 3SD of the absorbance value for the standard 50 mg L $^{-1}$ GABA. As shown in Table 3, the tolerance limits for all investigated interferences are higher than the concentrations that may exist in samples [22–24]. This suggests that the developed method is not affected by these compounds.

3.7. Application to sample and validation

To verify that developed method is fit for the purpose, it was applied to analysis of nine samples, including GABA-supplemented tablets/capsules, grains of germinated brown rice, instant green tea powder and GABA-enriched milk. Recovery study was first carried out. Standard solution of GABS was added to the sample in the donor chamber to give the spiked concentration of 50 mg L $^{-1}$. It is observed in Table 4 that the recoveries ranged from 97.4 to 102.2% (mean recovery: 99.8% ± 1.5). This result demonstrates that the method is free from sample matrix effect.

The GABA contents determined using the developed method and the reversed-phase HPLC, were compared and the results are listed in Table 5. The results are not significantly different using the Pearson linear regression test ($r^2 = 0.9999$) [25]. The GABA contents are compared to the label values and they are in good agreement.

Table 3
Tolerance limit of the interfering compounds.

Coexisting interferences	Tolerance limit (mg L $^{-1}$)
Isoleucine, Methionine, Serine, Threonine	100
Phenylalanine, Tryptophan, Arginine, Histidine	200
Leucine, Valine, Glutamic acid, Vitamin B12	300
Lysine	500
Aspartic acid	1000

Table 4
Percentage recovery of spiked GABA using the developed SI system.

Sample	GABA concentration in mg L $^{-1}$ (mean ± SD, n = 3)			Percentage recovery (%)
	Original	Added	Found	
GABA supplement-1(Tablet)	98.5 ± 0.3	50.0	149.3 ± 0.5	99.6
GABA supplement-2 (Capsule)	201.4 ± 1.0	50.0	251.3 ± 0.3	99.8
GABA supplement-3 (Capsule)	502.7 ± 0.5	50.0	552.3 ± 0.2	99.2
GABA supplement-4 (Capsule)	500.3 ± 0.1	50.0	549.9 ± 0.1	99.2
GABA supplement-5 (Capsule)	750.9 ± 0.6	50.0	801.7 ± 0.4	101.6
GABA-enriched milk-1	14.7 ± 0.3	50.0	63.4 ± 0.1	97.4
GABA-enriched milk-2	11.5 ± 0.1	50.0	61.0 ± 0.5	99.0
Germinated-brown rice	20.7 ± 0.5	50.0	71.8 ± 0.3	102.2

Table 5
Comparison of the GABA content in foodstuff and beverages determined by the developed SI system and the HPLC method.

Sample	GABA content (mean ± SD, n = 3)		Label value
	This work	HPLC method	
GABA supplement-1(Tablet)	98.5 ± 1.3	100.8 ± 0.03	100[a]
GABA supplement-2 (Capsule)	202.4 ± 2.0	202.9 ± 0.5	200[b]
GABA supplement-3 (Capsule)	502.7 ± 1.5	499.9 ± 1.4	500[b]
GABA supplement-4 (Capsule)	500.3 ± 2.1	498.6 ± 2.4	500[b]
GABA supplement-5 (Capsule)	743.4 ± 1.6	751.9 ± 0.2	750[b]
GABA-enriched milk-1	3383.5 ± 0.3	3519.0 ± 0.01	3,412[c]
GABA-enriched milk-2	2637.3 ± 0.1	2645.0 ± 0.02	2,656[c]
Germinated brown rice	31.6 ± 0.5	30.4 ± 0.04	30.5[d]
Instant green tea powder	20.1 ± 0.1	20.7 ± 0.6	20[e]

Note: The GABA contents are.
[a] : mg tablet $^{-1}$,
[b] : mg capsule $^{-1}$,
[c] : μg carton $^{-1}$,
[d] : mg 100 g $^{-1}$ and,
[e] : mg pack $^{-1}$.

4. Conclusions

The new 3D printed dialysis unit was designed and was effectively applied for the direct analysis of solid and liquid samples. Using 3D printing technology, the homemade dialysis unit was easily and rapidly fabricated. By adding a stainless steel sieve inside the donor chamber, the problem of the clogging of the dialysis membrane by suspended particulates or macromolecules in the sample matrices was eliminated. More than one 3D printed dialysis unit can be incorporated with the SI system for simultaneous dialysis of many samples. The dialysate from each dialysis unit is consecutively aspirated into the SI flow-line for automated on-line derivatization and absorbance measurement of the derivatized GABA. The developed method provides rapid analysis with high precision and accuracy.

Declaration of competing interest

The authors declare that they have no known competing financial interests or personal relationships that could have appeared to influence the work reported in this paper.

Acknowledgements

This work was financial supported by research grants from the National Research Council of Thailand and the Faculty of Science at King Mongkut's Institute of Technology Ladkrabang (KMITL) (to NC). The authors would also like to thank FIRST Labs @ KMITL and the Applied Analytical Chemistry Research Unit in the Department of Chemistry, Faculty of Science, KMITL for the instrumental and analytical support. The authors would also like to express our appreciation to Ms. Chayada Chiochan for her contribution to the fabrication of the 3D printed dialysis unit and to Assoc. Prof. Dr. Prapin Wilairat for editing the English of this article.

Appendix A. Supplementary data

Supplementary data related to this article can be found at https://doi.org/10.1016/j.aca.2019.10.074.

References

[1] J.F. van Staden, Membrane separation in flow injection systems. part 1. dialysis, Fresenius J. Anal. Chem. 352 (1995) 271–302.
[2] E.A. Nagul, C. Fontàs, I.D. McKelvie, R.W. Cattrall, S.D. Kolev, The use of a polymer inclusion membrane for separation and preconcentration of orthophosphate in flow analysis, Anal. Chim. Acta 803 (2013) 82–90.
[3] K. Grudpan, A.A. Quezada, J. Tanaka, A.N. Anthemidis, H. Murakami, N. Teshima, T. Sakai, Automatic on-line solid-phase extraction-electrothermal atomic absorption spectrometry exploiting sequential injection analysis for trace vanadium, cadmium and lead determination in human urine samples, Anal. Sci. 31 (2015) 383–389.
[4] Z.L. Fang, Flow Injection and Preconcentration, VCH publishers, Weinheim, 1993, Ch. 6.
[5] M. Miró, W. Frenzel, Automated membrane-based sampling and sample preparation exploiting flow-injection analysis, Trends Anal. Chem. 23 (2004) 624–636.
[6] J.F. van Staden, Simultaneous flow – injection analysis of three components with on – line dialyzer in series. Determination of sodium, potassium and chloride in blood serum, Talanta 38 (1991) 1033–1039.
[7] F.V. Silva, G.B. Souza, L.F.M. Ferraz, A.R.A. Nogueira, Determination of chloride in milk using sequential injection automated conductimetry, Food Chem. 67 (1999) 317–322.
[8] J.F. van Staden, Flow-injection analysis of chloride in milk with a dialyzer and a coated tubular inorganic chloride-selective electrode, Anal. Lett. 19 (1986) 1407–1419.
[9] D. Nacapricha, K. Uraisin, N. Ratanawimarnwong, K. Grudpan, Simple and selective method for determination of iodide in pharmaceutical products by flow injection analysis using the iodine–starch reaction, Anal. Bioanal. Chem. 378 (2004) 816–821.
[10] S. Morais, M.L. Alcaina-Miranda, F. Lazaro, M. Planta, A. Maquieira, R. Puchades, Evaluation of the dialysing yield of membranes with different composition. Application to the analysis of chloride in fruit juices by flow injection, Anal. Chim. Acta 353 (1997) 245–254.
[11] M. Miró, W. Frenzel, A novel flow-through microdialysis separation unit with integrated differential potentiometric detection for the determination of chloride in soil samples, Analyst 128 (2003) 1291–1297.
[12] B. Gross, S.Y. Lockwood, D.M. Spence, Recent advances in analytical chemistry by 3D printing, Anal. Chem. 89 (2017) 57–70.
[13] V. Cerdà, J. Avivar, D. Moreno, Chips: how to build and implement fluidic devices in flow-based system, Talanta 166 (2017) 412–419.
[14] D.J. Cocovi-Solberg, P.J. Worsfold, M. Miró, Opportunities for 3D printed microfluidic platforms incorporating sample handling and separation, Trends Anal. Chem. 108 (2018) 13–22.
[15] A.M. Abdou, S. Higashiguchi, K. Horie, M. Kim, H. Hatta, H. Yokogoshi, Relaxation and immunity enhancement effects of gamma-aminobutyric acid (GABA) administration in humans, Biofactors 26 (2006) 201–208.
[16] M.Y. Khuhawar, A.D. Rajper, Liquid chromatographic determination of γ-aminobutyric acid in cerebrospinal fluid using 2-hydroxynaphthaldehyde as derivatizing reagent, J. Chromatogr. B 788 (2003) 413–418.
[17] A. Hayat, T.M. Jahangir, M.Y. Khuhawar, M. Alamgir, A.J. Siddiqui, S.G. Musharraf, Simultaneous HPLC determination of gamma amino butyric acid (GABA) and lysine in selected Pakistani rice varieties by pre-column derivatization with 2-Hydroxynaphthaldehyde, J. Cereal Sci. 60 (2014) 356–360.
[18] A. Hayat, T.M. Jahangir, M.Y. Khuhawar, M. Alamgir, Z. Hussain, F.U. Haq, S.G. Musharraf, HPLC determination of gamma amino butyric acid (GABA) and some biogenic amines (BAs) in controlled, germinated, and fermented brown rice by pre-column derivatization, J. Cereal Sci. 64 (2015) 56–62.
[19] C.K. Zacharis, G.A. Theodoridis, A.N. Voulgaropoulos, On-line coupling of sequential injection with liquid chromatography for the automated derivatization and determination of γ-aminobutyric acid in human biological fluids, J. Chromatogr. B [illegible] (2004) 169–175.
[20] T. Tsukatani, K. Matsumoto, Sequential fluorometric quantification of γ-aminobutyrate and L-glutamate using a single line flow-injection system with immobilized-enzyme reactors, Anal. Chim. Acta 546 (2005) 154–160.
[21] A. Jumrat, P. Anantawichai, A. Infanis, S. Fungladda, N. Choengchan, P. Wilairat, D. Nacapricha, S. Teerasong, Sequential injection for determination of gamma-aminobutyric acid based on its effect on second order light scattering of silver nanoparticles, J. Food Compos. Anal. 51 (2016) 69–75.
[22] E.L. Beach, S.S. Bernstein, O.D. Hoffman, D.M. Teague, I.G. Macy, Distribution of nitrogen and protein amino acids in human and in cow's milk, J. Biol. Chem. 139 (1941) 57–63.
[23] A. Moongngarm, N. Saetung, Comparison of chemical compositions and bioactive compounds of germinated rough rice and brown rice, Food Chem. 122 (2010) 782–788.
[24] R. Hamani, U.H. Engelhardt, Determination of amino acids in white, green, black, oolong, pu-erh teas and tea products, J. Food Compos. Anal. 31 (2013) 94–100.
[25] J.N. Miller, J.C. Miller, Statistics and Chemometrics for Analytical Chemistry, fourth ed., Pearson Education, 1993.

Appendix A2

Conference proceedings

PACCON Proceedings 2016: Analytical Chemistry (ANC-1727)

Sequential injection system for automated derivatization with subsequent spectrophotometric determination of GABA

Pronrawee Tanpramoon,*[1,2] Nathawut Choengchan[1,2]
[1]*Flow Innovation-Research for Science and Technology Laboratories (FIRST Labs), King Mongkut's Institute of Technology Ladkrabang, Bangkok 10520, Thailand*
[2]*Applied Analytical Chemistry Research Unit, Department of Chemistry, Faculty of Science, King Mongkut's Institute of Technology Ladkrabang, Bangkok 10520, Thailand*
*e-mail: pronravee.tan@gmail.com

Abstract:

In this work, an automated system for derivatization with subsequent determination of γ-aminobutyric acid or GABA was developed. The system was based on using sequential injection analysis (SIA) with spectrophotometric detection. GABA was derivatized with 2-hydroxy-1-naphthaldehyde (6% w/v) in the presence of 0.1 mol L^{-1} borate buffer (pH 8.0). Pure acetonitrile was used as carrier. The derivative was monitored at 425 nm which is the maximum absorption wavelength. Linear calibration was observed in the concentration range of 300 to 2000 mg L^{-1} GABA with good linearity ($Abs_{425} = 2.21 \times 10^{-3}$ [GABA] - 0.0418, r^2 = 0.999). Increasing in derivatization temperature from room temperature to 60°C resulted in greater sensitivity. The SIA system provided good precision (RSD = 0.2% at 300 mg L^{-1} GABA) and good recovery (94-107%). The developed system was applied to GABA supplemented products (tablet and capsule) and was validated against batchwise method with the same detection reaction. By statistical paired *t*-test, the results obtained by both methods were not significantly different at 95% confidence level (t_{stat} = 0.27, t_{crit} = 2.23, d.f. = 10). This implies that the system was successfully developed.

1. Introduction

γ-Aminobutyric acid (GABA) is the main inhibitory neurotransmitter in the mammalian central nervous system. It is produced from glutamate by glutamate decarboxylase[1]. GABA can affect various bioactivities on human heath.[1,8] Nowadays, there are large numbers of commercial dietary GABA supplemented products, it is therefore important to monitor GABA concentration for control quality of the products.

Various analytical methods have been presented for determination of GABA such as high performance liquid chromatography,[9,10] gas chromatography[11] and capillary electrophoresis.[12] It was observed that derivatization was necessary prior to analysis. Derivatizing agents that were reported such as, 2-hydroxy-1-naphthaldehyde (HN),[9] ethyl-chloroformate,[11] (4-carboxybenzoyl)-2-quinoline-carboxaldehyde (CBQCA).[12] The separation techniques are very useful for determination of GABA in complicated matrix samples such as cerebrospinal fluid[9] and brain tissue.[10] For simple matrix sample, namely supplemented tablet, non-separation technique such as spectrophotometric method, is more interesting in term of simplicity and cost-effectiveness. However in cases of large number of samples, batchwise method is not convenience for derivatization and determination.

The aim of this work is therefore to develop an analytical method for automated derivatization with subsequent spectrophotometric determination of GABA. Sequential injection analysis or SIA was selected for method development since the technique is regarded as the fully automated method with the advantages of simplicity and rapid analysis. HN was

exploited as derivatizing agent because the delivatization procedure is simpler, compared to the other procedures.[10,12] Factors affecting sensitivity were studied. Application to GABA - supplemented samples and validation against batchwise method were also investigated.

2. Materials and Methods

2.1 Reagent and Sample preparation

All chemicals were analytical reagent grade and deionized - distilled water was used throughout. A HN solution (6 % (w/v)) was prepared by dissolving 1.5 g of 2-hydroxy-1-naphthaldehyde (Sigma Aldrich, USA) in 25.00 mL of pure acetonitrile (RCI Labscan, Thailand). Standard stock solution of 2000 mg·L^{-1} GABA (Sigma Aldrich, USA) was prepared by dissolving 0.0500 g in 25.00 mL of water. Working standards were prepared by freshly dilution from the stock solution. Borate buffer (pH 8.0) was prepared by mixing of 0.1 mol·L^{-1} boric acid (Sigma Aldrich, USA) with 0.1 mol ·L^{-1} potassium chloride (Sigma Aldrich, USA).

The GABA supplemented samples were purchased in retail stores in Bangkok. There are two forms of commercial products which are tablet and capsule. For tablet, the sample was grinded. The powder was exactly weighed (0.3000 g) and was then dissolved in 25.00 mL of water. The capsule was peeled and the powder was weighed (0.7600 g). An aliquot of 25.00 mL of water was added to dissolve the sample. Both kinds of sample solutions were filtered through 0.22 µm nylon (National Scientific, USA) membrane filter prior to analysis.

2.2 SIA system and manipulation

A schematic diagram of the SIA setup is shown in Figure 1. The system consists of syringe drive module equipped with 12.5 mL Gastight® syringe and an 8 - port multi - selection valve. All devices were purchased from Hamilton, USA. The system was automatically manipulated by Auto - pret® software (MKG Company, Japan). Spectrophotometric detection was carried out at 425 nm on Jasco v - 630 UV-visible spectrophotometer (USA). The 'Lab - built' heating system is composed of water bath with hot plate and temperature control device. (Heidolph, MR 1000, Germany) standard and reagent solutions as well as mixing coil (not show in Figure) are immerged into the bath. System manipulation for on - line derivatization with subsequent determination of GABA is summarized in Table 1.

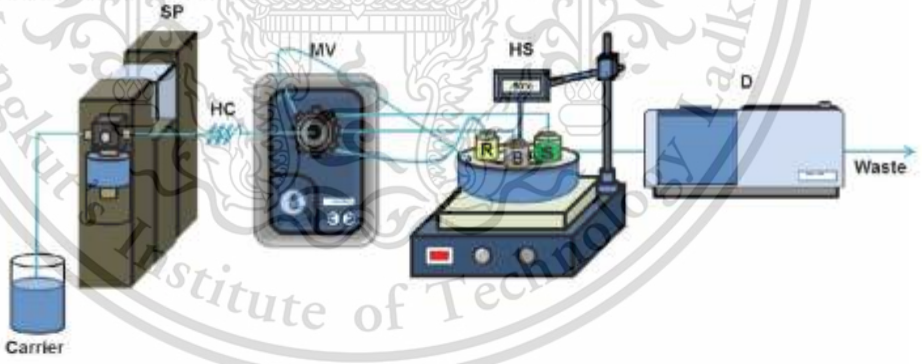

Figure 1. SIA system set up for 'on - line' derivatization with subsequent determination of GABA. Carrier: acetonitrile, SP: syringe pump, HC: holding coil, MV: multi - selection valve, R: derivatizing solution (6 % w/v HN in acetonitrile), B: borate buffer pH 8.0 (0.1 mol L^{-1}), S: standard GABA/sample, HS: heating system and D: detector.

Table 1. Operation sequence of the SIA system for automated derivatization with subsequent determination of GABA in a complete measurement cycle.

Step	Flow rate ($\mu L\ sec^{-1}$)	Volume (μL)	Valve position	Action description
1	10	50	2	Aspirate of sample to holding coil
2	10	30	3	Aspirate of borate buffer to holding coil
3	10	100	4	Aspirate of derivatizing solution to holding coil
4	50	600	8	Propulsion of reaction mixture to mixing coil
5	-	-	8	Incubation at 60°C for 5 min
6	50	4580	8	Sending to detector

3. Results & Discussion

3.1 Maximum absorption wavelength of the derivative.

Preliminary 'off line' derivatization procedure was carried out in order to study absorption spectrum of the GABA derivative in the range of 200 to 800 nm. Results in Figure 2(a) indicate that a maximum absorption wavelength of the derivative is located at 425 nm. This wavelength was selected as a detection wavelength. By batchwise measurement, linear calibration (Figure 2(b)) was obtained up to 40 mg GABA L^{-1} with good linearity ($Abs_{425} = 1.04 \times 10^{-2}$ [GABA] + 3.8×10^{-2}, $r^2 > 0.994$).

3.2 Optimization of SIA system

3.2.1 Effect of the derivatizing agent concentration

Effect of the concentration of HN, which is the derivatizing agent, was studied from 0.3 to 7.5 % w/v. Results are shown in Table 2. When the concentrations were increased from 0.3 to 6 % w/v, sensitivities were also improved by approximately two times. However, the sensitivity obtained by 6 and 7.5 % w/v were not difference. The concentration of 6 % w/v was selected as appropriate concentration.

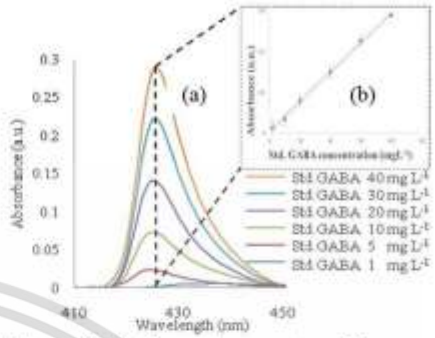

Figure 2. (a) Absorption spectra of the derivatives when 6 % (w/v) HN in 0.1 mol L^{-1} borate buffer (pH 8) was used. (b) Example of linear calibration curve by batchwise detection.

Table 2. Effect of concentration of derivatizing agent.

HN concentration (% w/v)	Calibration equation	r^2
0.3	y = 0.0156x + 0.216	0.773
3	y = 0.0188x + 0.344	0.551
6	y = 0.0324x + 0.246	0.997
7.5	y = 0.0327x + 0.699	0.998

3.2.2 Effect of pH

Effect of pH of borate buffer was studied at pH 8, 9 and 10. Results are presented in Table 3. The highest sensitivity was achieved when the pH of the derivatization reaction was kept at pH 8.0. This might be because this pH was appropriated for GABA to become stable derivative form[9]. Therefore, pH 8 was regarded as suitable pH.

Table 3. Effect of pH of borate buffer.

pH	Calibration equation	r^2
8	y = 0.0311x + 0.216	0.996
9	y = 0.0185x + 0.344	0.992
10	y = 0.0076x + 0.246	0.180

Table 4. The concentration of GABA in commercial supplemented products.

Sample	Type	Concentration of GABA (mg L^{-1})		
		Label	Batch wise method	SIA
1	tablet	20	20.9 ± 0.0006	21.5 ± 0.003
2	tablet	20	21.2 ± 0.0001	21.5 ± 0.0006
3	tablet	20	21.3 ± 0.0001	22.0 ± 0.005
4	tablet	20	21.4 ± 0.0007	22.1 ± 0.003
5	tablet	20	21.4 ± 0.0002	22.3 ± 0.006
6	capsule	500	501 ± 0.005	503 ± 0.001
7	capsule	500	502 ± 0.0001	511 ± 0.002
8	capsule	500	501 ± 0.0009	488 ± 0.0005
9	capsule	750	757 ± 0.0001	759 ± 0.005
10	capsule	750	758 ± 0.0002	757 ± 0.004
11	capsule	750	755 ± 0.0003	757 ± 0.001

3.2.3 Effect of incubation time

Incubation time is defined as the period of time that the reacted zones between sample and derivatizing agent were held in mixing coil which was immersed in heating bath during derivatization process (see Figure 1).

Effect of incubation time was studied from 1 to 5 min. Results were shown in Figure 3. When incubation time was increased, the sensitivity was also increased. Since the highest sensitivity was obtained at 5 min, this period of time was therefore selected. This led to sample throughput of 11 sample h^{-1}.

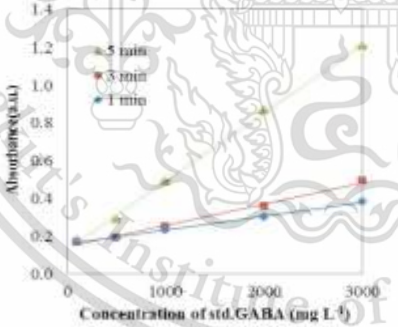

Figure 3. Effect of incubation time on absorbance reading.

3.2.4 Effect of temperature

The effect of temperature on derivatization reaction was studied by varying the temperature from room temperature to 70 °C. As the temperature was increased, sensitivity was also increased. However, at 70 °C, air bubble was observed. Therefore, temperature of 60 °C was chosen as the suitable temperature.

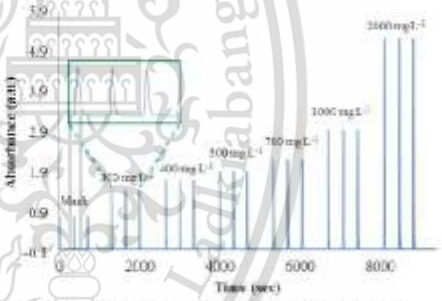

Figure 4. Typical SIA peak profiles for GABA standards (0-2000 mg L^{-1} GABA).

3.3 Analytical performances

Analytical performances of the developed method were studied and were summarized as the following. At the 300 mg L^{-1} of standard GABA, RSD was lower than 0.2 % and SIA profiles were shown in Figure 4. These signals gave high reproducibility. Limit of detection (y_b+3S_b).[13] and limit of quantification ($y+10S_b$) were obtained at 104 and 347 mg

L^{-1}, respectively. Analytical recoveries were found from 94 ± 0.006 to 107 ± 0.002 %. These results demonstrate that our method gave high precision and accuracy.

3.4 Application to GABA -supplemented products

The developed SIA system was applied to determine the GABA content in GABA - supplemented tablet and capsule. Results are shown in Table 4. It was observed that the results were not significantly difference from the results obtained by batchwise method, at 95 % confidence level (t_{stat} = 0.27, t_{crit} = 2.23). There results imply that the method was successfully validated.

4. Conclusion

In this work, an on - line derivatization system with subsequent spectrophotometric determination of GABA was successfully developed. This method gave good precision and good accuracy. The method was also applicable for determination of GABA in GABA supplemented tablet and capsule.

Acknowledgements

Applied Analytical Chemistry Research Unit, Department of Chemistry, Faculty of Science, King Mongkut's Institute of Technology Ladkrabang and National Research Council of Thailand (NRCT) are grateful acknowledged for equipments and financial supports.

References

1. Lujan, R.; Shigemoto, R.; Lopez bendito, G. *Neuroscience* **2005**, *130*, 567–580.
2. Inomata, N.; Ishihara, T.; Akaike, N. Br. *J. Pharmacol.* **1988**, *93*, 679–683.
3. Norikura, T.; Kojima-Yuasa, A.; Kennedy, D. O.; Matsui-Yuasa, I. *Amino Acid* **2007**, *32*, 419–423.
4. Brioni, J. D.; Nagahara, A. H.; Mcgaugh, J. L. *Brain Research* **1989**, *487*, 105–112.
5. Genazzani, A. D.; Stomati, M.; Bersi, C.; Luisi, S.; Fedalti, M.; Santuz, M.; Esposito, G.; Petraglia, F. Genazzani, A. R. *J. Endocrinol. Invest.* **2000**, *23*, 526–532.
6. Vescovi, P. P.; Volpi, R.; Coiro, V. *Alcohol* **1998**, *16*, 325–328.
7. Menzies, J. R. W.; Ludwig, M. Leng, G. *J. Neuroendocrinol.* **2010**, *22*, 585–592.
8. Reisi, P.; Alaei, H.; Babri, S.; Sharifi, M. R.; Mohaddes, G.; Soleimannejad, E.; Rashidi, B. *J. Res. Med. Sci.* **2010**, *15*, 172–174.
9. Khuhawar, M. Y.; Rajper, A. D. *J. Chromatogr. B* **2003**, *788*, 413–418.
10. Clarke, G.; O'Mahony, S.; Malone, G.; Dinan, T. G. *J. Neurosci. Met.* **2007**, *160*
11. Moini, M.; Cao, P. *J. Chromatogr. A* **1995**, *710*, 303–308.
12. Bergquist, J.; Vona, M. J.; Stiller, C. O.; O'Connor, W. T.; Falkenberg, T.; Ekman, R. *J. Neurosci. Met.* **1996**, *65*, 33–42.
13. Miller, J. N.; Miller, J. C. Statistics and Chemometrics for Analytical Chemistry, 4th ed., Pearson Education: Essex, **1993**; pp 223–230.

PACCON 2020
Chemistry for Catalyzing Sustainability and Prosperity

Flow injection system for detection of albumin based on gold nanoparticles-catalyzed luminol chemiluminescence

Bhoonnarasa Kasetsoontorn[1,2*], Nathawut Choengchan[1,2]
[1]Flow Innovation-Research for Science and Technology Laboratories (FIRST Labs),
[2]Department of Chemistry and the Applied Analytical Chemistry Research Unit, Faculty of Science,
King Mongkut's Institute of Technology Ladkrabang, Bangkok 10520, Thailand
*E-mail: bh.kasetsoontorn@gmail.com

This work presents a simple flow injection (FI) system for the determination of albumin based on chemiluminescence (CL) detection. Gold nanoparticles (AuNPs)-catalyzed luminol CL were employed as the detection reaction. In the presence of albumin, aggregation of the AuNPs was induced and this inhibited the CL light caused by the luminol-H_2O_2 system. The AuNPs were synthesized using the Turkevich's method. Surface plasmon peak of the as-prepared colloidal gold was located at 520 nm. TEM image showed that monodispersed nanoparticles were observed (average size: 18.4 ± 0.04 nm). The AuNPs were off-line mixed with the standard/sample for 10 min. Aliquots of 500 µL of the mixed solution and 400 µL of 0.01 mol L^{-1} luminol in 0.1 mol L^{-1} NaOH were injected into the FI manifold. A detection flow cell was designed as spiral configuration and was attached in front of the photomultiplier tube. This flow cell was fabricated quickly and easily using three-dimensional printing technology. Increasing in the concentration of albumin resulted in decreasing in the CL intensity. Calibration plot was observed from the concentration range of 0.1 to 70 mg albumin L^{-1} with good linearity (r^2 > 0.99). The detection limit was 0.05 mg L^{-1} (3SD/slope) with a relative standard deviation of 0.57 %. High sample throughput (66 samples h^{-1}) was also achieved.

1. Introduction

Kidney disease is a global health problem. Urinary albumin excretion is one of the important key parameters for diagnosis of kidney dysfunction.[1,2] Many analytical methods based on various detection principles have been presented for the determination of albumin such as spectrophotometry,[3] resonance light scattering,[4,5] voltammetry,[6] surface plasmon resonance,[7] surface enhanced Raman spectroscopy,[8] near infrared reflectance spectroscopy[9] and fluorometry.[10]

Nowadays, gold nanoparticles (Au NPs) are probably the most outstanding metal nanoparticles because of the advantages of chemical inertness, easy modification, simple control of particle size and high extinction coefficient. There are some works report that the AuNPs can easily form conjugates with bovine serum albumin (BSA)[11,12] via electrostatic interactions.[13,14] The AuNPs can be also exploited as a catalyst for the chemiluminescence (CL) reaction of the luminol-H_2O_2 system.[15]

In this work, we aim to employ the AuNPs-catalyzed CL reaction between luminol-H_2O_2 for the determination of albumin in urine by flow injection (FI) technique. In the presence of albumin, aggregation of the AuNPs is occurred and then the CL light is inhibited. The three-dimensional (3D) printing technology[15,16] was employed for construction of the spiral flow-through cell due to its single-step and fast fabrication.

2. Materials and Methods

2.1 Reagents and chemicals

All standard and reagents were of analytical reagent grade. Glassware were soaked in 10 % (v/v) of HNO_3 and rinsed with distilled water prior to use. Deionized-distilled water (18 MΩ ·cm) purified by

AC140

Zeneer up 900 (Human corporation, USA) was used through all experiments.

An albumin standard stock solution (1,000 mg L^{-1}) was prepared by dissolving 0.1002 g of solid powder of bovine serum albumin, BSA (Thermo Fisher Scientific, USA) in 100.0 mL of water and was adjusted to pH 6.0 with 0.01 mmol L^{-1} HCl. This standard stock solution was kept at 4 °C. The working standard solutions (0.1 to 70 mg albumin L^{-1}) were appropriate diluted from this stock solution with water and were adjusted to pH 6.0. The working standard solutions were left overnight to ensure complete protein dissolution. A 1.0×10^{-2} mol L^{-1} stock solution of luminol sodium salt was prepared by dissolving 0.1772 g of luminol (Sigma, USA) in 100.0 mL of 0.10 mol L^{-1} NaOH. 0.15 mol L^{-1} of H_2O_2 was daily prepared by dilution of 3.83 mL of 30 % (v/v) H_2O_2 (Merck, Germany) and made up with water to 250.0 mL.

2.2 Synthesis of AuNPs

The AuNPs were prepared by the modified procedure of the Turkevich's method[18]. Aliquot of 100.0 mL of 1 mmol L^{-1} chloroauric acid ($HAuCl_4{\cdot}H_2O$) (Sigma-Aldrich, USA) was heated to 95 °c and stirred vigorously. Then, 7 mL of 38.8 mmol L^{-1} of trisodium citrate solution (Sigma-Aldrich, Japan) was immediately added. The color of the solution was changed from pale yellow to deep red. This mixture was further boiled for 10 min and was cooled to room temperature. The as-prepared AuNPs colloidal was kept at 4 °C overnight before using.

2.3 Sample preparation

Urine samples were collected from healthy volunteers. After filtration through a 0.45-µm cellulose membrane filter, 5 mL of sample was pipetted into a 10.0 mL volumetric flask and made up with water prior to injection into the FI system in Figure 1.

2.4 FI system

The developed FI system for the determination of urinary albumin is presented in Figure 1. PTFE tubing (1.0 mm i.d., Cole Parmer, USA) was used. An Ismatec™ peristaltic pump (model IS7610, Switzerland) depicted as P, was used for liquid delivery. Two 6-Port valves (model V-450, USA), V_1 and V_2, were used for injection of luminol and a mixed solution of AuNPs and standard albumin or urine, respectively. The 3D-printed spiral flow cell (F) was attached in front of a PMT in a Jasco spectrofluorometer (model FP-8200, Japan) for monitoring of the emitted light intensity at 425 nm.

A volume of 400 µL of luminol (1 x 10^{-2} mol L^{-1}) was injected via V_1 into the stream of 0.1 mol L^{-1} of NaOH and flown to merge with the H_2O_2 stream. The standard albumin/sample (200 µL) was off-line mixed with AuNPs (2000 µL) for 10 min. The mixed solution (500 µL) was injected trough V_2.

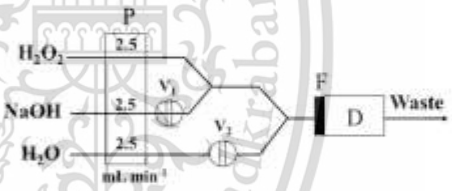

Figure 1. A schematic diagram of the developed FI system for the determination of albumin based on the AuNPs-catalyzed reaction between luminol-H_2O_2. P; peristaltic pump, V; 6-Port injection valves, F; the 3D-printed spiral flow cell (Ø of spiral: 350 mm) and D; spectrofluorometer.

3. Results & Discussion

3.1 Characterization of the AuNPs

AC141

Results by transmission electron microscopy (TEM) image in Figure 2A show that the monodispersed and spherical nanoparticles are observed (average size: 18.4 ± 0.04 nm). Maximum absorption wavelength of the as-prepared AuNPs is located at 520 nm (Figure 2B). These results are agreed with the literature report.[19] TEM image in Figure 2C reveals that aggregation of AuNPs in the presence of albumin is occurred. This results in red shift of the absorption spectrum of the AuNPs as shown in Figure 2D.

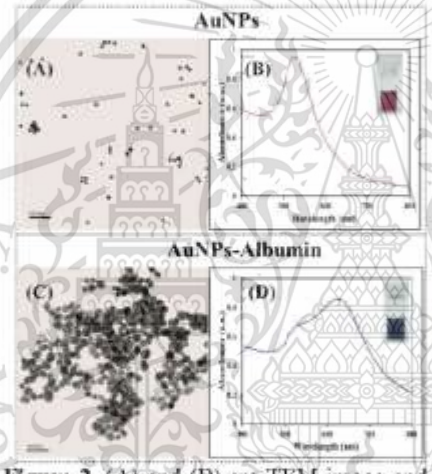

Figure 2. (A) and (B) are TEM image and absorption spectra of the prepared AuNPs, respectively. (C) and (D) are TEM image and absorption spectra of AuNPs in the presence of standard albumin (50 mg L^{-1}), respectively. The inset pictures of (B) and (D) are the observed colors of the AuNPs solutions.

3.2 Aggregation of AuNPs by albumin

Albumin can simply bind on the AuNPs surface through the displacement mechanism, where the stabilized citrate ion around the nanoparticles can be displaced by BSA upon adsorption, with the amino acids (functional groups) lysine (amine), histidine (imidazole), and cysteine (thiol).[20] After binding, the AuNPs became aggregate. Figure 3A indicates that increasing in the concentration of albumin, induce aggregation of the AuNPs. The color of the AuNPs solutions are changed from red to dark blue (Figure 3B). This confirm that the formation of AuNPs-albumin conjugate is occurred.

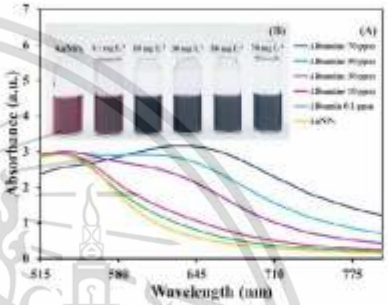

Figure 3. (A) Absorption spectra and (B) the color of the AuNPs (8.38 nmol L^{-1}) with various concentrations of standard albumin (0.1 to 70 mg L^{-1}).

3.3 Catalytic effect of AuNPs on the CL reaction between luminol and H_2O_2

Results in Figure 4 indicate that when the concentration of AuNPs is increased, the CL intensity is also increased. This is an evidence that the as-prepared AuNPs can catalyze the CL reaction of luminol and H_2O_2.

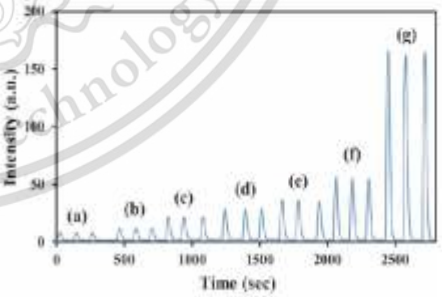

Figure 4. Signal profiles, obtained by injection of various concentrations of AuNPs into the developed FI in Figure 1:

AC142

(a) 0, (b) 0.59 x 10^{-9}, (c) 1.42 x 10^{-9}, (d) 2.57 x 10^{-9}, (e) 4.30 x 10^{-9}, (f) 8.38 x 10^{-9} and (g) 9.72 x 10^{-9} mol L^{-1}.

3.4 Effect of incubation time

Incubation time is defined as the period that the mixed solution was kept after standard albumin and AuNPs were mixed. This effect was investigated by various concentrations of AuNPs while standard albumin was fixed at 10 mg L^{-1}. Results in Figure 5 imply that when incubation time is increased, the absorbance ratio (A_{620}/A_{520}) is also increased. The ratio is not significantly different after 10 min. Therefore, 10 min is selected.

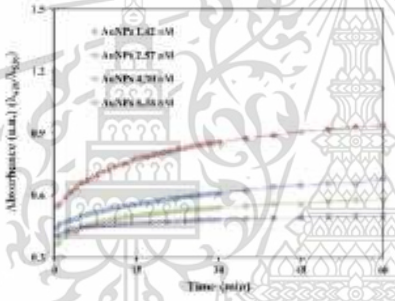

Figure 5. Effect of incubation time.

3.5 Optimization of FI system

3.5.1 Effect of sample volume

The effect of the sample volume (the mixture between AuNPs and standard albumin/urine) was studied when the volume of luminol was fixed at 400 µL. Results in Figure 6 indicates that the sensitivities are increased when the volume are increased from 100 to 500 µL. The sensitivity was decreased at higher volume. The doublet peak was also observed at 600 µL. The injection volume of 500 µL was therefore chosen.

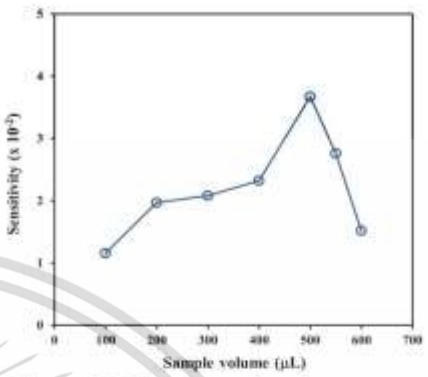

Figure 6. Effect of sample volume

3.5.2 Effect of flow rate

Effect of flow rate was studied from 1.0 to 3.0 mL min^{-1}. Results in Figure 7 show that increasing in the flow rate results in increasing in the sensitivity and the throughput. However, at 3.0 ml min^{-1}, the sensitivity was decreased. The flow rate of 2.5 mL min^{-1} was selected as compromising between the sensitivity and the throughput. By this flow rate the throughput of 66 samples h^{-1} was achieved.

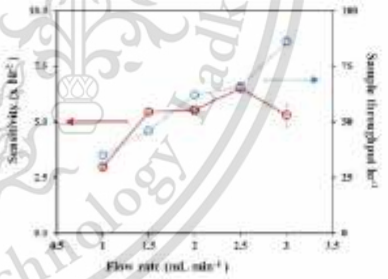

Figure 7. Effect of flow rate.

3.6 Analytical performances

AC143

Under the optimal conditions, the examples of signal profiles and linear calibration with its corresponded linear equation (0.1 to 70 mg L^{-1} albumin, Intensity = -17.1[Albumin] + 6976.3, r^2 = 0.992)) were obtained as demonstrated in Figure 8B. Good reproducibility (RSD: 0.57 %, n = 10 at 30 mg L^{-1} albumin) and limit of detection (3SD/slope) was obtained at 0.05 mg L^{-1}.

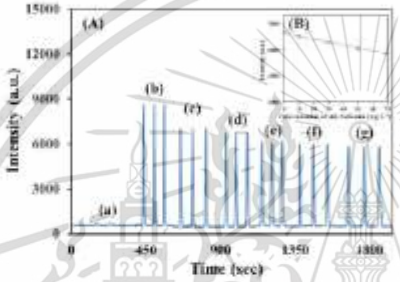

Figure 8. (A) An example of the signal profiles of the calibration: (a), luminol-H_2O_2 without AuNPs and (b)-(g), (AuNPs)-catalyzed luminol-H_2O_2 CL in the presence of standard albumin concentration of 0, 0.1, 10, 30, 50, and 70 mg L^{-1}, respectively and (B) the corresponded linear calibration curve.

3.7 Application to urine samples

The developed FI system was applied to the spiked urine, from normal volunteers. Good recovery was obtained (95.7 to 101.1 %) as shown in Table 1. These results can guarantee that the method was free from the sample matrix effect.

Table 1. Percentage recovery of albumin in urine samples, evaluated by the developed method.

Sample	Albumin concentration (mg L^{-1})			% Recovery
	Original	Added	Found	
1	13.1±0.02	10	23.4±0.47	101.1
2	8.7±0.02	10	18.5±0.28	98.1
3	1.3±0.01	10	22.9±0.17	95.7
4	15.2±0.02	10	25.0±0.07	98.2

4. Conclusion

This work presents a simple FI for the determination of albumin in urine based on CL detection. The method was successfully developed and was possible for the determination of urinary albumin. The method also gave high precision and high accuracy with high throughput.

Acknowledgements

Applied Analytical Chemistry Research Unit and FIRST Labs@KMITL, Department of Chemistry, Faculty of Science, King Mongkut's Institute of Technology Ladkrabang are grateful acknowledged for equipment supports.

References

1. Malin, B.; Kine, M.K.S.; Jeannette, N.; Inger, S.; Jan, T.A. *J. Control. Release.* **2015**, *211*, 144-162.
2. Mogensen, C.E.; M.D. *Engl. J. Med.* **1984**, *310*, 356-360.
3. Wei, Q.; Wu, D.; Du, B.; Li, Z.; Huo, Y. *J. Food Compos. Anal.* **2006**, *19*, 76-82.
4. Hui, Z.; Na, L.; Fenglin, Z.; Ka-an, L. *Talanta.* **2004**, *62*, 37-42.
5. Zhong-Xian, G.; Han-Xi, S. *Spectrochim. Acta A.* **1999**, *55*, 2919-2925.
6. Loganathan, B.D.; Sheela, B.; Asit, B. M. *J. Electroanal. Chem.* **2012**, *665*, 20-25.
7. Ananth, A.N.; Daniel, S.C.G.K.; Sironmani, T.A.; Umapathi, S. *Colloids Surf. B.* **2011**, *85*, 138-144.
8. Juqiang, L.; Rong, C.; Shangyuan, F.; Jianji, P.; Yongzeng, L.; Guannan, C.; Min, C.; Zufang, H.; Yun, Y.; Haishan, Z. *Nanomedicine.* **2011**, *7*, 655-663.
9. Cai-Jing, C.; Wen-Sheng, C.; Xue-Guang, S. *Chin. Chem. Lett.* **2013**, *24*, 67-69.
10. Xiaowei, Z.; Fenglin, Z.; Ke-an, L. *Microchem. J.* **2001**, *68*, 53-59.
11. Tapasi, S.; Krishna, K.H.; Amitava, P. *J. Phys. Chem. C.* **2008**, *112*, 17945-17951.

AC144

12. Justin, L.B.; Claudia, G.W.; Mario, M.Y.; Miguel, J.Y. *Langmuir.* **2004**, *20*, 11778-11783.
13. Li, S.; Yizhe, W.; Junguang, J.; Shaojun, D. *Langmuir.* **2007**, *23*, 2714-2721.
14. Smritimoy, P.; Platu, B.; Arindam, s.; Subhash, C.B. *J. Lumin.* **2008**, *128*, 1969-1974.
15. Zhi-Feng, Z.; Hua, C.; Chun-Ze, L.; Li-Juan, L. *Anal. Chem.* **2005**, *77*, 3374-3329.
16. Elodie, M.; Fabien, R.P.; Catherine, B.; Kinga, P.; Andre, M.; Christophe, B.P.; Joel, K.; Jean-Luc, B.; Bruno, C. *Talanta.* **2017**, *168*, 298-302.
17. Bethany, G.; Sarah, Y.L.; Dana, M.S. *Anal. Chem.* **2017**, *89*, 57-70.
18. Kimlong, J.; Maier, M.; Okenve, B.; Kotaidis, V.; Ballot, H.; Plech, A. *J. Phys. Chem. B.* **2006**, *110*, 15700-15707.
19. Monica, I.; Valentin, C.; Simion, A. *J. Photochem. Photobiol. A.* **2011**, *217*, 395-401.
20. Scott, H.B.; Wihelm R.G.; Marcus C.J.; Magne K.K.; Stefan, F. *Langmuir.* **2005**, *21*, 9303-9307.

AC145

Author Biography

Name	Miss Bhoonnarasa Kasetsoontorn
Date of Birth	1 October 1987
Address	575/84 Moo. 4, Klongkut, Mueang District, Satun, 91000 Thailand
Education	(2010) Bachelor of Science in Industrial Chemistry - Analytical Instrumentation, GPA 2.96 King Mongkut's Institute of Technology Ladkrabang. (2014) Master of Science in Analytical Chemistry, GPA 3.68 King Mongkut's Institute of Technology Ladkrabang.

International Publications

1. **Bh. Kasetsoontorn**, and N. Choengchan. *Towards direct analysis of solid and liquid samples exploiting a 3D printed dialysis unit and sequential injection: Application for automated derivatization and determination of gamma-aminobutyric acid in foodstuff and beverages*, Analytica Chimica Acta 1097 (2020) 103–109.

Conference Proceedings

1. **Bh. Kasetsoontorn**, and N. Choengchan. *Sequential injection system for automated derivatization with subsequent spectrophotometric determination of GABA*, Proceedings of Pure and Applied Chemistry International Conference, pp. 105-109, 2016.

2. **Bh. Kasetsoontorn**, and N. Choengchan. *Flow injection system for detection of albumin based on gold nanoparticles-catalyzed luminol chemiluminescence*, Pure and Applied Chemistry International Conference, pp. 140-145, 2020.